UCLouvain
Institute for Information
and Communication Technologies,
Electronics and Applied Mathematics
Institute of NeuroScience

Short- and long-term adaptation of grip dynamics and arm kinematics to novel gravito-inertial environments

Laurent Opsomer

Thesis submitted in partial fulfillment
of the requirements for the degree of

Doctor in Engineering Sciences

September 2021

Thesis committee

Prof. Philippe Lefèvre (Advisor), UCLouvain, Belgium
Prof. Jean-Louis Thonnard (Advisor), UCLouvain, Belgium
Prof. Frédéric Crevecoeur (Secretary), UCLouvain, Belgium
Prof. Roland Keunings (Chair), UCLouvain, Belgium
Prof. Francesco Lacquaniti, University of Rome Tor Vergata, Italy
Prof. Joseph McIntyre, Ikerbasque Science Foundation, Spain
Dr. Fabrice Sarlegna, CNRS, France

"The stars don't look bigger,
but they do look brighter."
Sally Kristen Ride

Acknowledgments

Je souhaiterais ici remercier du fond du cœur toutes ces personnes grâce auxquelles j'ai pu découvrir un univers très pointu mais bougrement intéressant et mener à bien un travail de cinq ans.

Merci, tout d'abord, Philippe et Jean-Louis, pour votre confiance, votre science, votre gentillesse et vos encouragements. Merci d'avoir pris le risque de m'embarquer dans cette aventure hors norme. Jean-Louis, merci pour ton enthousiasme et ta volonté, pour les bons restaurants et le blues. Philippe, merci pour ta patience à toute épreuve, pour ta rigueur attentive et pour ta bonne humeur.

Merci Fred et Joe, pour vos précieux conseils et feedbacks durant ces cinq années, que ce soit en tant que membres de mon comité d'accompagnement, co-auteurs, ou membres du jury de cette thèse. Merci également au Dr. Fabrice Sarlegna, au Prof. Roland Keunings et au Prof. Francesco Lacquaniti pour avoir accepté de faire partie de ce jury, pour les discussions très instructives lors de la défense privée et pour celles à venir.

Merci à tous les membres du labo avec qui j'ai pu partager une vie de bureau, des voyages inoubliables, une ou deux bières, des rires, des frustrations et... ah oui, des discussions scientifiques constructives. J'espère avoir la chance de pouvoir continuer à côtoyer tous les jours des gens aussi brillants et ouverts.

J'aimerais également remercier l'équipe du CADMOS pour leur support efficace depuis Toulouse lors des opérations à bord de l'ISS et pour m'avoir accueilli comme un presque CADMOS OPS n°3.

Enfin, merci à mes parents, qui auraient trouvé un moyen de m'amener à bord de l'ISS si cela s'était avéré nécessaire, et à mes petites sœurs, les meilleures.

Contents

Chapter 1

General introduction

To survive, humans need oxygen, food and shelter. The next items on the list would probably be gravity and tools. All life on Earth has evolved in a constant and omnipresent gravitational field and each species has developed specific ways to use gravity at its advantage. Prolonged exposure to weightlessness has serious effects on human physiology and behavior (Hupfeld et al., 2021; Iwase et al., 2020; Demontis et al., 2017). Likewise, life as we know it today would seem almost impossible without tools, which were already used by our ancestors millions of years ago. Surprisingly though, decades of space science have taught us that the human sensorimotor system can adapt rapidly to weightlessness when it comes to manipulating objects or moving around a space module. The question of how the central nervous system achieves this is however far from being settled. The present thesis continues a work started more than twenty years ago and driven by this interrogation. This work focused on the study of sensorimotor coordination, and in particular dexterous object manipulation, in altered gravito-inertial environments. We had the opportunity to study object manipulation in Mars and Moon gravity environments aboard a reduced-gravity aircraft, in negative gravity in an inversion chair and even on the International Space Station (ISS), where the well-known grip-load force paradigm has been brought for the first time. These experiments allowed us to study the short- and long-term adaptation of grip dynamics and arm kinematics during object manipulation in microgravity and other unusual gravitational contexts. But before diving into a detailed analysis of these results, an introduction of the field is required. This is the objective of this first chapter. We introduce the different senses that the brain has at its disposal to perceive gravity on Earth and how

they could be used to build internal representations of gravity for accurately predicting the behavior of objects and the consequences of movements. We then describe a scientific paradigm that has been used for decades and will be used repeatedly in this work: the grip force/load force coupling during object manipulation. This rather simple protocol can be used to study the predictive abilities of the brain in a large variety of contexts. In addition, we review the results of past studies focused on the adaptation of hand and arm motor control to altered-gravity environments and introduce the concept of reference frame in the context of sensorimotor control. Finally, we summarize the major contributions of the present work.

1.1 Why study motor control in Space ?

From the point-of-views of the neuroscientist and the engineer, the act of brushing one's teeth is as much an amazement as the acrobatic twirls performed by an experienced astronaut in weightlessness. Indeed, even for the simplest movements, the brain must theoretically deal with a huge number of degrees of freedom (more than 60 for the hand only; Santello et al. 2013), an infinity of possible limb trajectories, transmission and computational delays, noise, uncertainty, and much more. The exact mechanisms used by the brain to solve these problems are still misunderstood and actively studied.

An efficient way to study a system such as the central nervous system (CNS) is to see how it adapts to perturbations. For instance, in the nineties Lackner and DiZio (1994) studied simple reaching arm movements performed in a room rotating at constant speed. The rotation of the room induced significant Coriolis forces on the moving arm during the reaching movements, causing deviations of the arm away from the pre-rotation straight paths. Straight paths were retrieved after a few trials of practice, but deviated in the opposite direction once the rotation of the room had stopped. This experiment brought evidence that the CNS makes use of flexible predictive mechanisms to anticipate movement dynamics. Hence, the rotating room environment has brought interesting new insights on how motor control works, even though (or precisely because) motor adaptation to a rotating environment is almost never encountered in everyday life.

Similarly, sensorimotor-control experiments conducted in weightlessness or in other altered-gravity environments are not only driven by the necessity to best prepare for future space explorations, but also by the desire to better

understand how the brain controls our movements on Earth and how gravity affects them. Currently, the ISS is the only place where long-term sensorimotor adaptation to microgravity can be studied. Parabolic flight maneuvers allow to reproduce the exact same weightless condition as onboard the ISS, but only for periods of 20 to 30 seconds straight, therefore the extent of adaptation during these maneuvers is rather limited.

A much more accessible environment is water immersion, which allows to greatly reduce the sensation of weight as the buoyant force counteracting the gravitational force is distributed more evenly on the body than the contact reaction force on the ground. However, the effects of gravity on the internal organs, including the vestibular end-organs, are exactly the same under water as on dry ground, which means for instance that somatosensory and vestibular cues still inform about body orientation relative to gravity. Microgravity is the only environment where the influence of the gravito-inertial axis on spatial orientation can be removed. Furthermore, water considerably increases drag forces during movements. Thus, the microgravity environment of the ISS provides the best way to study the role of gravity in motor control and neurophysiological adaptation to microgravity. At last, a better understanding of the mechanisms underlying sensorimotor adaptation in general can help develop new rehabilitation methods for people suffering from sensorimotor deficits caused by injury or disease (Bastian, 2008).

This thesis presents experiments carried out on the ISS, in parabolic flights and on Earth with these motivations in mind. These experiments more specifically studied how a change in gravity affects sensorimotor coordination during dexterous object manipulation.

1.2 Sensing gravity

Gravity makes the world anisotropic: moving "left" and "right" is different from moving "up" or "down". It is therefore important for the CNS to construct a gravity-based reference frame defining where is "up" and where is "down" in order to make accurate predictions about the behavior of our body and of the external world. In that sense, gravity both allows and requires to orient oneself in space relative to it. Moreover, gravity gives weight to every object on Earth. Because the magnitude of the gravitational acceleration is sensibly always the same on Earth, the weight of familiar objects can be easily predicted. And if our predictions are completely erroneous and we accidentally drop the object,

we know which way it will fall.

Now, how is graviception, the perception of gravity, achieved ? Because it acts on every part of our body, a multitude of receptors can inform us about the intensity and orientation of the gravitational force. Our inner ear detects departures of head orientation from the vertical axis; touch and proprioception allow us to feel the weight of our own body and of the objects we manipulate; our eyes allow us to see trees and buildings standing up and the rain falling down. Both spatial orientation and weight perception therefore rely on multisensory information which must be combined to build a consistent percept. Here, we briefly present the main sensory systems that allow us to build internal representations of gravity.

1.2.1 The vestibular system

In all experiments that were conducted in the present work, participants manipulated an object equipped with accelerometers and gyroscopes measuring the linear acceleration and angular velocity of the object. Similar inertial sensors can be found in every smartphones and, more importantly, buried deeply in our temporal bones. Indeed, in addition to the cochlea dedicated to the sensing of acoustic waves, the inner ear comprises another pair of peripheral components: the labyrinths, dedicated to the sensing of self-motion and head orientation (Fig. 1.1). Each labyrinth is made up of three semi-circular canals and two otolith organs (the utricle and the saccule). The former are sensitive to angular accelerations of the head, while the latter are sensitive to linear accelerations and head tilt.

The semi-circular canals are filled with a fluid named the endolymph and comprise a small chamber, the ampulla, crossed by a gelatinous mass, the cupula (Fig. 1.1, top-left). When the head rotates, the cupula is deflected due to its own inertia and to the inertia of the endolymph. These deflections are sensed by hair cells inside the cupula, transduced into neural impulses and conveyed to central structures via the vestibular nerve[1].

The otolith organs contain a gelatinous membrane supporting small crystals, the otoconia, which are displaced relative to the supporting sensory epithelium as a consequence of head acceleration or head tilt (Fig. 1.1, bottom-left). These displacements are also sensed by hair cells. The utricle is mostly sensi-

[1] Note that the integrating properties of the endolymph fluid mechanics make the deflection of the cupula proportional to head angular velocity for relatively short stimuli such as natural head movements (Rabbitt et al., 2004).

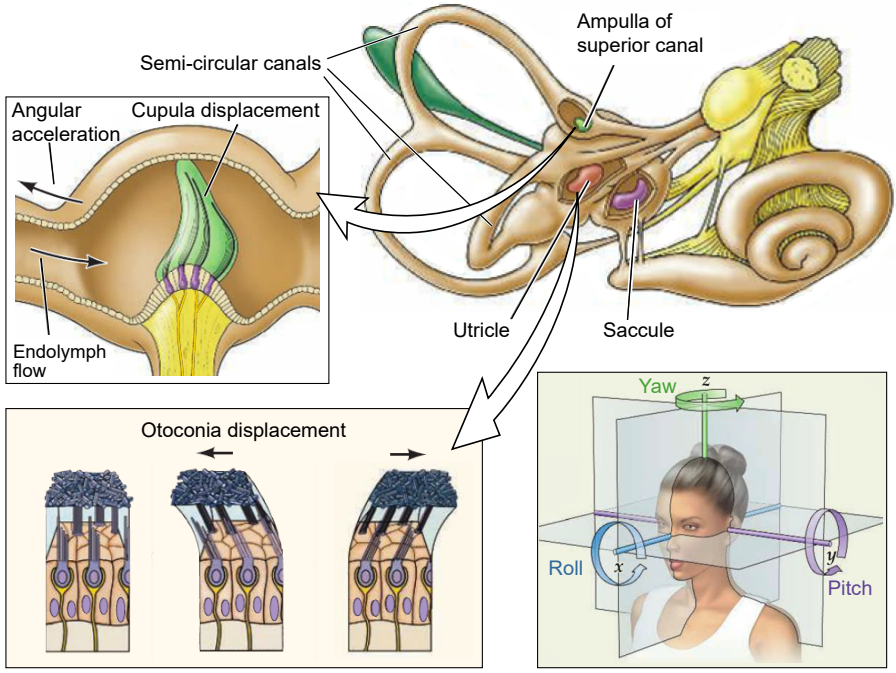

Figure 1.1 – The labyrinth of the inner ear. The labyrinth (top-right) is composed of three semi-circular canals and two otolith organs (the utricle and the saccule). The cupula within the ampulla of the semi-circular canals is displaced following angular acceleration of the head (top-left). The otoconia of the otolith organs are displaced following linear acceleration or rotation of the head (bottom-left). Adapted from Purves et al. 2012.

tive to linear accelerations in the horizontal plane and head tilts in the sagittal plane, while the saccule is mostly sensitive to linear accelerations and head tilts in the vertical plane.

Thanks to their three semi-circular canals and two otolith organs, the labyrinths can transmit information about head orientation and rotation velocity in three dimensions. Vestibular signals are essential to stabilize gaze (via the vestibulo-ocular reflex) and posture (via the vestibulo-cervical and vestibulospinal reflexes) and could even help trigger sympathetic reflexes to regulate blood pressure following a change in body posture (McCall et al., 2017; Shortt and Ray, 1997).

But vestibular signals are also crucial at higher levels for the perception of spatial orientation and self-motion, e.g. for the subjective perception of

the vertical (Mittelstaedt, 1999; Bisdorff et al., 1996) or for motor corrections following unexpected body motions (Bresciani et al., 2002; Keyser et al., 2017; Smith et al., 2017). In the microgravity (0-g) environment of Space, the otolith organs cannot be used anymore to measure head tilt, since no gravitational load is acting on the otoconia. This is one reason why spatial orientation can be drastically impaired in 0-g (Lackner and Graybiel, 1979; Kornilova, 1997).

1.2.2 Touch and proprioception

Gravity can also be sensed via the feeling of the weight of our own body and of the objects that we manipulate as well as via the sense of effort during self- or object motion. Touch and proprioception are therefore fundamental components of the somatosensory system for perceiving gravity (Fig. 1.2).

The skin is innervated by diverse mechanoreceptors (Merkel cells, Meissner corpuscles, Ruffinni corpuscles and Pacinian corpuscles) that are sensitive to stretch, pressure and/or vibrations (Johansson and Vallbo, 1983; Delhaye et al., 2018). Thousands of these cutaneous mechanoreceptors populate the glabrous skin of the human hand and provide critical information about interaction forces during object manipulation as the skin of the fingertips is stretched under the load. On Earth, object mass can be inferred from the weight of the object since the gravitational acceleration is constant. In microgravity, object weight is always zero, such that object mass cannot be estimated in static conditions. This could explain why mass-discrimination is impaired in Space (Ross et al., 1986).

Additionally, cutaneous mechanoreceptors can provide information about self orientation by monitoring how the reaction force of the supporting surface is distributed on the body (Bringoux et al., 2003; Trousselard et al., 2003; Lackner and Graybiel, 1979). During free-floating in weightlessness, it has been observed that providing pressure cues on the body can hence influence the perception of body orientation (Carriot et al., 2004; Clément et al., 2007; Lackner and Graybiel, 1979).

Another way of sensing object and limb weights is to monitor muscle activity. Mainly two kinds of receptors are able to provide this kind of information: the muscle spindles, located in the belly of skeletal muscles, and the Golgi tendon organs, embedded in the collagen fibers of the muscle tendons. Muscle spindles are formed by innervated intrafusal fibers that shorten when the muscle contracts and stretch out when the muscle relaxes; they are thereby sensitive to changes in muscle length and to limb position (Proske and Gande-

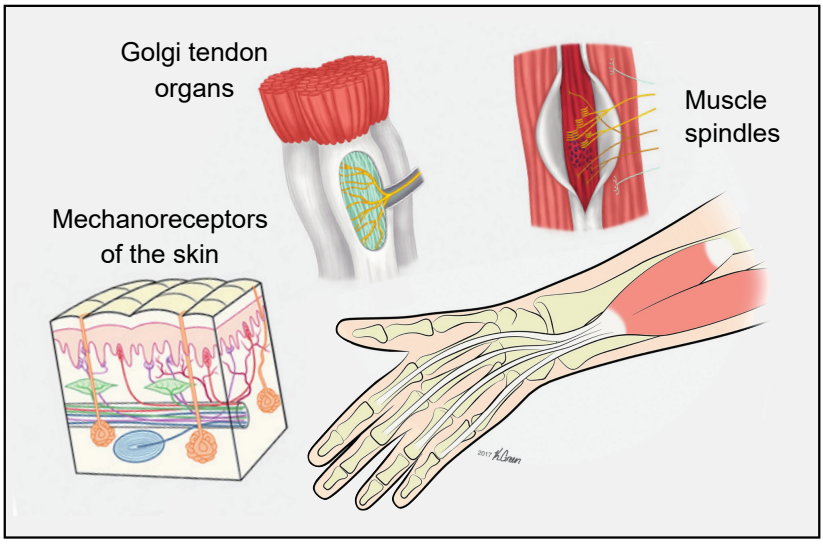

Figure 1.2 – Mechanoreceptors used for touch and proprioception. The mechanoreceptors of the skin are sensitive to stretch, pressure and vibrations; muscle spindles detect changes in muscle length; Golgi tendon organs provide information about muscle tension. Adapted from Delhaye et al. 2018.

via, 2009). High-frequency stimulation of a muscle can actually elicit illusions of limb motion (Goodwin et al., 1972). This effect was used to test and confirm the hypothesis that proprioceptive signals from muscles contribute to the internal representation of the vertical (Barbieri et al., 2008).

The Golgi tendon organs, on the other hand, are sensitive to muscle tension. The passive stretch of a muscle following the application of an external load as well as the muscular tension developing when the muscle contracts to counteract the load both inform about the magnitude of this load. Interestingly, motor efferences sent to the arm can also be used to estimate weight through a "sense of effort" (McCloskey et al., 1974; Gandevia et al., 2006).

Finally, movements of the viscera, stretching of blood vessels and variations of the hydrostatic pressure of the blood following a change in body posture can also be sensed by mechanoreceptors located more deeply in the body ("visceral graviceptors") and provide cues about body position in space (Mittelstaedt, 1996; Trousselard et al., 2004).

1.2.3 Vision

Vision is probably the first sense one thinks about if asked how the brain builds an internal reference frame for spatial orientation. In almost any place on Earth, visual cues about the direction of the vertical can be found: buildings, walls, trees, the floor, the sky,... It is therefore obvious that vision plays a primordial role in estimating the direction of gravity.

For instance, tilting a visual scene (while the body stays perfectly aligned with gravity) biases the subjective vertical and the perception of the upright (Asch and Witkin, 1948; Jenkin et al., 2003). This effect probably arises because many important features of the static visual field are usually either parallel or perpendicular to gravity (Coppola et al., 1998). The preponderance of horizontal and vertical visual stimuli is also thought to be at the origin of the oblique effect (Coppola et al., 1998; Appelle, 1972), which refers to the greater perceptual sensitivity along the vertical and horizontal axes compared to oblique axes.

In the same vein, a rotating visual background can elicit illusory sensations of body tilt (Dichgans et al., 1972). Dynamic stimuli from moving objects can also provide prominent information about the magnitude and direction of the gravitational acceleration, e.g. when observing objects falling or rolling down a slope. Moreover, visual feedback of arm velocity during object lifting has been shown to provide important cues about object weight in deafferented patients deprived of somatosensory feedback (Fleury et al., 1995). So, although gravity itself is invisible, the visual system plays a central role in graviception.

Vision is especially important for three-dimensional spatial orientation in extreme situations such as flying an aircraft or a helicopter, where sustained accelerations can be mistakenly interpreted by the vestibular system as body rotations. In poor visibility conditions, pilots can become rapidly disoriented, which can be fatal in the absence of reliable flight instruments.

1.2.4 Multisensory integration

Graviception therefore necessitates the integration of multiple signals. Combining multiple sources can solve ambiguities. For instance, signals from the semi-circular canals are used to distinguish the contributions of linear acceleration and head tilt to the otolith signals (Merfeld et al., 1993; Angelaki et al., 1999). Visual and somatosensory feedback can also be used to solve this otolithic ambiguity or to distinguish between head movements and whole-body

rotations. Convergence of vestibular, visual and proprioceptive information is indeed found already in the vestibular nuclei, the first stop of vestibular signals (Barmack, 2003; Jian et al., 2002).

But convergence of sensory signals for gravity and verticality perception occurs at multiple stages of sensory processing, because another goal of multisensory integration is to reduce uncertainty caused by sensory noise and to ensure a certain continuity and stability of the environment. Optimal reduction of estimation uncertainty is performed by weighting each signal according to its reliability (Seilheimer et al., 2014). For example, it has been hypothesized that the reliability of the otolith signals decreases with body tilt, which results in a higher weight given to visual and somatosensory signals relative to vestibular signals at large body tilts (Alberts et al., 2016).

Multisensory combination may sometimes come with the cost of increasing perceptual errors if one signal is biased: for instance, pilots can experience the illusion that the aircraft is pitching up excessively during take-off, because the sustained acceleration is interpreted as a body tilt. This somatogravic illusions can also be experienced (and studied) in human centrifuges (Mittelstaedt, 1996; Clément et al., 2001; Graybiel, 1952). At the same time, the centripetal acceleration experienced in human centrifuges can also induce an oculogravic illusion, i.e. the visual illusion that a target fixed relative to the body is actually moving upward to follow the sensation of tilt (Graybiel, 1952). Static and dynamic rotations of the visual field also impact the perception of body tilt (Asch and Witkin, 1948; Dichgans et al., 1972) and so do muscle spindles (Barbieri et al., 2008). Visual feedback can additionally affect the perceived weight of an object, as evidenced by the well-documented (but not yet fully understood) size-weight illusion. This illusion refers to the strong sensation that a small object feels heavier than a larger object of the same weight. Furthermore, the sensation of heaviness can also be biased by muscle fatigue (McCloskey et al., 1974).

In general though, the multitude of receptors capable of sensing gravity's effect allows the brain to construct a reliable estimation of gravity's effects in different contexts. But for a really efficient control of our movements and a stable and continuous perception of our environment, sensory feedback and multisensory integration are not enough: the CNS combines them to a large extent with sensorimotor predictions performed by *internal models*. These are introduced in the next section.

1.3 Predicting the effects of gravity

To explain how gravity is accounted for during motor planning and control, an "internal model of gravity" is very often mentioned in the literature (Lacquaniti et al., 2014; Lackner and DiZio, 2018; Zago and Lacquaniti, 2005; Jörges and López-Moliner, 2017). To understand what is meant by these terms, one must first look into the concept of internal model, a concept that is broadly used in the literature and can have various significations. Here, we briefly present the different meanings that can be hidden behind this concept and in particular behind the concepts of forward and inverse models, and where it comes into play for sensorimotor adaptation (for a much more detailed and complete review of the different forms of internal models in neuroscience, see McNamee and Wolpert 2019).

1.3.1 Internal models

Due to transmission delays, sensory feedback is not available instantaneously; moreover, it is corrupted by noise, subject to ambiguities, sometimes unavailable. To cope with these limitations, the brain develops predictive mechanisms that rely on internal representations of the world. In the context of sensorimotor control, internal models encapsulate this notion of a neural system capable of *mimicking musculoskeletal or environmental dynamical processes* (McNamee and Wolpert, 2019). Internal models serve multiple purposes, such as mental imagery, motor planning, improving state estimation, reafference cancellation, solving sensory ambiguities or overcoming transmission delays.

Let's imagine that you leave your building and realize you forgot your keys inside. Fortunately, your flatmate is still in the apartment and offers to throw you the keys from the window of the third floor. For this typical catching task to be successful, you have to estimate the location of the interception point, based on the direction of the fall; plan the hand trajectory to the interception point; transform the coordinates of the trajectory into joint coordinates, joint coordinates into muscle torques, muscle torques into motor commands; estimate the time-to-contact; close the hand at the right time and absorb the impact; and make corrective movements very quickly if the interception does not go exactly as planned. This is a lot to think about.

Fortunately, internal models intervene, potentially at each of these stages, to make things smoother and more predictable. For instance, when tilting your head back to look at your friend at the window, internal models are used to

make sure that the otolith signals are perceived as head tilt and not as forward acceleration (Merfeld et al., 1999; Green and Angelaki, 2010). When the keys are dropped, the direction of the fall is easily anticipated; a 7-month-old child knows that a dropped object will move downward and speed up (Kim and Spelke, 1992). During the fall, the oculomotor system predicts the upcoming position of the key by using an estimate of the velocity and acceleration of the keys (Bennett et al., 2010) sharpened by an internal model of the gravitational acceleration (McIntyre et al., 2001; Senot et al., 2005) allowing predictive saccades and an accurate prediction of the time-to-contact. Furthermore, efferent copies of the motor commands sent to the eye muscles are also sent to internal models that predict the upcoming eye movements, so that the visual flow on the retina caused by these eye movements are not mistakenly perceived as motion of the world (Haarmeier et al., 2001). When planning the catching action, internal models of the arm dynamics (weight, moment of inertia, interaction torques between segments,...) can be used to transform a desired arm trajectory into motor commands (Kurtzer et al., 2008; Kawato, 1999). An estimation of the mass of the keys (which you feel almost every day) is also used in combination with an estimation keys velocity to predict the momentum at the time of impact and tune muscular co-activation anticipatively (Lacquaniti and Maioli, 1989b; Johansson and Westling, 1988a). And so on: internal models can potentially be used at every level of sensorimotor control.

1.3.2 Forward and inverse models

Two classes of internal models are of particular interest for sensorimotor control. The first one, the *forward models*, assembles models that take as input the current state of the body and a set of motor commands, simulate the limb dynamics and give as output a prediction of the consequences of the motor action, be it the future state of the body or the expected sensory feedback (Miall and Wolpert, 1996; Todorov, 2004).

Forward models can be used for reafference cancellation, i.e. the action of suppressing sensory afferences caused by voluntary movements to better detect external perturbations and motor errors. Reafference cancellation can be achieved by feeding a copy of the motor command (an efference copy) into a forward model (von Holst and Mittelstaedt, 1950; Cullen, 2004; Miall and Wolpert, 1996). Efference copies and forward models can also be used to predict the consequences of arm movements on the load force at the fingertips when holding an object, to coordinate arm movements and grip forces and prevent

accidental slips (Flanagan and Wing, 1997; Flanagan et al., 1993; Johansson and Westling, 1984). The concept of grip-load-force coupling will be introduced in more details below and is at the core of the experiments conducted for this work.

The second class of internal models, the *inverse models*, refers to models that take as input a desired state (or trajectory) and compute the motor commands required to move to the desired state (Miall and Wolpert, 1996; Kawato, 1999). Inverse models can furthermore be sub-divided into inverse kinematics models, which compute intrinsinc coordinates (e.g. joint angles) from extrinsinc coordinates (e.g. hand trajectory); inverse dynamics models, which compute muscle torques from a planned sequence of joint angle; and inverse sensory output model, which compute intrinsic coordinates from sensory feedback (Miall and Wolpert, 1996; Papaxanthis et al., 1998c; Hollerbach and Flash, 1982).

Just like the forward models, the inverse models require some kind of knowledge about limb and object dynamics. Note that some computational models of motor control, for instance optimal feedback control theory, do not include an inverse model and prefer the notion of controller (Todorov, 2004; Todorov and Jordan, 2002). Optimal feedback control does include the notion of internal forward models for the process of state estimation, though.

1.3.3 The internal models of gravity

Internal models of gravity can take the form of forward models predicting gravity's effects, e.g. the acceleration of a falling object, the weight of the limbs and objects or the gravitational torques at the joints; inverse models accounting for theses effects at the stage of motor planning; or, an internal representation of body tilt relative to gravity (see Section 1.6 below). Hence, very distinct internal models of gravity are probably stored in the CNS. These internal models of gravity are essential for spatial orientation and motor planning (Pozzo et al., 1998). They would allow, for instance, to take into account gravitational torques at the planning level of arm movements in order to program appropriate muscular torques instead of compensating for gravitational torques only at the execution level by feedback control (Papaxanthis et al., 1998c).

Anticipation of gravity's effects are especially highlighted during interception of falling objects (Lacquaniti and Maioli, 1989a; Senot et al., 2005). Importantly, when asked to catch a ball "dropped" from above their head in 0-g, astronauts tend to initiate the catching arm response slightly too soon, as if they still expected the ball to accelerate because of gravity (McIntyre et al., 2001). In

virtual-reality environments, object accelerations congruent with Earth gravity are associated with activity in the insular cortex and temporoparietal junctions (Indovina et al., 2005), brain regions that are sometimes considered as the main location of the vestibular cortex involved in verticality perception (Brandt and Dieterich, 1999).

Anticipation of gravity's effects is also required to predict the consequences of self-generated movements. For instance, on Earth arm movements when standing are accompanied by muscular activity in the legs to maintain balance. A similar coordination between upper and lower limbs was observed during early exposure to microgravity although such postural adjustments are useless in 0-g (Clément et al., 1984). As we will see later, predicting gravity's effects is furthermore essential for motor coordination during object manipulation and for optimizing arm movements.

1.3.4 Adaptation

Another advantage of using internal models is that they enhance motor flexibility. In particular, they facilitate the generalization of learned skills to new contexts and the adaptation to novel limb or object dynamics.

Motor adaptation refers to the gradual modification of the motor patterns of a specific action to adapt to novel dynamics (Bastian, 2008). In scientific experiments, novel dynamics can for example take the form of a force field generated by a robotic arm or fictitious inertial forces encountered in a rotating environment, in parabolic flight or during space flight.

Adaptation can actually hide very different mechanisms (Fleury et al., 2019). One of them is the modification of an internal forward model. A leading variable for this type of adaptation is presumably the sensory prediction error (Tseng et al., 2007), i.e. the mismatch between the sensory consequences predicted by the (obsolete) forward model and the actual sensory feedback. This error can be used to re-calibrate the forward model (Bastian, 2008; Tseng et al., 2007), which allows not only to achieve the desired action in the future but also to find new trajectories that are more optimal (Izawa et al., 2008). The downside is that the re-calibration of the forward model can generate after-effects when the perturbation is removed: a period of *de*-adaptation is needed to return to baseline performance (Lackner and DiZio, 1994; Shadmehr and Mussa-Ivaldi, 1994; Nowak et al., 2004b; Martin et al., 1996). Interestingly, the times of adaptation and of de-adaptation progressively decrease following repeated exposures to the perturbation and eventually adaptation is not required any-

more (Martin et al., 1996), suggesting that a new forward model specific to the perturbation has been learned and stored, allowing rapid switching between the "old" and the new forward models (Bastian, 2008).

In microgravity, the forward models used on the ground to predict the consequences of our own actions are expected to need some kind of re-calibration, because the absence of gravitational load means that the relationship between net muscular torque and limb acceleration is changed. Experiments performed in parabolic flight suggest that the CNS accomplishes this relatively quickly (Augurelle et al., 2003a; Papaxanthis et al., 2005; Casellato et al., 2012).

Theoretically, in altered gravity the CNS should only update the predictions of limb and object dynamics, leaving the internal representations of the intrinsic properties of the limbs and manipulated objects unchanged. Whether the brain actually does that is not clear. Some results for instance suggest that the brain erroneously attributes the change in object weight to a change in object mass in hypergravity (Crevecoeur et al., 2010b, 2014).

In addition to updating forward models, the CNS must also modify the movements themselves, because movements that are optimal on Earth for a given task are not necessarily optimal in weightlessness. Such movement re-optimization has indeed been observed in parabolic flight and during space flight for arm movements (Papaxanthis et al., 2005; Gaveau et al., 2016; Mechtcheriakov et al., 2002; Crevecoeur et al., 2009b) and postural control (Clément et al., 1984; Casellato et al., 2012).

1.3.5 Neural substrates for internal models in motor control

Although the concept of internal model can be quite abstract, neural circuits satisfying the definition of an internal model have been found experimentally and/or theorized in various fields, brain regions and species.

One famous example is the mechanism of reafference cancellation studied in the weakly electric fish. This fish uses two electrosensory systems for electrolocation: a passive electrosensory system comprising electroreceptors and an active electrosensory system comprising specialized organs capable of generating electric organ discharges (Sawtell, 2016). To avoid interferences between the active and passive systems, the sensory reafferences caused by the electric organ discharges must be predicted and cancelled. A copy of the motor efference is presumably used to that end (von Holst and Mittelstaedt, 1950). Strikingly,

evidence for the existence of such efference copy and for the existence of a negative image of the sensory reafference have been found in cerebellum-like structures in the weakly electric fish (Sawtell, 2016; Bell, 1981).

In the context of upper-limb motor control in primates, one particular brain region stands out when looking for neural substrates of forward internal models: the cerebellum (Wolpert et al., 1998; Kawato, 1999; Shadmehr and Krakauer, 2008). A very popular hypothesis is that the cerebellum uses forward internal models to compute a prediction of the sensory consequences of a motor command from an efference copy. This prediction is then compared to the actual sensory feedback to compute a sensory prediction error. It has also been hypothesized that, since the sensory prediction error is represented in sensory coordinates, the cerebellum should also include inverse internal models to convert the sensory error into a motor error (Wolpert et al., 1998).

The importance of the cerebellum for movement control has long been established, as cerebellar damage can lead to great difficulties in performing smooth, accurate and well-coordinated multi-jointed movements and to tremor. Importantly, these impairments seem to affect predictive control especially, rather than reactive control (Bastian, 2006). For instance, patients with cerebellar ataxia have more difficulties to adapt to novel force fields or visuomotor perturbations, show less generalization of learned movements to new targets and little to no aftereffects when the perturbation is removed (Tseng et al., 2007; Maschke et al., 2004). Cerebellar patients also show a poorer coordination between grip force and arm movements than control subjects during object manipulation, indicating that their ability to accurately predict the consequences of voluntary arm movements is impaired (Nowak et al., 2002b; Rost et al., 2005). Finally, patients with cerebellar ataxia have been shown to suffer from an increased central vestibular noise affecting their perception of the gravitational vertical (Dakin et al., 2018), consistent with the finding of a population of cerebellar Purkinje cells that encode an estimate of the gravitational vector (Laurens et al., 2013).

Functional imaging studies and transcranial magnetic stimulation studies involving healthy participants have brought additional pieces of evidence that the cerebellum is crucial for motor predictions (see Popa and Ebner 2019 for a review). For instance, activity in the cerebellar cortex has been found to be correlated with the delay between the expected and actual somatosensory feedback following arm movements (Blakemore et al., 2001). Additionally, cerebellar activity during object manipulation in a MRI scan has been found to be consistent with the activity of a forward model computing the consequences or

arm movements (Kawato et al., 2003).

Single-unit recordings of cerebellar neurons in the monkey have furthermore shown that the cerebellum computes a mismatch between expected and actual sensory feedback during active head movements (Brooks et al., 2015). This estimation can be used to distinguish passive from active head motions (Roy and Cullen, 2004). Furthermore, the same study provided evidence that the forward models implemented in the cerebellum can be updated rapidly when the actual sensory feedback does not match the expected sensory feedback (Brooks et al., 2015).

Another brain region that has been hypothesized to incorporate forward models for sensorimotor control is the posterior parietal cortex (PPC). More precisely, this region has been associated with forward state estimation (Shadmehr and Krakauer, 2008). During arm movements, the role of PPC could be to compute a real-time estimate of hand location despite sensory delays (Desmurget et al., 1999; Mulliken et al., 2008). In agreement with this theory, fMRI studies have also suggested that PPC could be involved in the anticipatory control of fingertip forces during object manipulation (Ehrsson, 2003; Kuhtz-buschbeck et al., 2001).

Regarding the internal models of gravity, imaging studies have highlighted key brain regions whose activity could reflect the computations of an internal model simulating the effects of gravity. During an interception task involving visual motion of an object in a virtual reality environment, it was found that activity in the insula, the temporoparietal junction and the medial cerebellum was higher when the acceleration of the object was coherent with Earth gravity than when it was not (Indovina et al., 2005). Furthermore, the posterior insula (presumably part of the vestibular cortex involved in the perception of verticality and self-motion) was also more active during visually simulated vertical self-motion coherent with gravity than during vertical self-motion at constant speed or horizontal self-motion (Indovina et al., 2013).

1.4 Gravity impacts grip control during object manipulation

Thanks to its opposable thumb, its highly independent fingers and its dense population of mechanoreceptors, the human hand has developed highly dexterous skills that are particularly useful for manipulating objects. One fundamental aspect of object manipulation is the adjustment of the grasping forces

as a function of the properties of the manipulated object (mass, slipperiness, fragility) and of the inertial forces generated to move the object. We can bring a delicate *praline* to our lips as easily as a bottle of champagne and, if the situation is festive enough, can shake the latter vigorously without it slipping out of our hands. That humans can achieve complex manipulative actions in a large variety of contexts demonstrates the precision, rapidity and robustness of the sensory system but also the accuracy and flexibility of the predictive abilities of the brain which are essential for fast, smooth and reproducible movements. One crucial input to these predictive mechanisms is of course the action of gravity. In this section, we present a scientific paradigm that has been used for decades to study sensorimotor coordination in humans: the grip-load force coupling during object manipulation. We review why and how gravity must be taken into account during such tasks and summarize the results from several studies showing how finger-arm coordination adapts to new gravito-inertial environments such as hyper- and microgravity. These studies have constituted the bedrock for the experiments presented in chapters 2-4 of this work.

1.4.1 Grip-force tuning to object properties

One of the most obvious effect of gravity is that all objects have weight. This weight influences the amount of pinching force (or *grip force*) that the fingers must exert to hold the object securely.

When holding an object with a precision grip, i.e. between the thumb and index fingers, the forces applied by the fingers can be decomposed into two components (Fig. 1.3A). The first component, the normal force F_n, is perpendicular to the contact surface; the second component is the friction force F_t, tangential to the contact surface. The maximal friction force that can be applied depends on the normal force and on the static coefficient of friction μ_s of the skin-object interface, such that:

$$F_t \leq \mu_s \cdot F_n \tag{1.1}$$

If the tangential force exceeds this maximum value or, in other words, if the normal force is not high enough, slipping occurs between the skin and the object.

When the grip axis is perpendicular to gravity and the object is stationary, as is the case in Fig. 1.3, the sum of the tangential forces $\vec{F}_{t,thumb}$ and $\vec{F}_{t,index}$ applied by the thumb and index fingers must exactly compensate for the weight

of the object, while the normal forces $\vec{F}_{n,thumb}$ and $\vec{F}_{n,index}$ cancel out but ensure that sufficient friction force can be supplied on each contact surface. Typically, one refers to the sum of the tangential forces as the *load force* (LF) and to the average of the absolute values of the thumb and index normal forces as the *grip force* (GF; see Fig. 1.3B).

Under the assumption that the grip axis passes through the center of gravity of the object, the minimum amount of grip force that must be applied to prevent slipping (the *slip force*, SF) only depends on the weight of the object and on the static coefficient of friction in static conditions. The excess of applied grip force relative to the slip force defines the *safety margin*, a normalized quantity that reflects the safety margin applied to guard grasp stability against external perturbations, sensorimotor noise and prediction inaccuracies.

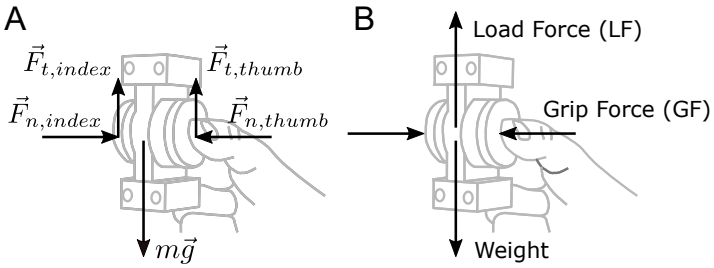

Figure 1.3 – Finger forces during static holding of an object in precision grip. A: Normal (F_n) and tangential (F_t) components of the forces applied by the thumb and index fingers. B: Grip force (GF) and load force (LF). The former is computed as the average between $||\vec{F}_{n,thumb}||$ and $||\vec{F}_{n,index}||$, the later is computed as the vectorial sum of $\vec{F}_{t,thumb}$ and $\vec{F}_{t,index}$. m, mass of the object; $\vec{g}$, gravitational acceleration.

A seminal study by Westling and Johansson (1984) has shown that, in adults, GF is finely tuned to the weight and frictional properties of the object (Fig. 1.4A), such that it is always proportional to SF (Fig. 1.4B). This fine control of GF relies on sensory inputs from mechanoreceptors (Johansson and Vallbo, 1983; Westling and Johansson, 1984; Johansson and Westling, 1984; Augurelle et al., 2003b; Witney et al., 2004) but also heavily on sensorimotor memories (internal models) of the manipulated objects, which allows to predict the weight, mass distribution and friction properties of the object to adjust GF anticipatively (Johansson and Westling, 1984, 1988a; Gordon et al., 1993). This way, a stable but economical grip is achieved.

If the grip axis does not pass through the center of gravity of the object, then the gravitational force also generates torques that can cause accidental

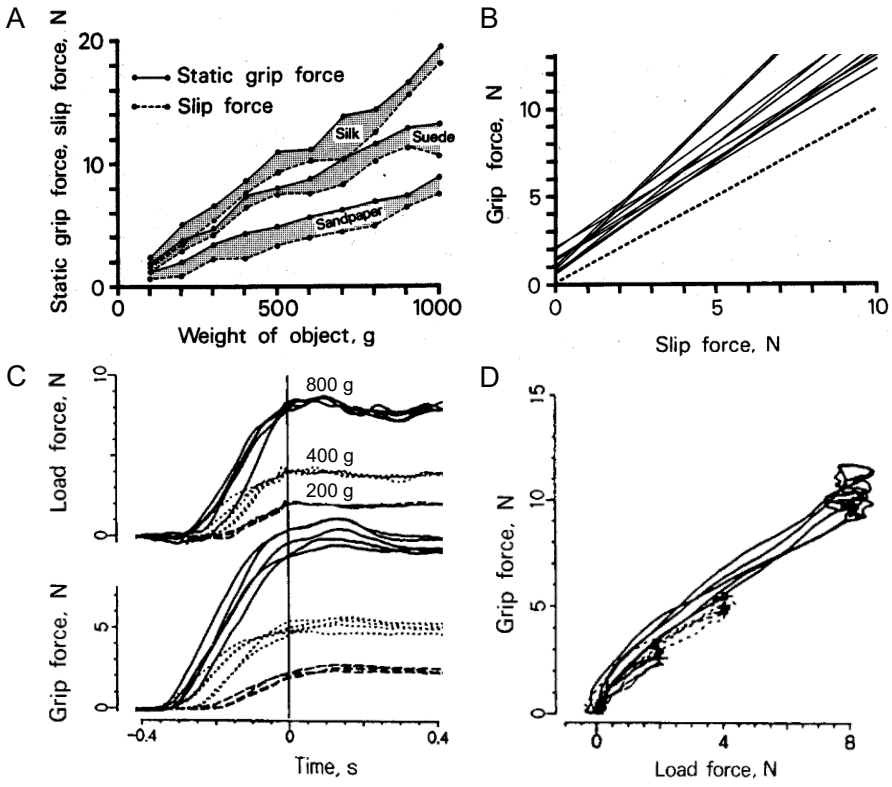

Figure 1.4 – Fine tuning of the grip force to the physical properties of the object and to the load force variations during lifting of an object held in precision grip. A: Grip force and slip force as a function of object weight during static holding, for three different surface materials. B: Linear regressions that best fit the grip-slip force relationship for ten subjects. C: temporal evolution of LF and GF during object lifting. D: GF versus LF during object lifting. A and B, adapted from Westling and Johansson 1984; C and D, adapted from Johansson and Westling 1988a.

slips during object lifting (Kinoshita et al., 1997). These gravitational torques have also been shown to be anticipated by the CNS, either by choosing contact points that minimize torques (Lukos et al., 2007) or by scaling the grip force appropriately if the contact points are imposed (Kinoshita et al., 1997; Crevecoeur et al., 2011).

Note that if the slip force at one finger is significantly different from the slip force at the other finger (because of differences in surface friction for instance), one looses important information when aggregating the forces into a LF and a GF component. Interestingly, several studies have shown that the local friction

at each individual fingertip was accounted for and the load distribution across fingers adjusted so that an adequate safety margin was maintained at each fingertip (Edin et al., 1992; Birznieks et al., 1998; Burstedt et al., 1997, 1999).

1.4.2 Grip-load force coupling during arm movements

If one starts to move the arm while holding the object, inertial forces come into play. The load force can then be computed as the vectorial sum of the gravitational and inertial forces[2]. Calling m the mass of the object and $\vec{a}$ its acceleration, we have:

$$\vec{LF} = m(\vec{a} - \vec{g}). \tag{1.2}$$

From there, it becomes obvious that the total load at the fingertips will depend on the direction of the acceleration relative to gravity. Movement direction relative to gravity must therefore be accounted for during the programming of finger forces.

When acceleration is aligned with gravity, LF varies linearly with the acceleration of the object. Upward acceleration will increase LF relative to a static condition, while downward acceleration will decrease it (as long as the absolute value of the acceleration is smaller than the gravitational acceleration). Strikingly, Johansson and Westling (1984) have shown that, during lifting of an object, GF rises synchronously with LF (Fig. 1.4C). Similarly, GF decreases in parallel with LF during replacement of the object. Consequently, an almost linear relationship is maintained between the two forces during movements (Fig. 1.4D). The absence of sensible delay in this synchronization, as well as the influence of previous lifts on the peak grip force rate, show that the coupling relies on internal forward models (Johansson and Westling, 1988a) and not solely on feedback control. The role of internal models in the planning of grip forces is further reinforced by the observation that visual feedback about object size (usually correlated with object weight) influences the anticipatory component of GF (Gordon et al., 1991; Buckingham and Goodale, 2010).

Since then, the tight coupling between GF and LF has been observed in a large variety of tasks, such as point-to-point arm movements (Flanagan and

[2]From the point-of-view of an inertial reference frame, there are no inertial forces here: only the load force and the gravitational force, which impart acceleration to the object if unbalanced. However, one can take the point-of-view of a non-inertial reference frame rigidly attached to the accelerating object. In that case, a fictitious inertial force needs to be added to Newton's second law so that the object is not accelerating relative to that reference frame. For convenience, this view is often considered when studying the coupling between GF and LF.

Wing, 1993), rhythmic arm movements (Flanagan and Wing, 1995; Gao et al., 2008), self-triggered impacts (Johansson and Westling, 1988b; Turrell et al., 1999; White et al., 2011), postural adjustments (Wing et al., 1997), locomotion (Gysin et al., 2003), jumping (Flanagan and Tresilian, 1994), etc. Importantly, the orientation of the axis of object motion relative to gravity (e.g. vertical versus horizontal movements) is taken into account during GF control (Flanagan and Wing, 1993; Crevecoeur et al., 2014).

All in all, the GF-LF paradigm appears to be a powerful tool for studying the forward models used by the brain to predict the consequences of arm movements. The quality of the GF-LF coupling can be studied as a proxy for the accuracy of these internal models. It can be characterized by means of several parameters, including: (1) the correlation coefficient between GF and LF; (2) the delay between the two force signals; (3) the GF/LF ratio; (4) the GF gain, i.e. the ratio between the amplitude of the GF modulations and the amplitude of the LF modulations. Studying how these parameters adapt as a function of movement condition, object dynamics or environmental dynamics can provide precious insights on the mechanisms used by the CNS to manipulate objects.

1.4.3 Mechanisms underlying the grip-load force coupling

As emphasized earlier, anticipatory grip control probably relies essentially on two mechanisms: sensory feedback and internal forward models. The forward models predict the consequences of self-generated arm movements and allow to adjust the grip force in anticipation to these consequences (model-based predictions). Sensory feedback allows the computation of sensory prediction errors which can be used to refine GF, update the forward models and respond to unexpected perturbations. Hence, there is a strong collaboration between the two mechanisms (Witney et al., 2004).

On the one hand, forward models are crucial for an efficient coordination between finger forces and arm movements. Reflexive grip responses to unpredictable load changes are delayed by approximately 60-70 ms relative to LF step increase (Johansson and Westling, 1988b; Turrell et al., 1999). By contrast, GF responses to predictable movement-induced load variations show typically no delay relative to these LF variations. If the consequences of arm movements cannot be accurately predicted, because the dynamics of the object have been artificially modified for instance, the GF-LF coupling is initially disrupted, with GF being delayed and excessively elevated relative to LF (Flanagan et al., 2003). During object manipulation in virtual-reality environment, incongru-

ent visual feedback about the direction of object motion can affect the GF-LF coupling, which shows that the predictive mechanisms take into account the direction of motion relative to gravity to adjust GF (Toma et al., 2020).

On the other hand, sensory feedback is necessary for an accurate control of finger forces during object manipulation, even for simple tasks that are accomplished everyday. The leading source of feedback during object manipulation is the tactile information originating from the cutaneous mechanoreceptors (Witney et al., 2004; Johansson and Vallbo, 1983). These receptors inform about the forces applied on the fingertips (Birznieks et al., 2009; Westling and Johansson, 1987), about friction (Smith and Scott, 1996; Johansson and Westling, 1984) and about partial slips (Barrea et al., 2016; Johansson and Westling, 1987a). Proprioceptive feedback from receptors in the hand and arm muscles also provides information about finger forces. If sensory feedback is blocked by local anesthesia, control of grip force is substantially impaired, even in very basic movements. This impairment is mainly characterized by an inadequate and more variable GF/LF ratio and by the occurrence of accidental slips (Augurelle et al., 2003b; Nowak et al., 2002a; Johansson and Westling, 1984). In addition, the alignment between the index and thumb fingers is less accurate, leading to additional destabilizing torques (Monzée et al., 2003). However, the temporal coupling between GF and LF is preserved. In a chronically deafferented patient, both the scaling and the timing of GF was impaired (Nowak et al., 2004a), however GF still showed modulations in response to arm movements. These studies show that a continuous input from the sensory systems is required to maintain and update the accuracy of the forward models, but that motor efferences are sufficient to elicit GF modulations.

These experiments nicely illustrate the complementary roles played by predictions and online sensory feedback in object manipulation. Predictions allow for a tight synchronization between GF and LF and anticipate the minimum GF required based on the predicted mass and frictional properties of the object; sensory feedback more finely regulates GF scaling and timing, prevent prediction errors to accumulate and is used to update the forward models. This interplay between predictions and feedback could take place at various levels of the sensorimotor system. Furthermore, the different characteristics of GF (timing, offset, gain,...) could be controlled by distinct mechanisms or even distinct brain regions (Oya et al., 2020).

The cerebellum, which is strongly associated with motor adaptation and the ability to compute sensory prediction errors and is thought to be a good candidate for the location of internal forward models (see Section 1.3.5), likely

plays an important role in GF-LF coordination. This idea was corroborated by studies investigating the GF-LF force coupling in patients with cerebellar atrophy. These patients tended to apply higher GF/LF ratios than healthy controls and to show a poorer correlation between GF and LF during movements, although the accuracy of GF timing was preserved (Nowak et al., 2002b). Other brain regions that have been suggested to play an important role in object manipulation include the primary motor and sensory areas, the ventral and dorsal premotor cortex and the posterior parietal cortex (Olivier et al., 2007; Davare, 2006; Ehrsson, 2003).

1.4.4 Alternative mechanisms for grip control

Alternative mechanisms have been put forth to explain the GF-LF coupling during arm movements without invoking internal models of limb and object dynamics (model-free mechanisms).

For instance, an automatic co-activation of arm and finger muscles during object manipulation could develop with practice and contribute to the temporal coordination between grip force and arm movements. A "grip-force" motor command could be sent automatically in parallel with any arm motor command to stabilize the object during arm movements. Unnecessary grip force adjustments have indeed been observed in subjects performing the "barman task" during which the stationary arm is loaded or unloaded without inducing changes of load force at the fingertips (Danion, 2004). Furthermore, GF modulations during rhythmic arm movements are still observed even when the subjects are instructed to apply an excessive amount of grip force such that these modulations are unnecessary (Flanagan and Wing, 1995). However, when loading the arm with a ballast (White et al., 2005) or with an elastic cord (Descoins et al., 2006), the GF/LF force ratio remains fairly similar to the ratio with no loading, despite a substantial increase in the muscular activity required to move the arm.

Another theory, called the threshold position control theory, explains the grip force modulations during arm movements by concomitant shifts in the equilibrium configuration of the arm and finger muscles. These equilibrium configurations would be calibrated by previous experience and online sensory feedback but would not rely on an internal model of the dynamics of the system (Pilon et al., 2007).

The biomechanics of the fingerpad could also contribute to the GF-LF coupling: the compression of the elastic pulp between the bone and the object

during tangential loading could increase the normal component of the finger forces in synchrony with hand acceleration (Pilon et al., 2007; Crevecoeur et al., 2017). However, anticipatory GF modulations are observed in a large variety of grip types, including the "inverted grip" where the contact surfaces are on the dorsal side of the thumb and index fingers and in which case the contribution of skin deformation is probably negligible (Flanagan and Tresilian, 1994).

Other authors suggested that the GF-LF coupling during arm movements could arise from a global modulation of the stiffness of the group of muscles responsible for the movement (Viviani and Lacquaniti, 2015). In addition, it has been shown that wrist movements can affect grip force independent of load force (Werremeyer and Cole, 1997). This is explained by the fact that the extrinsinc finger muscles cross the wrist. Consequently, activating these extrinsic muscles can produce wrist flexion torques. These muscles could thus be recruited to assist wrist movements or wrist stabilization during object manipulation, which would also have an effect on grip force and could account for a portion of the GF-LF coupling. Such contribution would however be quite low for slow movements (Werremeyer and Cole, 1997).

It is probable that at least some of the alternative mechanisms listed above contribute to the fluctuations of grip force observed during self-generated arm movements. Some experimental results are however difficult to explain without invoking internal models. For instance, delaying the visual feedback about object motion (Sarlegna et al., 2010) or providing incongruent visual feedback about movement direction (Toma et al., 2020) using a virtual-reality environment have been shown to affect grip control, strongly suggesting the use of flexible forward models incorporating the dynamics of the object and the action of gravity to predict the consequences of arm motor commands. Furthermore, the fast adaptation of grip feed-forward control to novel object dynamics (Flanagan and Wing, 1997; Diamond et al., 2015) and to novel environmental dynamics (Barbiero et al., 2017; Augurelle et al., 2003a; Nowak et al., 2004b) highlights the important contribution of flexible mechanisms to the GF-LF coupling. These latter studies are reviewed hereafter.

1.4.5 Adaptation of the grip-load force coupling to altered gravito-inertial environments

If the CNS relies on forward models to control grip force during object manipulation, one would expect the GF-LF coordination to be impaired in novel gravito-inertial environments. This is one reason why GF-LF coupling during

object manipulation is a particularly interesting paradigm to study in parabolic flights, human centrifuges and rotating chambers.

Both parabolic flight and centrifuges rely on Einstein's equivalence principle according to which gravitational forces cannot be distinguished from the fictitious forces experienced by an observer in a non-inertial reference frame (e.g. an accelerating aircraft or a rotating room). This equivalence principle justifies the use of terms such as "altered gravity", "microgravity" or "hypergravity" when referring to the conditions experienced in parabolic flight, orbital flight or centrifuges, despite the fact that gravity itself remains unchanged.

During parabolic flight maneuvers, periods of around 20 s of hypergravity can be created during the initial phase of the maneuver, during which the aircraft is accelerated upward to enter the parabolic trajectory (Fig. 1.5A; Karmali and Shelhamer 2008). During this phase, the reaction force between the aircraft floor and the participant is almost two-fold the reaction force during level flight, which from the point-of-view of the occupant is equivalent to a two-fold increase in gravitational force. During the second phase of the maneuver, which also lasts around 20 s, the aircraft and its occupants are accelerated downward with an acceleration equal to that of gravity (they are in free-fall). For the occupants inside the aircraft, the experience is equivalent to experiencing a condition of zero gravity. This is why this phase is usually called the microgravity (or zero-g) phase. The parabola ends with a new phase of hypergravity that brings the aircraft back to level flight. It should be noted that, depending on the downward acceleration of the aircraft during the parabola, intermediate values of "gravity level" can be obtained (see Chapter 2 for instance).

In human centrifuges, a gondola is rotated at relatively high speed so that a centripetal force is added to the gravitational force, creating an environment of "hypergravity" as the norm of the resulting gravito-inertial vector is greater than 1-g. Depending on the orientation of the gondola relative to the rotation axis, the orientation of the gravito-inertial vector relative to the occupant's body can also be varied, so that a sensation of tilt is induced (Mittelstaedt and Fricke, 1988). If the rotation radius is small relative to the movements performed by the participant, Coriolis effects become important and can further perturb the predictive mechanisms used by the CNS (Lackner and DiZio, 1994).

Interestingly, the temporal coupling between GF and LF appears to be conserved during the hypergravity (1.8-g) and microgravity (0-g) periods of parabolic flights (Fig. 1.5B; Nowak et al. 2001; Hermsdörfer et al. 1999; Au-

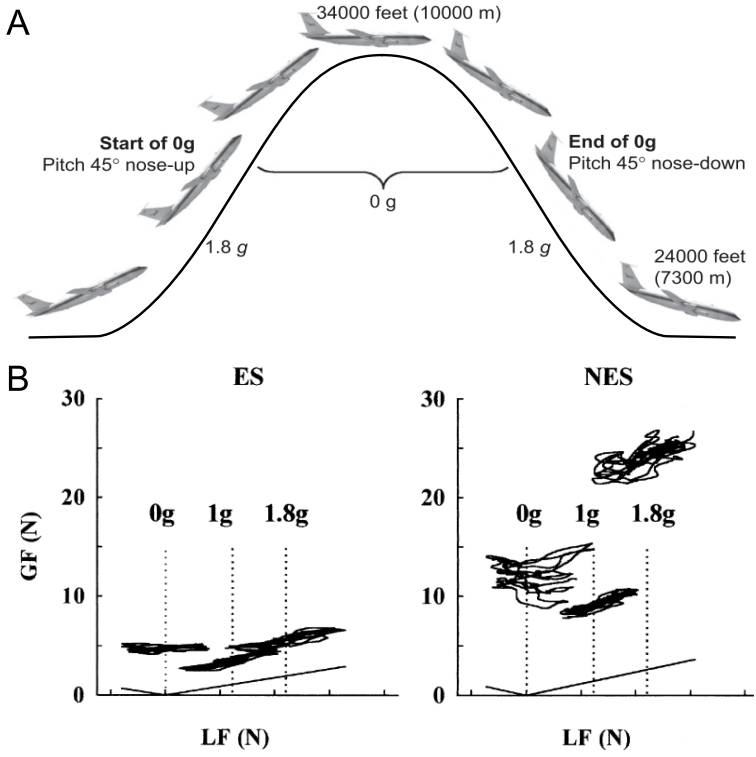

Figure 1.5 – Grip-load force coupling in parabolic flight. A: Parabolic maneuver of a reduced-gravity aircraft. B: GF versus LF during rhythmic arm movements in parabolic flights. The figure contrasts the behavior of experienced subjcets (ES) with the behavior of non-experienced subjects (NES) during the first parabola. A, adapted from Karmali and Shelhamer 2008; B, adapted from Augurelle et al. 2003b.

gurelle et al. 2003a; Crevecoeur et al. 2009a; White et al. 2005) and in the hypergravity environment created by centrifuges (Barbiero et al., 2017). The grip force even seemed to anticipate the negative LF peaks that occur during downward acceleration of the arm in 0-g (Crevecoeur et al., 2009a; Augurelle et al., 2003a). On Earth (in 1-g), such negative LF peaks only occur for downward hand accelerations that exceed the gravitational acceleration, which is rare during natural movements involving object manipulation. Some effects of the gravito-inertial level on the GF-LF coupling have however been observed.

First, participants tend to apply an excessive amount of mean GF in 0-g, at least during the first parabolas (Augurelle et al., 2003a; Crevecoeur et al., 2009a, 2010a; Nowak et al., 2001). This could be a strategy to increase the

safety margin against accidental slips to cope with a higher uncertainty surrounding LF predictions (Hadjiosif and Smith, 2015). Uncertainty about the consequences of arm movements in 0-g has been attributed to a poorer somatosensory information about object mass and friction during stationary holding (Nowak et al., 2001) and to inaccurate internal models (Crevecoeur et al., 2010a).

Second, GF modulations are much more variable during early exposure to 0-g and 1.8-g than in 1-g in non-experienced subjects (Fig. 1.5; Augurelle et al. 2003a). This could also be linked to poor predictions of LF amplitude, even though the timing of LF peaks is correctly predicted.

Finally, the GF increment for a unit increment of LF has been shown to be greater in hypergravity than in normal gravity, for both vertical and horizontal movements (Crevecoeur et al., 2010b, 2014). This suggested that the CNS may have incorrectly attributed the increase in weight to an increase in mass, thereby overestimating the inertial forces resulting from arm movements.

All in all, these results speek in favor of an important contribution of somatosensory information about tangential loads before movement onset in the control of precision grip (White et al., 2020). They also suggest that the putative forward models underlying grip control adapt very quickly to new gravito-inertial environments and/or are very flexible (White et al., 2005).

Another interesting study investigated the GF-LF coupling in participants seated in a rotating chamber and performing horizontal movements along the radial axis (Nowak et al., 2004b). This situation is very different from parabolic flights because here the gravito-inertial forces acting on the object depend on the position of the object on the movement axis (variations in ficticious centrifugal forces) and on its velocity (variations in ficticious Coriolis forces). The grip-load force coupling was initially impaired when the room was rotating, in terms of GF/LF ratio, GF timing and GF/LF correlation, but progressively improved with practice. Strikingly, after-effects were observed in the GF-LF coupling following adaptation to the rotational environment. These observations provide evidence that the forward models underlying grip control can be more sophisticated than just a "simple" mapping between arm motor command, somatosensory feedback during initial static holding and grip motor commands.

1.5 Gravity shapes hand trajectories

In the previous section, a series of studies were reviewed which indicated that an internal representation of gravity is probably used during object manipulation to coordinate finger forces and arm movements. Here we review the results of other studies performed on the ground, in parabolic flights and in Space that indicate that an internal representation of gravity is also used for arm movement planning and control. These studies motivated the development of an experiment deployed on the ISS and presented in Chapter 5.

1.5.1 Influence of gravity on arm kinematics on the ground

In the horizontal plane, hand trajectories during point-to-point arm movements are generally characterized by smooth, straight paths and symmetric bell-shaped velocity profiles that are relatively independent from movement direction, speed and load (Fig. 1.6A; Morasso 1981; Flash and Hogan 1985; Soechting and Lacquaniti 1981; Hollerbach and Flash 1982; Gentili et al. 2007). These invariant characteristics of arm movements incited some authors to hypothesize that movements are planned by the CNS in terms of kinematics expressed in extrinsic coordinates (such as hand trajectory), not in terms of joint angles or muscular torques (Morasso, 1981; Hollerbach and Flash, 1982). Kinematic constraints, such as a maximization of movement smoothness (minimum-jerk model), have been put forth to explain the invariant bell-shaped velocity profiles and straight hand paths (Flash and Hogan, 1985).

According to this hypothesis, movement trajectory would be independent of dynamic considerations such as gravitational torques and the latter would be considered as a disturbance to be compensated for. The desired trajectory would be transformed into the required muscle torques at the planning stage using inverse dynamics. This would imply that the CNS is able to anticipate upcoming interaction torques between moving segments arising from inertial, centripetal and Coriolis forces as well as upcoming gravitational torques (Hollerbach and Flash, 1982). It was nonetheless argued that movement speed and load could be changed while preserving the shape of the velocity profile by independently scaling the dynamic torques (i.e. the inertial, centripetal and Coriolis contributions to the net torque) and the gravitational torque, thereby simplifying dynamics computations (Atkeson and Hollerbach, 1985; Hollerbach and Flash, 1982).

Later, a closer look at arm movements performed in the vertical plane ques-

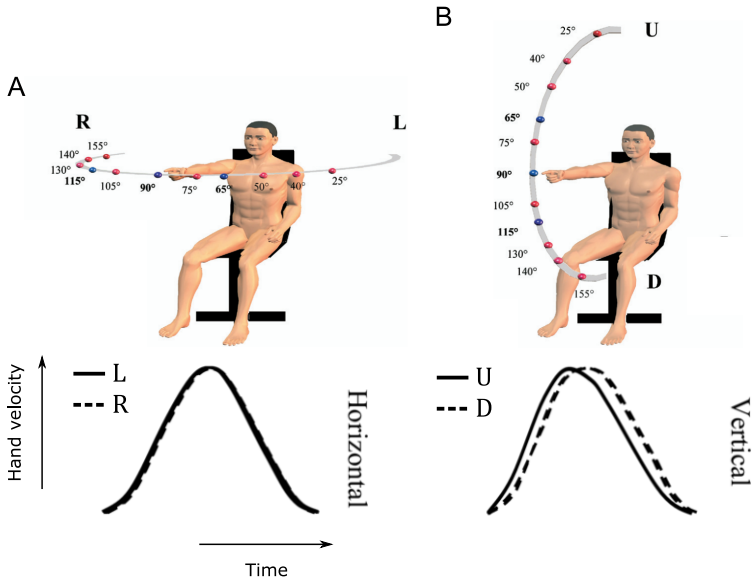

Figure 1.6 – Hand tangential velocity profiles during typical horizontal (A) and vertical (B) arm movements. L: Left; R: Right; U: Up; D: Down. Adapted from Gentili et al. 2007.

tioned this notion of an invariant shape for the velocity profile achieved by dynamics scaling. It was indeed observed that trajectories of vertical movements show a clear dependence on movement direction. For instance, during pointing and drawing tasks the velocity profiles of upward movements are more skewed than those of downward movements (Fig. 1.6B), while other parameters such as movement duration and hand path are unaffected by movement direction (Papaxanthis et al., 1998b,c; Gentili et al., 2007). Additionally, upward movements tend to be more curved than downward movements (Atkeson and Hollerbach, 1985; Papaxanthis et al., 1998a, 2003). These results indicate that gravity (a dynamic constraint) is internally represented and influences the selection of the appropriate trajectory at the planning level. Furthermore, it was hypothesized that this internal representation of gravity could be used as a reference axis for aligning different reference frames at the planning level during inverse kinematics and dynamics computations (Papaxanthis et al., 1998c). The observation that the direction dependencies of arm kinematics persist when vertical movements are performed while lying down in a reclined posture reinforced the idea that they are due specifically to gravity and not to biomechanical properties

(Le Séac'h and McIntyre, 2007).

The asymmetric velocity profiles of vertical arm movements have been explained by optimal control strategies that minimize muscle effort. Optimal control models in which an effort-related cost function is minimized have indeed reproduced these asymmetries. For instance, simulated vertical trajectories that minimize a combination of absolute work and smoothness present a skewed velocity profile and this skewness depends on movement direction (Berret et al., 2011; Gaveau et al., 2014, 2021). Optimal control models accounting for the gravitational force and minimizing a combination of control input and end-point error can also reproduce these asymmetries (Crevecoeur et al., 2009b).

During aiming tasks where accuracy is important, movement direction relative to gravity has additionally been shown to influence end-point error: downward movements are associated with larger undershooting of the target than upward or horizontal movements (Lyons et al., 2006). This can once again be explained by effort-related considerations: during downward aiming movements, the presence of gravity makes downward corrective sub-movements required when undershooting energetically less costly than upward corrective sub-movements required when overshooting (Lyons et al., 2006). This observation indicates once again that gravitational torques are anticipated during motor planning and control.

1.5.2 Adaptation of hand trajectories to altered gravito-inertial environments

Experiments conducted in parabolic flights and in orbital space flight have provided further evidence that the effects of gravity are anticipated during motor planning and control to optimize movements.

For instance, the direction-dependency of the velocity profile asymmetry initially persists during early exposure to 0-g, then progressively vanishes after repeated exposure (Papaxanthis et al., 2005; Gaveau et al., 2016). These observations suggest that the dynamics (muscle torques) adapt first, possibly via the adaptation of forward models (see Section 1.3.4), in order to reproduce the kinematics of the movements performed on Earth; then, new kinematics more appropriate to the novel gravitational background are progressively adopted (Papaxanthis et al., 2005). An optimal control model using a cost function discounting for absolute work and movement jerk has managed to reproduce the empirical results obtained in parabolic flight (Gaveau et al., 2016).

Exposure to microgravity has also been associated with slowing of arm movements, which could occur to maintain movement accuracy despite an increased uncertainty in the internal representation of limb dynamics (Mechtcheriakov et al., 2002; Crevecoeur et al., 2010a). In contrast, hypergravity has been associated with faster movements than in normal gravity, despite the increased effort required to move the arm but in agreement with optimal control predictions (Crevecoeur et al., 2009b). These results were once again seen as an indication of a central representation of gravitational torques used to optimize movements.

Results from parabolic-flight and spaceflight experiments have also indicated that proprioceptive feedback might be impaired in weightlessness, impacting movement accuracy (Fisk et al., 1993; Watt, 1997; Lackner and DiZio, 1992; Bock et al., 1992). Suggested explanations for this have included a decrease in muscle spindle gain (Lackner and DiZio, 1992), the absence of proprioceptive information originating from gravitational torque (Bringoux et al., 2003) and the development of slack in the intrafusal muscle fibers (Proske, 2019). Additionally, larger errors when pointing to remembered target locations with eyes closed in Space relative to Earth have also been attributed to disorientation rather than impaired proprioceptive feedback (Watt, 1997). This latter hyothesis has however not been tested thoroughly. Accuracy of reaching movements in Space will be examined in Chapter 5.

1.6 Gravity as a reference axis for motor planning and control

As evoked earlier, the timeless nature of the direction of the gravitational acceleration makes the latter a priceless tool for spatial orientation. Whatever the history of body motion, the upward and downward directions are always detectable once the body is static thanks to Earth gravity. This is why gravity plays an important role in building reference frames during motor planning and control. This is also why spatial orientation is so challenging in microgravity environments.

1.6.1 Reference frames in perception and motor control

A reference frame is a set of axes used to objectively and non-ambiguously define the position of an object, a limb or a goal. The notion of reference frame

is an important one in the field of perception and control since sensory signals come from peripheral organs whose orientation relative to one another and relative to gravity is not fixed. Thus, the reference frames of distinct sensory modalities (and distinct end effectors) are not necessarily aligned.

For instance, when scanning the environment with the eye, the coordinates of static objects change constantly in the retinal reference frame, while remaining unchanged in a body-centered reference frame. Conversely, during visual pursuit of a moving target, the position of the target in retinal coordinates is constant, while it varies continuously in body-centered coordinates. In both cases, the CNS can for instance use proprioceptive information from neck receptors and efference copies of oculumotor commands to disambiguate the visual information (Mittelstaedt, 1997).

To combine multiple sensory sources and coordinate sensory inputs with motor outputs, one possibility is that the CNS converts sensorimotor data into one or multiple common reference frames, the nature of which could change depending on the context (Cohen and Andersen, 2002; Zaehle et al., 2007; Angelaki and Cullen, 2008). Such a common reference frame can be a system of coordinates that represents the spatial organization of the external world and of limb movements in relation to one's own body (the retina, the head or the trunk), i.e. an *egocentric* reference frame; or, in relation to external cues, i.e. an *allocentric* reference frame (Le Séac'h et al., 2010; Zaehle et al., 2007; Tagliabue and McIntyre, 2012). On Earth, gravity obviously constitutes a prominent external cue which can be used to define the vertical axis of an allocentric reference frame. Therefore, gravity could play an important role in the alignment of reference frames for perception, motor planning and control as a complement to visual landmarks (McIntyre et al., 1998; McIntyre and Lipshits, 2008).

The perception of the gravitational vertical depends on the available sensory cues (visual, somatosensory, vestibular,...) and on the context. For instance, the subjective visual vertical can differ from the subjective postural and subjective haptic vertical (Dakin and Rosenberg, 2018). Static (Asch and Witkin, 1948; Jenkin et al., 2003) and dynamic (Dichgans et al., 1972) visual stimuli as well as somatosensory (Mittelstaedt and Fricke, 1988; Trousselard et al., 2003; Bringoux et al., 2003) and proprioceptive (Barbieri et al., 2008) stimuli affect the perception of body orientation. In addition, the subject visual vertical is often biased towards the longitudinal body axis, an effect referred to as the Aubert effect (Aubert, 1861; Mittelstaedt, 1983; Kaptein and Van Gisbergen, 2004) and that suggests the existence of interference between egocentric and

allocentric reference frames.

1.6.2 Gravitational reference frames during arm motor planning

We saw in Section 1.5.1 that optimal hand trajectories during arm movements depend on the direction of the movement relative to gravity. Furthermore, gravitational torques contribute to limb position sense (Worringham and Stelmach, 1985; Bringoux et al., 2012). It is therefore tempting to hypothesize that, during the planning and execution of arm movements, limb motion is represented in an allocentric, gravity-centered reference frame in which the vertical axis does not depend on the orientation of the body. During arm motor planning, gravity would then be considered both as a mechanical load and as a reference axis (Papaxanthis et al., 1998c). However, because most movements in everyday life are performed in an upright posture, it is also possible that limb kinematics are partly represented in an egocentric reference frame that would coincide with the gravity-centered reference frame most of the time (see Chapter 3). Moreover, directional asymmetries could have developed in the biomechanical properties of the arm themselves as a result of natural selection if these asymmetries make movements more efficient.

Le Séac'h and McIntyre (2007) examined this last possibility by asking participants to perform horizontal and vertical movements in both an upright and a reclined posture. They found that the asymmetry of the velocity profiles was consistent with an allocentric planning of kinematics when movements were performed with eyes open. This shows that this asymmetry does not stem from biomechanical asymmetries. However, when eyes were closed, the egocentric reference frame appeared to take over in the horizontal plane, suggesting that the reference frame used to define where is "up" and where is "down" at the planning stage is multimodal. Similarly, it appears that the reference frame defining the vertical and horizontal axes during visual perceptual tasks is also built by integrating information from multiple sensory sources (Dyde et al., 2006; Lipshits et al., 2005).

These results are consistent with the idea that one of the sources used to construct a sense of verticality is the internal representation of the longitudinal body axis, as suggested by the Aubert effect mentioned above. This effect leads to an underestimation of body tilt at relatively large tilt angles in the frontal plane (Aubert, 1861; Mittelstaedt, 1983; Kaptein and Van Gisbergen, 2004). This bias tends to increase with time during prolonged body tilt, as

if the credit given to egocentric cues increased with time (Tarnutzer et al., 2013; Wade, 1970; Schöne and De Haes, 1968). Interestingly, large backward tilts of the body are rather associated with an overestimation of body tilt (Ebenholtz, 1970; Bortolami et al., 2006a). During experimental tasks involving pointing movements to remembered target locations, it is expected that an erroneous internal representation of the vertical axis, caused for instance by the Aubert effect, could affect aiming accuracy[3]. This could explain why pointing movements to remembered targets are less accurate in upside-down, supine and prone postures than in an upright posture (Hondzinski et al., 2016; Smetanin, 1997).

The direction of gravity also serves as a reference axis in the context of object manipulation. As seen in Section 1.4.2, movement direction relative to gravity affects the shape of the LF profile and therefore the slip force. Interestingly, the latency of GF responses to unpredictable load perturbations has been found to be smaller when the load forces are in the direction of gravity, independent of the orientation of the hand (Häger-Ross et al., 1996). Therefore, haptic feedback about load direction plays a role in defining "up" and "down" during object manipulation.

1.6.3 Spatial orientation in altered gravito-inertial environments

Altered gravito-inertial environments provide a unique opportunity to better understand the role of gravity in defining an allocentric reference frame for spatial orientation and movement optimization. Human centrifuges are very useful in that matter as they allow to artificially change the orientation of the gravito-inertial vector. Microgravity environments, in contrast to partial- or hypergravity environments, allow to completely eliminate this gravito-inertial reference axis.

When a human subject is rotated in a centrifuge whose rotation axis is parallel to gravity, a centripetal contact force appears and combines with the ground contact force counteracting the gravitational force. The resultant force is tilted relative to gravity and relative to the longitudinal body axis if the latter is aligned with gravity. Because this resultant force is long-lasting, the CNS interprets it as being caused by a reorientation of the body relative to gravity and not by a centripetal acceleration of the body. For instance, if the subject is

[3]Reciprocally, active arm movements can influence the perception of the vertical (Fouque et al., 1999; Bringoux et al., 2004; Tani et al., 2021).

facing the axis of rotation, he/she experiences a strong illusion of being tilted backward (the somatogravic illusion) and that objects in the visual field are moving upward (the oculogravic illusion; Graybiel 1952). These illusions affect the accuracy of pointing movements to visible targets (Scotto Di Cesare et al., 2011).

Human centrifuges have been used to test the contributions of vestibular and somatosensory cues to the perception of the visual vertical (Lechner-Steinleitner et al., 1979; Mittelstaedt and Fricke, 1988). They have also been used during and after orbital space flights to study vestibular-related adaptations to microgravity (Clément et al., 2001; Hallgren et al., 2016). In microgravity, all gravitational cues, whether vestibular or somatosensory, disappear; spatial orientation is severely impaired, especially when visual feedback is precluded (Lackner and Graybiel, 1979; Clément et al., 2007; Kornilova, 1997; Carriot et al., 2004; Clément et al., 1987; Young et al., 1993). Head tilts are not detectable by the otolith organs anymore and neither are body tilts by internal or superficial mechanoreceptors. The absence of gravitational load can lead to a deconditioning of the otolith system, affecting vestibular-related reflexes upon return to Earth, making postural control very difficult (Young et al., 1984; Reschke et al., 1984; Hallgren et al., 2016; Young et al., 1993). One hypothesis is that this deconditioning is caused by a reinterpretation of the otolith signals by the brain: after adaptation to weightlessness, otolith signals would be interpreted as pure linear acceleration signals, not tilt signals (Young et al., 1984). However, in microgravity sustained centripetal accelerations generated by off-axis centrifugation are still perceived as body tilts, not linear motion (Clément et al., 2001).

Despite the loss of gravitational cues, a sense of verticality is usually maintained in weightlessness, either by using visual cues such as walls, texts or orientation of other persons, or by aligning the vertical with the longitudinal body axis (Kornilova, 1997; Lackner and Graybiel, 1979). This sense of verticality is used for instance in catching tasks in microgravity, during which objects falling from above the head are still expected to accelerate downward (McIntyre et al., 2001). Anticipation of gravity's effects along the "vertical" axis is also reflected by the direction-dependent kinematics of vertical arm movements during early exposure to microgravity (see Section 1.5.2 above).

Experiments in microgravity have also allowed to study the influence of gravity on the perception of the upright during visual perception tasks. For instance, one parabolic flight study found that the perceived direction of illumination of a shaded disk was influenced by the gravito-inertial background

(Jenkin et al., 2005). Furthermore, long-term exposure to microgravity could result in changes in the way visual and egocentric cues are combined to construct a reference frame for visual perception (Harris et al., 2017). The role of gravity in the processing and storage of visual information has also been investigated by studying the influence of body tilt and of microgravity on the oblique effect. The results showed interesting interactions between the egocentric and gravitational allocentric reference frames (Lipshits and McIntyre, 1999; Lipshits et al., 2005). While gravity influences the oblique effect on Earth, an egocentric reference frame is sufficient to elicit an oblique effect during space flight, consistent with the idea that a sense of verticality is maintained in microgravity.

1.7 Aim of this work

Although the grip-load force coupling has been studied for almost 40 years, it has not revealed all its secrets yet. Similarly, space and parabolic-flight studies related to motor control have been conducted for decades, yet the sensorimotor adaptation to altered gravity is far from being fully understood.

In particular, the following questions remain unanswered and will be addressed in this work: Can grip control adaptation to one reduced-gravity environment (such as Mars gravity) quicken adaptation to other reduced-gravity environments (such as Moon gravity)? Are the adaptation patterns of grip dynamics observed in altered gravity specific to a change in gravity level, or can they also describe adaptation to unusual body postures on Earth? What role does gravity play in defining a reference frame for grip force and trajectory planning? How is grip control adjusted after long-term exposure to microgravity?

In the framework of this thesis, we have addressed those questions by studying grip dynamics and arm kinematics in quite uncommon situations, from short periods of exposure to Mars, Moon or even "negative" gravity to months of exposure to microgravity.

- In Chapter 2, we investigate the adaptation of the GF-LF coupling in martian, lunar and micro- gravity reproduced in parabolic flight. We show that after some time of adaptation in Mars gravity, the parameters characterizing the quality of the grip-load force coupling stabilize and remain stable even when the gravitational level is subsequently changed to

Moon or micro- gravity. This might indicate that adaptation to a reduced gravitational field can quicken adaptation to other reduced gravitational fields. These results also corroborate results from previous studies that have highlighted the great flexibility of the predictive mechanisms underlying grip control.

- In Chapter 3, we ask a rather simple question: does body orientation impact the quality of the GF-LF coupling on Earth ? This question was addressed by asking participants to perform rhythmic arm movements while being upside-down. In that posture, the group of arm muscles that must be coordinated with the grip muscles is completely different from the one in the more standard upright posture. Moreover, from an egocentric perceptive, relative to the upright posture the direction of the load force reverses and its phase shifts by 180°. We show that in most participants, the tight temporal coupling between GF and LF is nevertheless preserved. This indicates that the CNS uses limb motion represented in an Earth-centered reference frame to accurately predict the consequences of movements. By contrast, hand velocity shows subtle adaptation patterns that reflect a planning in an egocentric reference frame.

In Chapters 4 and 5, we leave Earth's soil to study sensorimotor coordination in Space. These chapters present preliminary analyses of data collected on the International Space Station as part of the GRIP experiment, a set of protocols designed to study the long-term adaptation of grip dynamics and arm trajectories during object manipulation in microgravity (Thonnard et al., 2020). This experiment involves different types of arm movements performed with a manipulandum held in precision grip in a seated or supine posture. Six astronauts have so far participated in the study. They were tested prior to flight, three times during the course of their long-duration spaceflight mission and several times after their return on Earth.

- Chapter 4 examines the modulation of GF during rhythmic arm movements in various conditions of movement frequency, object mass and, of course, gravity level. We show that the grip-load force ratio and the GF-LF correlation stabilize very quickly, whether on Earth or in Space. Furthermore, the grip-load force ratio is finely tuned to take into account the LF range during the task, the load distribution between the thumb and index finger and the load direction in both gravitational contexts.

These observations highlight the efficiency of the interplay between sensory feedback and internal models during object manipulation.

- In Chapter 5, the study of grip dynamics is set aside to focus on the study of hand path during reaching arm movements in Space. Horizontal and vertical movements, performed in a seated or supine posture with eyes open or with eyes closed, are studied. We show that, without vision, gravity is crucial for movement accuracy. In Space, whatever the posture of the body and the direction of the movements, when eyes were closed hand paths tilted gradually away from the target axis. The direction of the tilt was consistently the same across participants and directions. This behavior was also observed in the supine posture on Earth. We discuss the hypothesis that these results are due to a biased subjective perception of body tilt.

The results from Chapters 2-5, their implications and limitations, are discussed in the last chapter. We furthermore expose a non-exhaustive list of open questions that could not be answered with or emerged from the data collected in the framework of this thesis. We suggest some ideas of experiments that could be conducted in the future to address those questions.

1.8 Publications and communications

Published

- **Opsomer L, Crevecoeur F, Thonnard J-L, McIntyre J, Lefèvre P.** Distinct adaptation patterns between grip dynamics and arm kinematics when the body is upside-down. *J Neurophysiol* 125: 862–874, 2021.

- **Opsomer L, Théate V, Lefèvre P, Thonnard J-L.** Dexterous Manipulation During Rhythmic Arm Movements in Mars, Moon, and Micro-Gravity. *Front Physiol* 9: 1–10, 2018.

- **Thonnard J-L, Opsomer L, Lefèvre P, Pletser V, McIntyre J.** GRIP: Dexterous Manipulation of Objects in Weightlessness. In: *Preparation of Space Experiments*, edited by Pletser V. IntechOpen, p. 1–19.

Proceedings

- **Opsomer L, Crevecoeur F., McIntyre J, Thonnard J-L, Lefèvre P.** Moving objects upside-down: the robustness of dexterous manipulation. *49th Annual Meeting of the Society for Neuroscience*, Chicago IL, 2019 (Poster presentation).
- **Opsomer L, Crevecoeur F., McIntyre J, Thonnard J-L, Lefèvre P.** Moving objects upside-down: the robustness of dexterous manipulation. *18th National Day on Biomedical Engineering*, Brussels, 2019 (Poster presentation).
- **Opsomer L, Crevecoeur F, McIntyre J, Thonnard J-L, Lefèvre P.** Multimodal reference frame during rhythmic arm movements in various body orientations with respect to gravity. *48th Annual Meeting of the Society For Neuroscience*, San Diego CA, 2018 (Poster presentation).
- **Opsomer L, Théate V, Lefèvre P, and Thonnard J-L.** Partial-gravity as an extended insight on the adaptive and learning mechanism of the CNS during rhythmic arm movements. *47th Annual Meeting of the Society For Neuroscience*, Washington DC, 2017 (Poster presentation).

Chapter 2

Grip dynamics in Mars, Moon, and micro- gravity

Published as: Opsomer L, Théate V, Lefèvre P, Thonnard J-L. Dexterous Manipulation During Rhythmic Arm Movements in Mars, Moon, and Micro-Gravity. *Front Physiol* 9: 1–10, 2018.

Predicting the consequences of one's own movements can be challenging when confronted with completely novel environmental dynamics, such as microgravity in Space. The absence of gravitational force disrupts internal models of the central nervous system (CNS) that have been tuned to the dynamics of a constant 1-g environment since birth. In the context of object manipulation, inadequate internal models produce prediction uncertainty evidenced by increases in the grip force (GF) safety margin that ensures a stable grip during unpredicted load perturbations. This margin decreases with practice in a novel environment. However, it is not clear how the CNS might react to a reduced, but non-zero, gravitational field, and if adaptation to reduced gravity might be beneficial for subsequent microgravity exposure. That is, we wondered if a transfer of learning can occur across various reduced-gravity environments. In this study, we investigated the kinematics and dynamics of vertical arm oscillations during parabolic flight maneuvers that simulate Mars gravity, Moon gravity, and microgravity, in that order. While the ratio of and the correlation between GF and load force (LF) evolved progressively with practice in Mars

gravity, these parameters stabilized much quicker to subsequently presented Moon and microgravity conditions. These data suggest that prior short-term adaptation to one reduced-gravity field facilitates the CNS's ability to update its internal model during exposure to other reduced gravity fields.

2.1 Introduction

The human central nervous system (CNS) is highly skilled in its ability to model, with great accuracy, the physics underlying bodily interactions with the world. The construction of accurate internal models enables the brain to generate appropriate motor commands and to anticipate the consequences of the resulting movements, thereby allowing rapid actions to be performed despite inevitable delays in the transmission of sensory feedback. In the context of dexterous object manipulation, such internal representations are of primary importance for fine tuning of grip force (GF) to the inertial and frictional properties of each object (Johansson and Westling, 1984, 1987a) and for feedforward modulation of that same GF to rapid fluctuations of the load force (LF) at the fingertips, including those induced by arm movements (Flanagan and Wing, 1993, 1995) or locomotion (Gysin et al., 2003). When exposed to novel dynamics, such as elastic or viscous force fields, internal models update rapidly to enable suitable adaptation of motor commands to the current context (Descoins et al., 2006; Flanagan and Wing, 1997).

On Earth, gravity is an omnipresent constraint with which our brains cope from birth. Thus, it is not surprising that our brains are able to anticipate its effects (Lacquaniti and Maioli, 1989b; McIntyre et al., 2001; Papaxanthis et al., 2003, 2005) and use it as a reference frame (Le Séac'h and McIntyre, 2007) as well as a driving force (Crevecoeur et al., 2009a; White et al., 2008) during arm movements. During object manipulation, gravitational and inertial forces are both liable to induce slippage at the fingertips. In microgravity, LF decreases by an offset equal to the weight of the object. Consequently, the minimum GF required to avoid slippage is lower when the object is weightless than it would be on the ground, and the same anti-slippage safety margin can thus be achieved with less GF. However, when confronted with a 0-g environment for the first time (in the context of parabolic flights), subjects adopt the opposite strategy: they increase GF relative to that used in 1-g (Augurelle et al., 2003a), thus producing an even greater safety margin. This initial increase in safety margin has been viewed as a strategy to cope with heightened uncertainty,

or noise, in one's ability to predict LF magnitudes (Crevecoeur et al., 2010a; Hadjiosif and Smith, 2015). With training in the new gravitational field, the GF and safety margin decrease as subjects adapt to the novel gravitational field (Hermsdörfer et al., 2000; Augurelle et al., 2003a).

It is not yet known whether experience with learning to adapt to one new gravity field can be transferred to other unknown gravity environments. We investigated this question by assessing upper-limb motor control in partial-gravity environments. Eight naive subjects were exposed successively to Mars gravity, Moon gravity, and microgravity and we analyzed data collected while each performed rhythmic vertical arm movements with a handheld object while being exposed repeatedly to short periods (20–32 s) of each gravity level during parabolic flight maneuvers. It might be that the CNS builds a new internal model that is applied solely to each new gravity environment specifically. Alternatively, the CNS may be sufficiently flexible as to benefit from the development of a prior new internal model when adapting to the gravitational accelerations of subsequent new gravitational environments. If the former possibility is true, then the adaptation times of serial gravitational environments should be similar. If the latter is true, then the adaptation times should lessen in succession.

2.2 Materials and methods

2.2.1 Participants

Eight men (22–47 years old) participated in the present experiment. All participants gave their informed consent and received approval to participate in parabolic flights from the National Center for Aerospace Medicine (class II medical examination). The experimental protocol was approved by the ESA Medical Board and by the local French Committee for Persons Protection. The experiment was carried out during the second Joint European Partial-g Parabolic Flights Campaign (JEPPFC) on board an Airbus A-300 ZERO-G aircraft. All participants were naive to parabolic flight. They were given scopolamine to prevent motion sickness.

2.2.2 Parabolic maneuvers

Each flight consisted of a sequence of 31 parabolas. Each parabola began with 20 s of hyper-gravity (1.8 g) during the pull-up phase, followed by a partial-

gravity or microgravity phase of 32 s (Mars gravity), 25 s (Moon gravity), or 20 s (microgravity). The parabola ended with a second period of hyper-gravity during the pull-out phase. The 31 parabolas were divided into three sessions of 13, 12, and 6 parabolas. The first session reproduced Mars gravity (0.38 g), the second Moon gravity (0.16 g), and the last microgravity (0-g).

2.2.3 Experimental procedure

Two participants were tested simultaneously per flight. An opaque curtain separated the two participants to prevent them from interacting. Each subject was seated in front of two visual targets (LEDs) fixed on a vertical bar 250 mm above and below shoulder level and at a distance of 800 mm from the chair back. Each subject was secured to his chair with straps (see Fig. 2.1A).

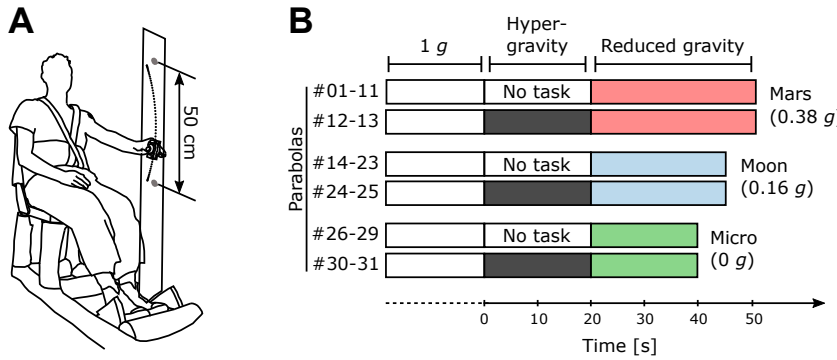

Figure 2.1 – Protocol. (A) Illustration of the experimental setup. (B) Distribution of the 31 parabolas in the protocol among the three main sessions (*Mars*, *Moon*, and *Micro*). The participants performed the task in hyper-gravity during the last two parabolas of each session.

Each subject held a 260-g manipulandum between the thumb and index finger of his right hand with his right arm extended. They were asked to perform vertical oscillations of the extended arm at their preferred pace (i.e. a pace each subject felt to be spontaneous and comfortable).

Prior to flight, the participants performed a training iteration of the experiment on the ground consisting of four blocks of at least 10 s each. Onboard the aircraft, they first performed four blocks of at least 10 s at 1-g during stationary flight, before the first parabola. Then, they performed the task during the

1-g period preceding each pull-up phase and during the reduced gravity phase of each parabola (Fig. 2.1B). During the last two parabolas of each session, the participants performed the task without interruption throughout the entire parabola, including the transition phases and the hyper-gravity phase (Fig. 2.1B). The oscillations performed during the transition phases were not analyzed. After the last parabola, the participants performed another four blocks of at least 10 s each during stationary flight.

2.2.4 Data collection

Gravitational acceleration was sampled at 800 Hz with a three-dimensional accelerometer (Analog Devices, ref. ADXL330). The three-dimensional (3D) position of the manipulandum was recorded at 200 Hz with a Codamotion tracking system (Charnwood Dynamics, Leicester, UK) and its acceleration was recorded at 800 Hz with a 3D accelerometer embedded in the manipulandum (Analog Devices, ref. ADXL330). Finally, 3D forces and torques were recorded at 800 Hz with Mini 40 force/torque transducers (ATI Industrial Automation, NC, USA) placed under each finger.

2.2.5 Data post-processing

Data post-processing was carried out with custom routines in Matlab (Mathworks, USA). Position, acceleration, and force signals were filtered with a zero phase-lag Butterworth low-pass filter of order four with cutoff frequencies of 15 Hz, 10 Hz and 15 Hz, respectively. Gravitational acceleration was filtered with the same type of filter, but with a cutoff frequency of 5 Hz.

Two forces were measured for the analysis of movement dynamics: GF exerted by the fingers normally to the contact surfaces, computed as the mean of the normal component of the forces recorded by the two force/torque sensors; and LF, that is, the vertical component of the tangential load relative to the manipulandum reference frame (see Fig. 1.3).

One oscillation cycle was defined as the period between two consecutive minima of the vertical component of velocity relative to the aircraft reference frame (i.e. the first derivative of the vertical component of the position), which corresponds to the points at which the vertical component of the acceleration crosses zero during downward arm movement. Cycles with amplitudes <20 cm were rejected (<1 % of the cycles). When the mean gravitational acceleration of one cycle was out of pre-defined bounds (in g's: *Micro*: [-0.1,0.1]; *Moon*:

[0.1,0.3]; *Mars*: [0.3,0.5]; *1-g*: [0.9,1.2]), the corresponding cycle was also rejected (<5 % of cycles per condition). Mean ± standard deviation (SD) gravitational acceleration was 0.039±0.02 g in microgravity, 0.19±0.02 g in Moon gravity, 0.40±0.03 g in Mars gravity and 1.03±0.04 g in Earth gravity.

Mean GF was computed within each cycle. To study how well GF was adjusted to LF, we computed the ratio between GF and LF for each cycle at the time of peak LF (Fig. 2.2A). GF-LF correlation within the whole block was determined by calculating the coefficient of determination (R^2) from linear regression modelling of the GF-LF relationship for positive values of LF (Fig. 2.2B). The slope α of this regression was taken as the modulation gain of GF (Fig. 2.2C).

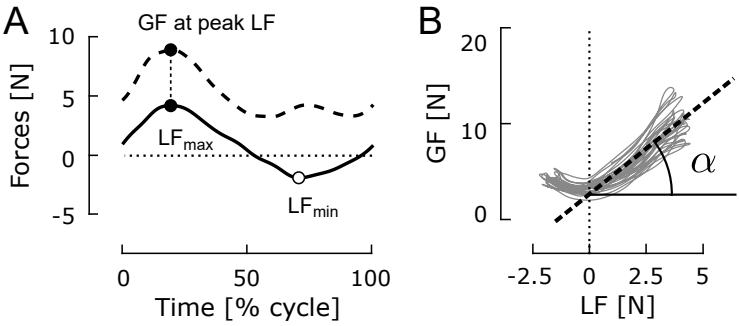

Figure 2.2 – Parameters characterizing the GF-LF coupling. (A) Typical GF and LF traces during one cycle of oscillation. (B) GF plotted against LF for one complete block (33 cycles here). The dashed line represents the linear regression computed for positive LF values with the ordinary least-squares procedure. The R^2 coefficient and slope α were computed for each block from this linear regression.

2.2.6 Statistical analysis

To analyze the participants' adaptation to each gravitational condition, the effect of the repetition of blocks was tested independently for each condition with a linear mixed-effects model, which generalizes the concept of linear regression models (Brown and Prescott, 2006). Mixed-effects models allow between-subject variability to be accounted for in terms of model intercept and slope. The (numeric) variable *Block* was considered a fixed effect, while the factor *Subject* was considered a random effect that can affect the model's intercept and slope. The variables studied were the frequency of arm oscillations, maximum and minimum LF, the mean GF during each oscillation cycle, the GF

gain α, the GF/LF ratio at the time of peak LF, and the R^2 coefficient of the linear regression between GF and LF for positive values of LF (Fig. 2.2C), computed for all cycles of one block.

Mathematically, the linear mixed-effects model with random intercept only (Model 1) can be written as

$$Y_{ij} = (b_0 + \beta_{0j}) + b_1 \cdot X_i + \epsilon_{ij}, \tag{2.1}$$

where Y_{ij} is here the value taken by the dependent variable on the i^{th} block of the j^{th} subject, X_i is the i^{th} block, $\beta_{0j} \sim \mathcal{N}(0, \sigma_0^2)$ is the random intercept associated with the factor *Subject*, b_0 and b_1 are the fixed effects, and $\epsilon_{ij} \sim \mathcal{N}(0, \sigma^2)$ are residuals. To account for between-subject variance in slope, a random slope associated with the factor *Subject*, $\beta_{1j} \sim \mathcal{N}(0, \sigma_1^2)$, was introduced into the model, yielding Model 2:

$$Y_{ij} = (b_0 + \beta_{0j}) + (b_1 + \beta_{1j}) \cdot X_i + \epsilon_{ij}. \tag{2.2}$$

Model 1 and Model 2 parameters were determined by maximum-likelihood estimation. Normal quantile-quantile plots were used to verify the normality of model residuals and random effects. We used Model 2 for all variables and conditions. The effect of block repetition (parameter b_1) was tested with Wald's t-test. Note that the last two parabolas of each gravitational condition, during which the participants performed the task throughout the entire parabolic maneuver (thus including the hypergravity and transition phases), were not included in this analysis to make sure that any trend observed across parabolas was due to task repetition and not to task performance in hypergravity or in unstable gravity levels. Including these last two parabolas does not change the conclusions though (see Appendix A). To assess whether the effect of block repetition differed significantly across participants, Models 1 and 2 were compared based on Bayesian information criterion (BIC) values and with the likelihood ratio test (Brown and Prescott, 2006). To avoid overloading the text, only the likelihood ratio test results are reported here; they were always in agreement with the BIC values.

The next step was to evaluate the effect of gravity level on movement kinematics and dynamics. Blocks pertaining to the same gravity condition and to the same subject were pooled together, unless specified otherwise. We found no evidence that performing the task in hyper-gravity (parabolas nos. 12, 13, 24, 25, 30 and 31) affected task performance in the subsequent *Mars*, *Moon*,

or *Micro* conditions (2-way repeated-measures analysis of variance (ANOVA) with the factors *Condition* and *Preceded by Hypergravity*), with the exception of movement amplitude, which was significantly smaller during these parabolas ($F_{(1,7)} = 5.64$, $p = 0.049$). Because this effect was small ($\eta^2 = 0.065$, difference in means of 2.6 mm) and did not affect peak LF, these parabolas were included in this analysis. The effect of gravity level was investigated with a one-way repeated-measures ANOVA. Generalized eta-squared is reported for effect size. Huyn-Feldt corrections were used when the condition of sphericity was violated (Mauchly's test for sphericity, 0.05 level). When the omnibus test revealed a significant effect of gravity condition, Tukey's pairwise multiple comparison test was used.

2.3 Results

Typical traces of GF plotted against LF for one subject are presented in Fig. 2.3. The first 15 cycles of the first (lightest color), third (normal color), and last (darkest color) blocks within the *1-g*, *Mars*, *Moon* and *Micro* conditions are plotted. These traces provide qualitative illustrations of the main results of this study. GF and LF show a clear correlation in each condition, from the very first block, even in microgravity. In *1-g*, LF was mainly positive and the relationship between LF and GF was essentially linear. As gravity decreased in the subsequent *Mars*, *Moon*, and *Micro* conditions, the LF values shifted towards negative values while the movement kinematics were unchanged. For negative values of LF, the correlation between the two forces became negative. Indeed, to avoid slippage of the object, GF must increase when the absolute value of the load acting on the fingertips increases, whatever the direction of the load.

There was more variance in the GF profile during early exposure to Mars gravity (light red traces) than during the last block of exposure to Mars gravity (darkest red trace). By contrast, the first block of the Moon condition presents more reproducibility in GF modulation, suggesting that the subject adapted much quicker to this second novel gravitational field. Lastly, GF appeared to be higher in microgravity than in the Mars and Moon conditions, suggesting that the subject felt the need to apply a stronger grip to avoid dropping the object, although the maximum LF did not increase in microgravity.

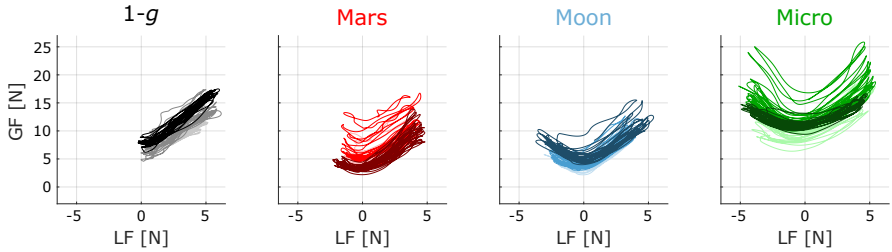

Figure 2.3 – Traces of GF versus LF for a typical subject within each condition. Lighter traces correspond to the first block, medium traces to the third block, and darker traces to the last block of the condition. Only the 15 first cycles are plotted. In the *1-g* condition, the blocks plotted are the first, third, and fourth blocks performed on board the aircraft before the first parabola.

2.3.1 Adaptation to different gravitational levels

The (vertical) amplitude of arm movement (imposed by target LEDs 50 cm apart) was 56.7±6.4 cm (Mean±SD across all participants, conditions and blocks). Movement amplitude was not affected by gravity condition ($F_{(4,28)} = 2.0$, $p = 0.12$, $\eta^2 = 0.057$) and did not evolve significantly across blocks, as revealed by the linear mixed-effects models (*Mars*: $b_1 = 1.5 \times 10^{-3}$, $t_{79} = 1.08$, $p = 0.28$; *Moon*: $b_1 = 6.0 \times 10^{-5}$, $t_{72} = 0.05$, $p = 0.96$; *Micro*: $b_1 = 1.6 \times 10^{-3}$, $t_{21} = 0.27$, $p = 0.79$).

Plots of the study cohorts' mean kinematic and dynamic variable values for each block within each condition are shown in Fig. 2.4. Regression lines that estimate the fixed effect of block repetition are plotted when the slope is significantly different from zero. Each gravity condition is detailed hereafter.

Earth gravity (1-g)

Movement pace increased significantly across the four preliminary stationary-flight blocks ($b_1 = 0.033$, $t_{23} = 4.74$, $p < 0.001$; left column in Fig. 2.4), but neither the GF/LF ratio at the time of peak LF nor the R^2 coefficient evolved significantly across these blocks ($b_1 = -0.024$, $t_{23} = -0.88$, $p = 0.39$ and $b_1 = -0.025$, $t_{23} = -1.20$, $p = 0.24$, respectively). We can therefore assume that the variables characterizing the arm-hand coordination were stable at 1-g before the task was performed in the *Mars* condition. participants also performed the task during the 1-g period preceding each parabola (not shown). Again, the variables were essentially stable across these 31 blocks ($p > 0.5$ for

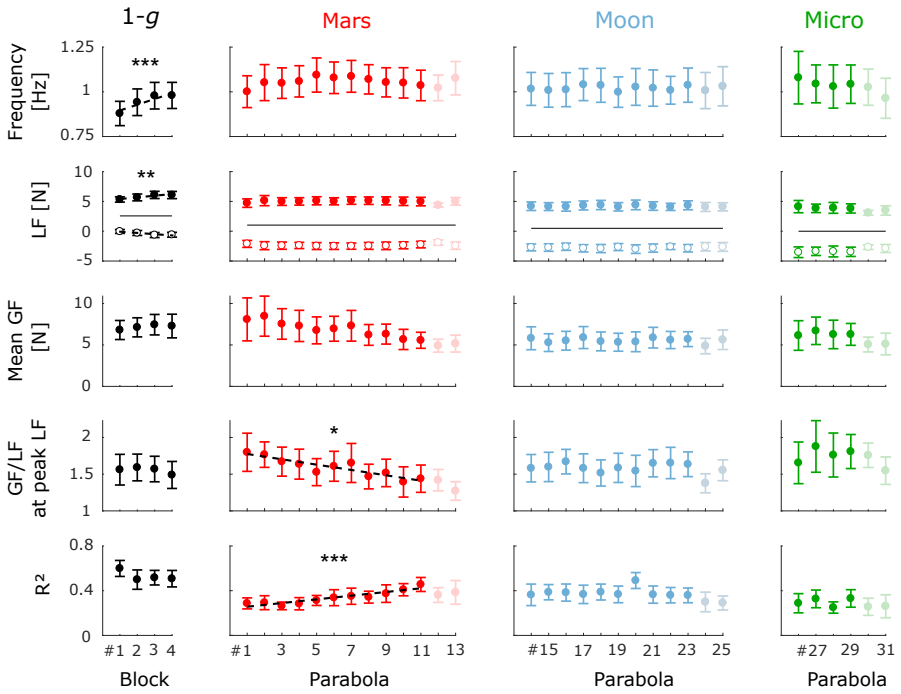

Figure 2.4 – Mean ($\pm$ standard error [$N = 8$]) kinematic and dynamic variable values by block number within each gravity condition. From top to bottom: movement frequency, LF minimum (open circles) and LF maximum (filled circles), mean GF, GF/LF ratio at the time of peak LF, and R^2 coefficient. The solid black lines in the LF plots represent the weight of the manipulandum. Blocks plotted in the *1-g* condition are the four first blocks performed onboard the aircraft. The regression lines estimated by the mixed-effects models are plotted (dashed lines) when their slope is significantly different from zero ($^{*}p < 0.05$; $^{**}p < 0.01$; $^{***}p < 0.001$). The last two parabolas of each session (faint dots), during which the participants performed the task throughout all phases of the parabola, were not included in the statistical analyses testing the effect of block repetition (see Section 2.2).

mean GF, GF/LF ratio at peak LF and R^2). Again, no effect of block number was detected after the last parabola when participants performed the task during stationary flight for the four final blocks (not shown). No differences were found between those last four blocks and the four first blocks performed in 1-g in terms of mean GF, GF/LF ratio and R^2 coefficient (paired t-test; $p > 0.4$), confirming that motor adaptation was complete after the four first blocks performed during stationary flight.

Mars gravity (0.38-g)

Because the participants performed the oscillations at their own pace, the number of cycles within each block varied across participants. In the *Mars* condition, the participants performed 32.5±8.2 oscillation cycles per block (Mean±SD).

The first block performed under Mars gravity was the first experience of reduced gravity for all participants. As expected, we observed a significant effect of block repetition on two dependent variables that characterize the dynamics of precision grip as the participants adapted to this new experience. The GF/LF ratio at the time of LF maximum decreased significantly from block 1 to block 11 ($b_1 = -0.036$, $t_{79} = -2.03$, $p < 0.05$), as depicted in Fig. 2.4, and there was a significant variance in slope across participants ($SD = 0.046$, $\chi^2_2 = 17.4$, $p < 0.001$). Estimated slopes and intercepts of the linear model for each subject are reported in Tab. 2.1. Six of the eight participants presented an overall decrease in GF/LF ratio. The linear mixed-effects model estimates that the participants decreased their GF/LF ratio by 20 %, on average, across the eleven blocks of the *Mars* condition. The decrease in the GF/LF ratio at the moment of maximum load (when risk of object slippage is greatest) indicates that motor control of the precision grip improved with time by progressively minimizing excess GF beyond that needed to ensure a stable grip. Note that the slope of the decrease in mean GF was not significantly different from zero ($b_1 = -0.265$, $t_{79} = -1.76$, $p = 0.08$) and varied significantly across participants ($SD = 0.41$, $\chi^2_2 = 64.7$, $p < 0.001$).

Table 2.1 – Estimates of slopes and intercepts for a block repetition effect on GF/LF ratio for each subject in the *Mars* condition.

Subject	Slope (b_1)	Intercept (b_0)
1	-7.6×10^{-3}	2.25
2	7.4×10^{-3}	0.86
3	−0.021	2.37
4	−0.125	2.66
5	−0.04	1.94
6	−0.069	1.50
7	7.2×10^{-3}	1.41
8	−0.041	1.46

In parallel, the correlation between GF and LF (R^2) increased significantly with block repetition ($b_1 = 0.016$, $t_{79} = 3.76$, $p < 0.001$; see last row in Fig.

2.4). The slope of the linear model did not vary significantly across participants ($SD = 7.5 \times 10^{-3}$, $\chi^2_2 = 4.49$, $p = 0.11$). From the first to the last block, R^2 increased by an average of 66 %, as estimated by the linear mixed-effects model. Because the coefficient R^2 characterizes the coordination between arm kinematics and the dynamics of prehension, the presently observed increase in R^2 may reflect an actual increase in force correlation within each cycle owing to improved arm-hand coordination. Decreased intra-block variability of the mean GF and/or GF modulation gain may also account for or contribute to the increased R^2. Additional analyses showed that none of these three possible effects were significant, suggesting that the increase in global intra-block R^2 was probably due to a combination of these three effects given that the number of oscillations performed (and selected) per block did not vary across blocks ($b_1 = -0.035$, $t_{79} = -0.14$, $p = 0.89$). Overall, these results reflect an increase in movement reproducibility as participants adapted to a new gravitational field.

In contrast, oscillation frequency (top row of Fig. 2.4) and GF modulation gain (α; not shown), did not evolve significantly across blocks in the *Mars* condition ($b_1 = 1.8 \times 10^{-3}$, $t_{79} = 0.30$, $p = 0.76$ and $b_1 = 3.8 \times 10^{-3}$, $t_{79} = 0.39$, $p = 0.69$; respectively). Again, the slope of the model varied significantly across participants (frequency: $SD = 0.016$, $\chi^2_2 = 57.0$, $p < 0.001$; α: $SD = 0.026$, $\chi^2_2 = 32.0$, $p < 0.001$).

Moon gravity (0.16-g)

In the Moon condition (parabolas 14–23), the participants performed 24.2±7.0 cycles per block (Mean±SD). Unlike the preceding *Mars* condition, there was no significant effect of block repetition on GF/LF ratio at the time of peak LF ($b_1 = 4.6 \times 10^{-5}$, $t_{72} < 0.01$, $p > 0.99$). This negative finding was consistent across all participants ($SD = 0.021$, $\chi^2_2 = 2.88$, $p = 0.24$). Moreover, the R^2 coefficient did not change significantly across blocks ($b_1 = -2.0 \times 10^{-3}$, $t_{72} = -0.53$, $p = 0.60$; $SD = 5 \times 10^{-3}$, $\chi^2_2 = 0.95$, $p = 0.62$) and we did not observe any significant effects of block repetition on any of the examined variables. This stability across blocks suggests that the participants adapted to the new gravitational field within the duration of one block (<25 s).

Microgravity (0-g)

In microgravity, the participants performed 20.1±6.5 cycles per block (Mean±SD). Even though all participants were experiencing microgravity for the very first

time, there was no significant effect of block number (parabolas 26–29) on mean GF ($b_1 = -0.063$, $t_{21} = -0.33$, $p = 0.75$), GF/LF ratio at the time of peak LF ($b_1 = 0.020$, $t_{21} = 0.46$, $p = 0.65$), or R^2 ($b_1 = 3.5 \times 10^{-3}$, $t_{21} = 0.19$, $p = 0.85$). However, the GF/LF ratio increased in microgravity, as will be emphasized below, a finding inconsistent with the conclusion that adaptation was complete after less than one block of training. Nevertheless, performance was close to that in the *Moon* condition.

2.3.2 GF adapts adequately to gravity changes

Figure 2.5 presents the effects of gravity level on frequency, mean GF, and GF/LF ratio at peak LF. Blocks from the same subject and condition were pooled, except in the *Mars* condition, where only the last six blocks (parabolas 8–13) were selected to avoid learning-phase artefacts. For the same reason, the first two blocks performed in 1-g on board the aircraft were withdrawn from the movement frequency analysis. Note that the last two parabolas of each session (where participants performed the task during the entire duration of the parabola) were included in this analysis. No effect of block repetition was found in the hyper-gravity condition; those blocks were therefore pooled as well.

Gravity level did not affect oscillation frequency ($F_{(4,28)} = 2.29$, $p = 0.84$, $\eta^2 = 0.027$). In addition to altering peak LF ($F_{(4,28)} = 57.5$, $p < 0.001$, $\eta^2 = 0.47$), gravity also had a strong effect on mean GF ($F_{(4,28)} = 20.5$, $p < 0.001$, $\eta^2 = 0.27$) and a relatively moderate effect on GF/LF ratio at the time of peak LF ($F_{(3.21,22.5)} = 3.1$, $p = 0.044$, $\eta^2 = 0.04$). Mean GF in 1-g was significantly higher than that in Mars gravity, Moon gravity, and microgravity (Tukey' s post hoc: $p < 0.05$ in all three cases) but lower than that in hyper-gravity ($p = 0.001$). Hence, mean GF was also significantly higher in hyper-gravity than in partial- and microgravity ($p < 0.001$ for the three comparisons). No differences were found in GF/LF ratio at the time of peak LF between any of the *Hyper*, *1-g*, *Mars* and *Moon* conditions, suggesting that grip control was equivalently adapted in all four conditions, after the adaptation process that occurred under Mars gravity. However, the GF/LF ratio was significantly more elevated in microgravity than in Mars gravity ($p = 0.004$).

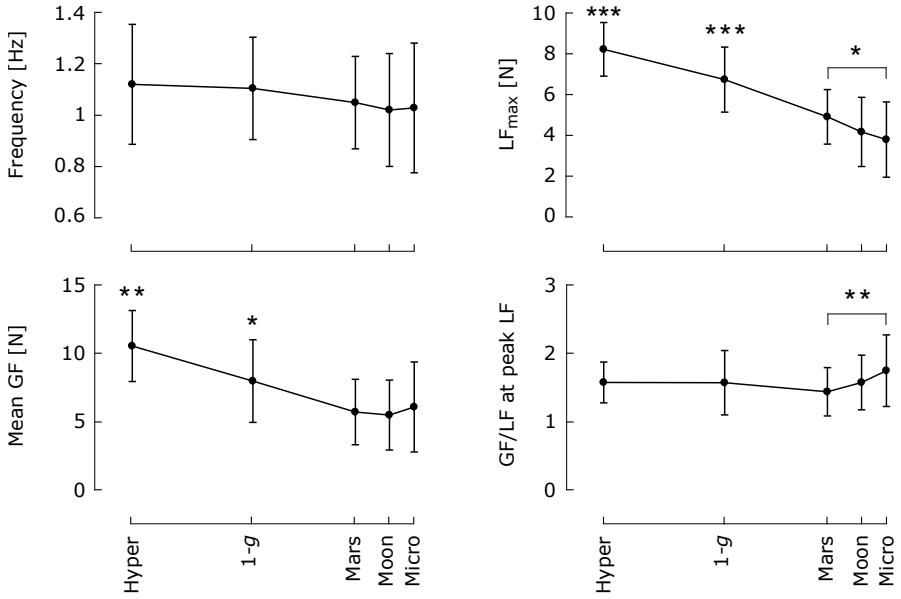

Figure 2.5 – Mean and 95-% confidence interval of the mean [$N = 8$] of frequency, maximum LF, mean GF and GF/LF ratio at the time of peak LF as a function of gravity condition. Means that differ significantly across conditions are marked with an asterisk ($^{*}p < 0.05$; $^{**}p < 0.01$; $^{***}p < 0.001$). Blocks within the same condition and subject were pooled. Only the last six blocks were selected in the *Mars* condition, and the first two blocks performed in 1-g on board the aircraft were excluded from the analysis of movement frequency.

2.4 Discussion

In this study, we found that prior (short-term) adaptation to Mars gravity quickened subsequent adaptation to Moon and 0-g environments, suggesting that the new internal model developed during exposure to Mars gravity is flexible enough to be adapted rapidly to other novel reduced gravitational fields. The rapid adaptation of the control of prehension dynamics in subsequent environments after practice is consistent with a transfer of learning from the *Mars* condition to the subsequent *Moon* and *Micro* conditions. Importantly however, in microgravity the participants applied a higher GF/LF ratio than in the *Mars* condition, producing a greater safety margin against slippage, which suggests that the adaptation to weightlessness may have been incomplete.

Although all eight participants were experiencing reduced gravity for the very first time, the temporal coupling between GF and LF and the GF modula-

tion gain adapted rapidly (in <1 parabola) to the novel environmental dynamics of the reduced gravity conditions (0.38-g, 0.16-g, and 0-g). These observations are in line with previous studies showing preserved synchronization between GF and LF during arm oscillations in weightlessness (Hermsdörfer et al., 2000; Augurelle et al., 2003a) and reinforce the view that control of average GF and GF modulation are independent (Augurelle et al., 2003b; Flanagan and Wing, 1993; Nowak et al., 2002a; Nowak and Hermsdörfer, 2003).

During the first parabola simulating Mars gravity, the participants tended to apply an excessive GF relative to the peak LF. They then learned throughout the 11-block session that they could safely loosen their grip. Similar, albeit more pronounced, practice-associated decreases in GF were observed previously in 0-g stationary holding (Hermsdörfer et al., 1999) as well as during rhythmic (Augurelle et al., 2003a) and discrete (Crevecoeur et al., 2009a, 2010a) arm movements performed while holding an object. The influence of the stress and excitement induced by an uncommon context such as parabolic flight should not be ignored given that stress-related hormones have been shown to increase in participants undergoing parabolic flight maneuvers (although only in participants that experienced motion sickness; Schneider et al. 2007). Notwithstanding, the increases in GF observed under reduced gravity conditions likely constitute a strategy to establish a higher safety margin to compensate for the uncertainty induced by an inaccurate internal model of the physics of the environment (Crevecoeur et al., 2010a). Indeed, GF control during reaching movements perturbed by a viscous force field of variable intensity was shown to be more sensitive to LF variability than to mean LF (Hadjiosif and Smith, 2015), supporting the idea that uncertainty per se favors augmentation of the safety margin against slippage. As participants integrate the dynamics of the novel environment into a new internal model, the uncertainty in load prediction should decrease, reflected by a decreasing GF/LF ratio with further task repetition. Moreover, we observed a highly significant increase in GF-LF correlation (decrease in the intra-block variance of the grip force profile) across the eleven blocks of the *Mars* condition as participants learned the dynamics of the new gravitational field, consistent with a progressive reduction in LF-prediction noise.

In contrast, and most interestingly, during the subsequent *Moon* condition, mean GF, GF/LF ratio, and GF/LF correlation were stabilized from the first parabola onward. Moreover, these variables were stable across the four microgravity blocks that followed the *Moon* condition. This is coherent with our hypothesis that there has been a transfer of learning from one environment to the

next. Although the increase in GF/LF ratio that we observed in microgravity, relative to that in Mars gravity, suggests that adaptation to microgravity might have been incomplete, it should be emphasized that the effect was quite small (+21 % vs. Mars gravity, +11 % vs. 1-g) relative to the results of Augurelle et al. (2003a), in which the safety margin (GF/LF ratio at peak LF minus half of the inverse of the coefficient of friction) was more than double that in 1-g during the first parabola in microgravity. Their protocol was similar to ours except that participants did not perform the task in partial gravity beforehand, suggesting that performing the task in a prior partial gravity attenuates this reactive increase in safety margin exhibited in weightlessness.

This contrast with the results of Augurelle et al. is a strong indication that training in partial gravity might actually be sufficient to reach the level of adaptation typically observed after 5–10 parabolas (Hermsdörfer et al., 1999; Augurelle et al., 2003a; Crevecoeur et al., 2010a, 2009a). This apparent transfer effect is not trivial given previous suggestions that when performing rhythmic arm movements in microgravity, the CNS may rely on a different motor strategy than when performing the same movements under the Earth's gravity, hyper-gravity, or partial gravity (White et al., 2008). More precisely, the presence of gravity could allow the CNS to rely on central pattern generators to produce rhythmic movements that are tuned to the resonant frequency of the arm-object system. And indeed, White et al. showed that the frequency of rhythmic arm movements is close to the estimated resonant frequency of the system. In weightlessness, however, central pattern generators can no longer rely on gravity to initiate movements and a new, higher-level strategy must be established. This change translates into a disruption of the frequency-gravity relationship in 0-g. Our results show that the implementation of this new strategy for the control of arm kinematics in microgravity does not necessarily alter the internal models used for the control of prehension dynamics, which were updated previously in the Mars and Moon gravity conditions.

Despite the apparent immediate adaptation of the participants to weightlessness, it appears that GF control may not be as finely tuned in microgravity as in Mars gravity. Indeed, GF/LF ratio at the time of maximum LF was moderately but significantly higher in the *Micro* condition than in the *Mars* condition. Generally, GF scaled to peak LF across gravity conditions, except in microgravity where mean GF was not decreased relative to the *Mars* or *Moon* conditions, leading to a slightly elevated GF/LF ratio. This divergence could mean that the adaptation to microgravity was incomplete, and that a second learning phase would be observed with longer exposure. In altered gravity,

participants tend to generate excessive isometric forces when instructed to produce forces of specific amplitude and direction (Girgenrath et al., 2005; Bock and Cheung, 1998; Mierau et al., 2008). Mierau and colleagues (2008) found no evidence that degraded segmental excitability or proprioception could explain this impoverishment in force estimation, and proposed that the cause should be looked for at a higher level. As mentioned above, Crevecoeur and colleagues (2010a) suggested that altered movement kinematics and dynamics in 0-g could be explained by elevated prediction noise. That is, our CNS may cope with greater LF uncertainty by increasing the GF safety margin (Hadjiosif and Smith, 2015). Further experiments under long-term exposure to microgravity in space should be carried out to investigate whether prediction uncertainty can be reduced to levels observed in the Earth's gravitational field. Notwithstanding, it is important to recognize that the increased safety margin in the first 0-g parabola was small (20 %) relative to the results of Augurelle and colleagues ($> 100\,\%$), and the difference was only significant compared to the Mars gravity condition.

This study had some limitations. First, during the last two parabolas of the *Mars*, *Moon*, and *Micro* sessions, the participants performed the task during the hyper-gravity phase preceding the reduced gravity phase. We cannot exclude the possibility that these trials impacted subsequent performance. However, intuitively, it makes more sense to attribute the quick motor-control adaptation in Moon gravity to the prior adaptation in Mars gravity than to practice in hyper-gravity. Second, due to restrictions inherent to parabolic flight protocols, only four microgravity blocks (after discarding the fifth and sixth blocks) were available for the analysis of motor adaptation across blocks. As a result, the statistical power of testing the effect of block repetition was reduced compared to that in the *Mars* and *Moon* conditions. Nevertheless, the constancy of the mean GF across the four blocks is striking given that previous studies showed a substantial decrease in GF over the first 5–10 blocks performed in weightlessness (Hermsdörfer et al., 1999; Augurelle et al., 2003a; Crevecoeur et al., 2010a). Third, we did not monitor participants' stress during the experiment, given the complex and invasive aspect of the measurement procedure. Schneider and colleagues (2007) observed an increase of stress-related hormones during the course of a parabolic flight but only in experiencing motion-sickness. During our experiment, two out of eight participants experienced motion-sickness, which lowers the potential impact of stress on the results. Finally, we did not account for possible variations in the coefficient of finger pad-object contact friction. The minimum GF required to avoid slippage is inversely proportional

to the static coefficient of friction; accordingly, a change in friction leads GF adjustment to maintain a constant safety margin (Johansson and Westling, 1987b). In addition, the static coefficient of friction is influenced by the applied normal force and skin moisture (Adams et al., 2007, 2013; Barrea et al., 2016; André et al., 2011; van Kuilenburg et al., 2013). Thus, it might be argued that the effect of block repetition or gravity on the GF/LF ratio may be a hidden effect of friction variation. In the present experiment though, GF at the time of peak LF exceeded 5 N for 80 % of the cycles. Generally, at that level, the influences of normal force and moisture on friction become negligible (André et al., 2009; Barrea et al., 2016). But even if the influence of friction variations cannot be entirely neglected, friction alone cannot explain the significant increase in GF-LF correlation observed in the *Mars* condition, nor the performance constancy observed in the *Moon* and *Micro* conditions.

In conclusion, our results show that experiencing partial gravity before microgravity may be sufficient to bypass the high increase in uncertainty typical of early exposure to weightlessness evidenced by the use of excessive GF. Prior exposure to partial gravity may produce a more accurate and flexible internal model, in addition to reducing stress and load-prediction noise, though that noise may remain slightly higher than in 1-g. While these results only apply to short, repeated exposures, we can speculate that if short-term exposure to Mars gravity facilitates motor adaptation to Moon gravity, long-term exposure likely does as well. One way to progress into the understanding of learning transfer across gravity levels could be to inverse the order of gravity changes: starting with 0-g, then 0.16-g and finally 0.38-g. This could help us in studying whether microgravity is indeed a "singularity" from the point of view of motor control (White et al., 2008). In addition, the current study was restrained to rhythmic movements: it would be relevant to perform a similar study with discrete movements, which are thought to rely on a higher-level control (Schaal et al., 2004). The present evidence of motor learning transfer from one partial gravity environment to another may be useful for the development of future training programs for astronauts.

Chapter 3

Distinct adaptation patterns between grip dynamics and arm kinematics when the body is upside-down

---

Published as: Opsomer L, Crevecoeur F, Thonnard J-L, McIntyre J, Lefèvre P. Distinct adaptation patterns between grip dynamics and arm kinematics when the body is upside-down. *J Neurophysiol* 125: 862–874, 2021.

In humans, practically all movements are learnt and performed in a constant gravitational field. Yet, studies on arm movements and object manipulation in parabolic flight have highlighted very fast sensorimotor adaptations to altered-gravity environments. Here, we wondered if the motor adjustments observed in those altered-gravity environments could also be observed on Earth in a situation where the body is upside-down. To address this question, we asked participants to perform rhythmic arm movements in two different body postures (right-side-up and upside-down) while holding an object in precision grip. Analyses of grip-load force coordination and of movement kinematics re-

vealed distinct adaptation patterns between grip and arm control. Grip force and load force were tightly synchronized from the first movements performed in upside-down posture, reflecting a malleable allocentric grip control. In contrast, velocity profiles showed a more progressive adaptation to the upside-down posture and reflected an egocentric planning of arm kinematics. In addition to suggesting distinct mechanisms between grip dynamics and arm kinematics for adaptation to novel contexts, these results also suggest the existence of general mechanisms underlying gravity-dependent motor adaptation that can be used for fast sensorimotor coordination across different postures on Earth and, incidentally, across different gravitational conditions in parabolic flights, in human centrifuges or in Space.

3.1 Introduction

The Central Nervous System (CNS) develops at an early age the ability to coordinate arm movements and finger forces during object manipulation (Blank et al., 2001; Forssberg et al., 1992b,a). To ensure a stable grip, the CNS must learn to synchronize grip force (GF), applied perpendicularly to the contact surfaces of the object, with the tangential load force (LF), varying as a function of the object weight and acceleration, so that any self-induced variation of load force is accompanied by a synchronized and finely tuned change of grip force. This tight coupling between GF and LF relies on accurate sensory feedback (Witney et al., 2004) and, importantly, on internal forward models that can be used to predict the sensory and physical consequences of our own actions (Blakemore et al., 1998; Flanagan and Wing, 1997). These predictive mechanisms must account for the dynamics of the environment. One crucial element of this environment is the omnipresent gravitational force. In particular, distinct directions of movement with respect to gravity can yield distinct LF profiles and therefore distinct required GF (Flanagan and Wing, 1993). In addition to impacting grip control, gravity also plays a central role in the planning of movement kinematics, as previous works have shown that the velocity profile of discrete arm movements depends on movement direction relative to gravity (Gaveau and Papaxanthis, 2011; Gentili et al., 2007; Papaxanthis et al., 1998b; Le Séac'h and McIntyre, 2007).

Quite remarkably, although the coordination between GF and LF is learnt exclusively in a constant Earth-gravity environment, the CNS has proven to be very swift in its ability to adapt dexterous manipulation control to altered-

gravity environments encountered for instance in parabolic flights or in human centrifuges. A good temporal synchronization between the two forces is usually observed within seconds of exposure to microgravity (Augurelle et al., 2003a; Hermsdörfer et al., 2000), partial gravity (see Chapter 2) or hyper-gravity (Augurelle et al., 2003a; Barbiero et al., 2017; Crevecoeur et al., 2010b; Hermsdörfer et al., 2000), suggesting flexible predictions of LF that adapt quickly to novel gravitational contexts. In contrast, adaptation of the kinematics of the movement to altered-gravity environments seems to be more progressive (Crevecoeur et al., 2009b; Gaveau et al., 2016; Papaxanthis et al., 1998a, 2005). The question arises as to whether the CNS can successfully anticipate load forces and dynamics in all terrestrials conditions or whether mechanisms of sensorimotor adaptation observed in novel gravitational contexts are also required to achieve adequate GF-LF coupling and kinematics planning in unusual circumstances such as when the body is inverted with respect to gravity.

We therefore set out to measure how GF-LF coordination and movement kinematics adapt in a situation where the body is upside-down. In particular, we ask whether the internal estimate of the direction of gravity allows for an allocentric predictive control of finger forces and arm movements, that-is-to-say a control that would use limb motion represented in an Earth-centered reference frame to accurately predict the forces acting on the arm and the fingers, regardless of the body's orientation with respect to gravity; or whether the CNS may have developed predictive mechanisms for load force and limb dynamics based on limb motions expressed in a body-centered reference frame, due to the overwhelming preponderance of movements performed when the body is aligned with gravity.

To answer this question, we asked human participants to perform rhythmic vertical arm movements with a manipulandum held in precision grip in two different body orientations: right-side-up and upside-down. During vertical arm oscillations performed in a right-side-up posture on Earth and at a moderate pace, LF acts upward on the object (towards the head) and reaches a maximum when object acceleration is maximal upward. If one performs the same movement in an upside-down body orientation relative to gravity, from an allocentric point-of-view the LF profile does not change. But from an egocentric point-of-view, LF now points towards the feet and reaches a maximum when object acceleration is maximal in the direction of the feet. We hypothesized that, if the GF-LF coupling operates in an allocentric reference frame, the quality of the coordination between the two forces should be high from the first movements performed in the upside-down posture. Indeed, by combining

all convergent sensory information indicating a reversal of the body with respect to gravity with flexible predictive mechanisms of movement dynamics, the CNS should theoretically be able to predict accurately the novel sensory consequences of a given motor command sent to the arm. Alternatively, if GF is programmed in an egocentric reference frame, the grip-load force coordination should be seriously impaired in the upside-down posture, at least during initial trials while the system adapts. In addition to the GF-LF coupling, we investigated how the kinematics of the movements adjust when the body is upside-down. Similar to the question of which reference frame is used for GF control, we studied which reference frame is used to plan direction-dependent vertical arm movements.

Our results suggest distinct adaptation processes and potentially distinct reference frames between the planning of GF and the planning of kinematics. In the upside-down body orientation, the tight temporal coupling between GF and LF was generally maintained, in agreement with the hypothesis of an allocentric control of GF. In contrast, the kinematics of the arm reflected an egocentric reference frame for trajectory planning, with a more gradual adaptation to this uncommon body posture. Furthermore, kinematics adaptation to upside-down orientation led to after-effects in the velocity profile of subsequent movements performed in right-side-up orientation, as opposed to the adaptation of GF control. These observations strengthen previous results suggesting distinct adaptation processes underlying trajectory and grip force planning (Danion et al., 2013; Flanagan et al., 2003). Furthermore, we argue that they support the hypothesis of general mechanisms underlying gravity-dependent motor adjustments that can ensure efficient sensorimotor coordination across different postures on Earth and allow for a rapid sensorimotor adaptation to novel gravitational contexts.

3.2 Materials and Methods

3.2.1 Participants

Thirty-six healthy participants took part in this study. Eighteen participants (aged 24±2.8; 10 males; 17 right-handed) participated in the first experiment and eighteen participants (aged 23.5±1.9; 10 males; 16 right-handed) participated in the second experiment. All participants were naïve with respect to the purpose of the study. The experiment was approved by the ethics committee

of the Université catholique de Louvain and all participants provided a written informed consent prior to the experiment.

3.2.2 Experimental setup

Participants were installed in a custom-built inversion chair consisting of a bucket seat (Evo XL VTR fiberglass seat, Sparco, Italy) fixed to a rotating frame (Fig. 3.1A). The rotating frame could be set at two different angles: 0° (the right-side-up (RU) posture) and 180° (the upside-down (UD) posture). The participants were securely attached to the seat with a 6-point harness (Sparco, Italy). Also fixed to the rotating frame was a target mast composed of two LED targets 32 cm apart and aligned to the longitudinal axis of the rotating frame. The position of the target mast could be adjusted along the horizontal and vertical axes to adapt to the participant's size. The participant's feet were held in place with foot straps. During the experiment, the participants held a manipulandum (mass 260 g; grip aperture 4.5 cm; Arsalis, Belgium; see Fig. 3.1B) in precision grip, i.e. between the thumb and the index finger. The cables of the manipulandum were attached to the participant's forearm with straps.

3.2.3 Procedure

Participants were instructed to perform smooth and continuous rhythmic arm movements along the vertical axis, with the arm extended and with the manipulandum held in precision grip. All participants performed the task with the right arm. Movement pace (1 Hz) was given by a metronome and movement amplitude (32 cm) was delimited by the two LED targets positioned next to the participant's hand, symmetrically above and below participant's shoulder.

Experiment 1

In Experiment 1, participants first performed three training blocks in the right-side-up posture to familiarize with the metronome pace, then performed eight blocks in a row in both the right-side-up (RU) and upside-down (UD) postures. The order of the sequence of the two postures was chosen pseudo-randomly for each participant. All blocks were identical and consisted of 25 arm oscillations at a pace of 1 Hz. A short break (lasting around 45 s for the RU condition and 90 s for the UD condition) was imposed between two consecutive blocks. The

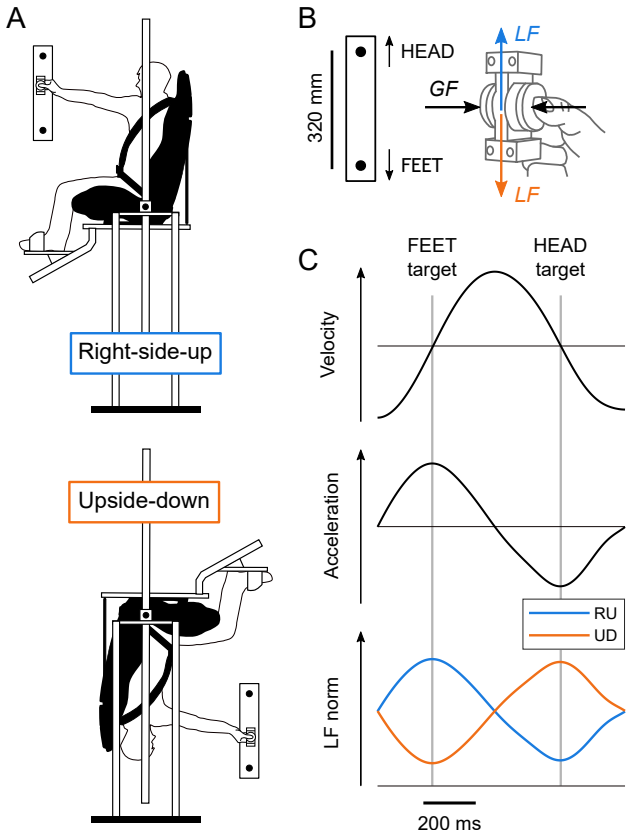

Figure 3.1 – Experimental setup. A: Participants were installed in an inversion chair that could be set in right-side-up (RU) and in upside-down (UD) posture. B: The task was performed with a manipulandum held between the right thumb and index finger. The manipulandum allowed measuring the grip force (GF), normal to the contact surface, and the load force (LF), tangential to the contact surface. C: Sketches of the vertical velocity, vertical acceleration and LF profiles during one cycle, expressed in egocentric coordinates. The horizontal lines represent the zero axis.

chair was reset back in the right-side-up posture during the break separating two blocks performed in an upside-down posture.

Experiment 2

Experiment 2 was designed to explore changes in arm kinematics over longer practice times in an upside-down posture and to assess the presence of after-effects in the right-side-up posture after repeated practice in the upside-down posture. The task was identical to Experiment 1, but the layout of the blocks

was different. Participants performed 6 blocks in the right-side-up posture (RU-PRE) followed by 16 blocks upside-down (UD) and then 10 blocks right-side-up again (RU-POST). All blocks consisted of 22 arm oscillations with the same pace (1 Hz) and the same amplitude (32 cm) as in Experiment 1. Again, the chair was reset back in the right-side-up posture between two blocks performed in an upside-down posture for a short break (2 min).

Evaluation of the slip force

In addition to the oscillation task, participants also performed a calibration task to evaluate the slip force (SF), i.e. the minimum normal force required to avoid slippage given a specific tangential force applied at the fingertip. This calibration task consisted of three blocks of 25 s during which the participant was instructed to rub the contact surfaces of the manipulandum using different levels of grip force (light, moderate and firm) and using the same finger configuration as during the oscillation task. This procedure, described in (Barrea et al., 2016), allows extracting phases during which the finger slides along the surface and the identification of the onset of these phases provides accurate measurements of the static coefficient of friction of the finger-object interface for various levels of normal force. The coefficient of friction was modelled as:

$$\mu_s = k \cdot (NF)^{n-1}, \tag{3.1}$$

where μ_s is the ratio between the tangential force (TF) and the normal force (NF) at the time of slip onset and k and n are parameters (Adams et al., 2013; Barrea et al., 2016). Because $TF = \mu_s \cdot SF$ at the time of slip onset, SF can be expressed as: $SF = (\frac{TF}{k})^{1/n}$. The fit parameters k and n in the above formula were computed using standard least-squares regression methods for the thumb and index finger of each participant and for the ulnar and radial directions separately. We also computed μ_s for a normal force of 2.25 N (typical value of the peak SF estimated during the oscillation task) using Equation 3.1 to compare the coefficient of friction in the ulnar and radial directions for both fingers. In Experiment 1, the participants performed the three blocks of the calibration task before and after each condition, thus four times in total. In Experiment 2, the participants performed the three blocks of the calibration task two times, once before and once after the 32 blocks of the oscillation task. Although the coefficient of friction can vary substantially from one subject to another, this method for computing SF can be considered reliable (Barrea et al., 2016) and the median (IQR) R-squared coefficient between the fitted SF

and the data was 0.94 (0.09) across all participants, fingers and load directions (both experiments combined).

3.2.4 Data collection

Forces applied by the fingers on the manipulandum were recorded with tridimensional force/torque sensors (Mini 40 F/T transducers, ATI Industrial Automation, NC, USA) located under each finger (see Figure 3.1B). The manipulandum was also equipped with a tridimensional accelerometer (Analog Devices, ref. ADXL78). Finally, CODA cameras (Codamotion CX-1 units, Charnwood Dynamics, Leicestershire, UK) tracked the position of four CODA active markers located on the front of the manipulandum shell. The position of the center of mass of the manipulandum was reconstructed from the position of the four markers using custom routines in Matlab.

3.2.5 Data postprocessing and analysis

All analyses were implemented in Matlab R2018a. Data signals were filtered with a dual-pass Butterworth low-pass filter of order 4. For force and accelerometer signals, a cut-off frequency of 40 Hz was used for the Butterworth filter, while for the position signal a cut-off frequency of 5 Hz was used. Signals were measured in an egocentric reference frame: the positive direction is always towards the head (HEAD direction in Fig. 3.1B) while the negative direction is always towards the feet (FEET direction).

The velocity of the manipulandum was obtained by numerical differentiation of the position. Arm movements were essentially 1-degree-of-freedom rotations around the shoulder, therefore the trajectories were slightly curved in the sagittal plane. We focused on the vertical component of the velocity, the horizontal component being on average less than ten percent of the vertical component. The peaks of the vertical component of the velocity were used to delimit individual cycles of oscillation of the arm (Fig. 3.1C). We studied the effect of body orientation on the kinematics of the movement by looking at the maxima of the vertical component of the velocity in the two movement directions (HEAD and FEET), as was done in previous studies for discrete arm movements (Gaveau et al., 2014; Gentili et al., 2007; Hondzinski et al., 2016; Papaxanthis et al., 2003, 2005). More precisely, within each cycle we computed the difference between the value of the positive peak velocity (PV_{HEAD}) and the absolute value of the negative peak velocity (PV_{FEET}). We expressed this

difference in velocity peaks (ΔPV) as a percentage of PV_{HEAD}.

The first cycle of each block was not included in the analyses of the kinematics of the arm, because we were interested in the kinematics of settled rhythmic movements. We nevertheless performed the same analyses after including the first cycle and reached the same conclusions. Note that the first cycle was included in the analysis of the finger forces, because we were particularly interested in the GF-LF coupling during the first movements performed upside-down.

The load force (LF) was defined as the norm of the force applied tangentially on the contact surfaces, computed as the vector sum of the tangential forces measured by the left and right sensors. The grip force (GF) was defined as the force applied by the fingers normally to the contact surfaces and was computed as the average of the normal force measured by the two sensors. We assessed the quality of the GF-LF coupling by computing, for each block, the Pearson correlation coefficient between GF and LF, using a sliding window of five cycles. Within each five-cycle window, we also computed the GF offset and gain, defined as the intercept and slope of the linear regression that best fits the GF-LF relationship in the least-squares sense. The lag of GF with respect to LF was computed as the time delay maximizing the cross-correlation between GF and LF within each five-cycle window. A positive value means that GF lags behind LF. As illustrated on the bottom graph of Fig. 3.1C, in an egocentric reference frame the LF profiles in the right-side-up and upside-down postures are 180° out-of-phase. A pure egocentric (predictive) control of GF would therefore yield a negative GF-LF correlation, a negative GF gain and a GF lag of half a cycle (500 ms) in the upside-down posture. Finally, we computed the grip safety margin within each cycle. The safety margin was first computed for each finger separately and was defined as the difference between the maximum value of the normal force and the maximum value of the slip force (computed as a function of the tangential force, as explained above), divided by the maximum value of the slip force. The minimum between the thumb safety margin and the index safety margin was taken as the final grip safety margin.

The left force sensor was defective for one participant in Experiment 2. For this participant, LF was computed using the accelerometer data and GF was taken as the normal force applied on the right sensor, as the difference between the left and right normal forces was small for the other participants (on average, the mean absolute difference between left and right NF was $<$ 1 N and the correlation between left and right NF was equal to 0.99). This

participant was however not included in the analysis of the safety margin, as computing the safety margin requires tangential force measurements from both force sensors.

3.2.6 Statistical analysis

In Experiment 1, we assessed the effect of body posture (RU vs. UD) on the dynamics of precision grip and on the kinematics of the arm by using linear mixed-effect (LME) models with factors *Posture* (two-level factor) and *Block* (numeric variable) as fixed effects, and a random intercept that captures inter-participants variability. To test the significance of each fixed-effect term, an F-test was used. In Experiment 2, we used paired t-tests to compare: (1) the average of the six RU-PRE blocks with the average of the first two UD blocks (UD-early); (2) UD-early with the average of the last five UD blocks (UD-late); (3) the average of the first two RU-POST blocks (RU-POST-early) with RU-PRE; and (4) RU-POST-early with the average of the last five RU-POST blocks (RU-POST-late). For all statistical tests, a significance threshold of 0.05 was used. Kolmogorov-Smirnov tests confirmed the normality of the residuals of the LME model and the normality of the differences between scores for the t-tests. All statistical analyses were performed using Matlab Statistical Toolbox.

3.3 Results

3.3.1 GF dynamics in right-side-up and upside-down body orientations

In Experiment 1, participants performed eight blocks of vertical arm oscillations in both a right-side-up and an upside-down body orientation. Movement frequency and amplitude were not significantly affected by the condition and were equal to 1.035±0.028 Hz and 36±4 cm in the RU condition (mean ± standard deviation), and 1.031±0.033 Hz and 35±4 cm in the UD condition, respectively. Participants were therefore able to follow the metronome pace (1 Hz) in both conditions. Figure 3.2 reports the GF and LF data of the first block of oscillations performed in right-side-up and upside-down body orientation by a typical participant. The phase diagram (Fig. 3.2A) illustrates that the two forces were positively correlated in both conditions. Considering all participants, we found no significant difference in the GF-LF correlation coefficient between the first

RU block and the first UD block (paired t-test: $t_{17} = -0.48$, $p = 0.63$; see Fig. 3.2C and Fig. 3.2F showing the distributions of the correlation coefficient across participants for UD and RU, resp.). This correlation coefficient was equal to 0.61 (0.49, 0.74) for RU movements and 0.64 (0.58, 0.71) for UD movements (mean + 95 % CI of the mean). The temporal traces of GF and LF during the first 10 seconds of each condition, depicted in Figures 3.2B and 3.2E, show that the two forces were furthermore tightly synchronized from the first oscillating movements. We verified that the lag between GF and LF during the first block was not significantly impacted by the posture condition ($t_{17} = 0.39$, $p = 0.70$) and was not significantly different from zero (95 % CI of the mean for RU movements: (-19, 40) ms; for UD movements: (-20, 30) ms). In both conditions, for at least 14 out of 18 participants the GF lag relative to LF was inferior to 25 ms (Fig. 3.2D and 3.2G), indicative of an immediate predictive control of GF. This still holds if one considers only the first five cycles of oscillation. A tight GF-LF coupling was therefore established very quickly in the UD condition despite the fact that, from an egocentric perspective, the direction of the load reversed relative to the RU condition and LF was phase-shifted by 180°.

When considering all blocks, the GF-LF correlation was not significantly different in the UD condition with respect to the RU condition (Fig. 3.3A). There was indeed no effect of *Posture* on the correlation coefficient ($F_{(1,283)} = 0.29$, $p = 0.59$), no effect of *Block* ($F_{(1,283)} = 0.001$, $p = 0.97$) and no significant interaction between those two factors ($F_{(1,283)} = 2.30$, $p = 0.13$). Likewise, the GF lag was not significantly impacted by body orientation (*Posture*: $F_{(1,283)} = 1.16$, $p = 0.28$; *Posture*×*Block* interaction: $F_{(1,283)} = 1.31$, $p = 0.25$) but decreased slightly across blocks ($F_{(1,283)} = 6.17$, $p = 0.01$). In contrast, the F-test revealed a significant effect of *Posture* on the GF gain (Fig. 3.3B; *Posture*: $F_{(1,283)} = 19.4$, $p < 0.001$; *Block*: $F_{(1,283)} = 3.42$, $p = 0.07$; *Posture*×*Block*: $F_{(1,283)} = 0.11$, $p = 0.74$). The GF gain was indeed more elevated in the UD condition than in the RU condition.

In addition to an increased gain, GF also presented a higher offset in the UD condition relative to the RU condition (main effect of *Posture*: $F_{(1,283)} = 100.7$, $p < 0.001$). This offset decreased across blocks in the UD condition but not in the RU condition (*Posture*×*Block* interaction: $F_{(1,283)} = 12.9, P < 0.001$). The grip safety margin (Fig. 3.3C) was also higher in the UD condition than in the RU condition (main effect of *Posture*: $F_{(1,283)} = 24.5$, $p < 0.001$) and decreased in the UD condition but not in the RU condition (*Posture*×*Block*: $F_{(1,283)} = 10.0$, $p = 0.002$). Importantly, after practice the safety margin was

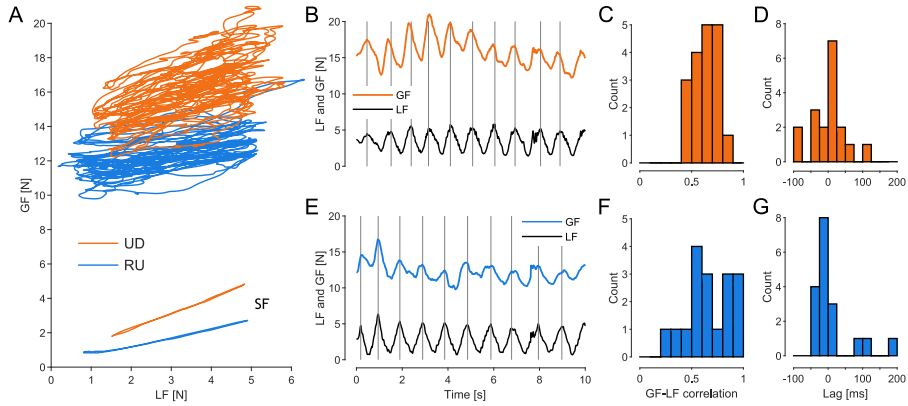

Figure 3.2 – Experiment 1: Grip dynamics during the first block performed in right-side-up and upside-down body orientations. A: GF versus LF for one typical participant (S9) during the RU (dotted line) and UD (plain line) conditions. The SF curves were averaged across all movement cycles. This participant started with the UD condition. B,E: GF and LF during the first ten seconds performed in the UD (B) and in RU (E) conditions for the same participant as in (A). Grey vertical lines represent the times of peak LF. C,F: Histograms showing the distributions of the GF-LF correlation coefficient across participants during the first block performed in the UD (C) and RU (F) conditions. D,G: Histograms showing the distributions of the GF lag (w.r.t. LF) across participants, during the first block performed in each condition

similar in the two body postures (paired t-test comparing the last two blocks of each condition: $t_{17} = -0.12$, $p = 0.90$) despite the fact that the GF offset and gain remained more elevated in the UD condition ($t_{17} = -4.69$, $p < 0.001$ and $t_{17} = -3.65$,$p = 0.002$, resp.). This is explained by the fact that the slip force was more elevated in the UD condition than in the RU condition (main effect of *Posture*: $F_{(1,283)} = 20.0$, $p < 0.001$; see example traces in Fig. 3.2A), for two reasons. The first reason is that the load force was not distributed equally on the two fingers in the UD condition: it was more elevated on the index finger side than on the thumb side. This was due to a misalignment of the centers of pressure of the two fingers in the upside-down posture. The second reason was that the coefficient of friction of the index finger was smaller in the radial (HEAD) direction relative to the coefficient of friction in the ulnar (FEET) direction ($t_{17} = 4.97$, $p < 0.001$; see Section 3.2). These two reasons both tend to increase the slip force, and therefore decrease the safety margin for a given grip force, on the index finger side in the UD condition.

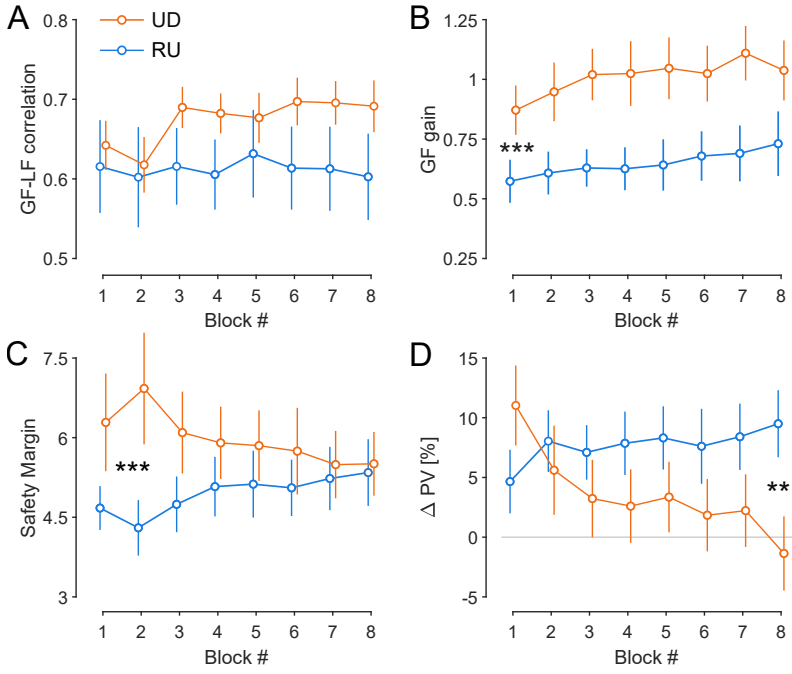

Figure 3.3 – Summary results from Experiment 1: GF-LF correlation coefficient (A), GF gain (B), Safety Margin (C) and ΔPV (D) across blocks in the UD and RU conditions (mean ± standard error). Asterisks show significant main effects of *Posture* ($^{**}p < 0.01$; $^{***}p < 0.001$).

3.3.2 Movement kinematics in right-side-up and upside-down body orientations

To investigate the impact of body posture on the kinematics of the movement, we looked at the dependence of the velocity profile on movement direction (Papaxanthis et al., 2005) by computing the difference ΔPV between the positive velocity peaks (PV_{HEAD}) and the absolute value of the negative peaks (PV_{FEET}). We express this difference as a percentage of PV_{HEAD}. Note that with such a convention, this asymmetry index is expressed in an egocentric reference frame. Figure 3.3D presents the evolution of ΔPV across blocks within each condition. ΔPV was positive in the right-side-up posture, meaning that PV_{HEAD} was on average greater than PV_{FEET}. In the upside-down posture, ΔPV showed a substantial evolution across blocks: it started higher relative to the RU condition, meaning that the difference between PV_{HEAD} (where the HEAD direction is now the downward direction with respect to

gravity) and PV_{FEET} (where the FEET direction is now the upward direction with respect to gravity) was increased. Thus, the asymmetry of the velocity profile was initially in the same direction in both conditions, when seen from an egocentric perspective. Strikingly, with practice this asymmetry progressively decreased in the UD condition. The statistical analysis confirmed those observations. The LME model revealed a significant main effect of *Posture* ($F_{(1,281)} = 8.60$, $p = 0.003$) as well as a significant main effect of *Block* ($F_{(1,281)} = 4.54$, $p = 0.03$) on ΔPV. Importantly, there was a large interaction effect between *Posture* and *Block* ($F_{(1,281)} = 36.8$, $p < 0.001$). This interaction confirms that, across blocks, ΔPV evolved in opposite directions in the RU and UD conditions. The asymmetry in the velocity profile increased with practice in the right-side-up posture, while it decreased with practice in the upside-down posture. Note that at the end of the eight blocks, the RU and UD asymmetries were not mirror image of each other, as one might expect if the kinematics were planned in a pure gravity-centered reference frame. We stated two hypotheses to explain that: (1) the asymmetry is different in the upside-down posture relative to the right-side-up posture because the muscles involved are different; or (2) the practice time was too short for a complete adaptation. The latter hypothesis motivated us to design a second experiment with an increased number of blocks.

3.3.3 GF dynamics in right-side-up orientation after repeated practice in upside-down orientation

In Experiment 2, participants performed six blocks in the right-side-up posture (RU-PRE condition), before performing 16 blocks in the upside-down posture (UD condition). The participants then performed 10 blocks back in the right-side-up posture (RU-POST condition) so that we could probe the presence of after-effects potentially induced by a motor adaptation to the upside-down posture. We first analyze GF-LF coupling, compare the results with those of Experiment 1 and check whether practice in the UD condition led to after-effects in the control of GF in the subsequent RU-POST condition.

In terms of grip dynamics, most participants reproduced the results observed in Experiment 1. More specifically, the GF was positively correlated with LF from the first movements performed in the UD condition (see participant S6 in Fig. 3.4 and averaged data in Fig. 3.5A). Interestingly though, in Experiment 2 there was an initial decrease in the GF-LF correlation during the first UD block (Fig. 3.5A). This decrease was not significant (RU-PRE vs.

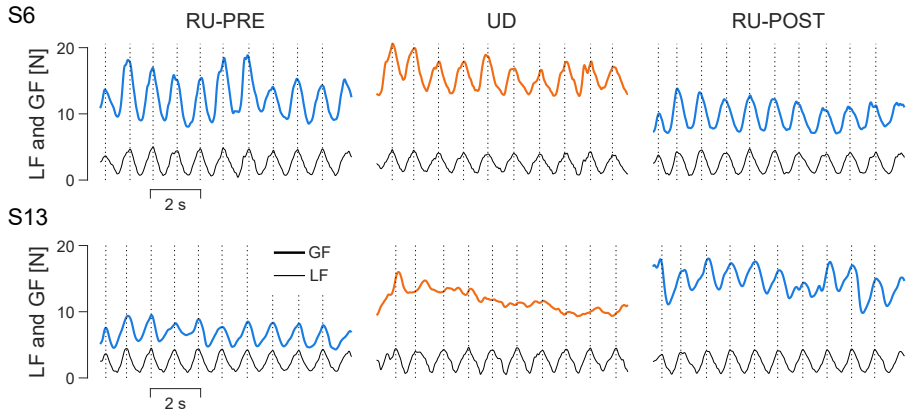

Figure 3.4 – GF and LF traces for two participants (S6 and S13) displaying distinct behaviors in terms of GF-LF coupling in the upside-down posture in Experiment 2. On the left: the last RU-PRE block; in the center: the first UD block; on the right: the first RU-POST block. For clarity, only the first 10 seconds of each block are plotted.

UD-early: $t_{17} = 1.88$, $p = 0.08$), but the correlation coefficient significantly increased with further practice in the UD condition (UD-early vs. UD-late: $t_{17} = -3.45$, $p = 0.003$) and regained the baseline value. The GF gain tended to increase across blocks (UD-early vs. UD-late: $t_{17} = -2.51$, $p = 0.02$), which probably contributed to the increase in the GF-LF correlation. For instance, participant S13 displayed a reduced GF gain and an out-of-phase modulation of GF during early blocks in upside-down posture (Fig. 3.4, bottom row, middle column), two phenomena that tend to decrease the correlation between GF and LF. This participant actually had a negative GF-LF correlation during the first UD block. It is noteworthy that this participant started feeling sick after a few blocks performed in the upside-down posture.

As in Experiment 1, the GF offset was significantly more elevated in the UD condition than in the preceding RU condition, both at the beginning (RU-PRE vs. UD-early: $t_{17} = -7.33$, $p < 0.001$) and at the end (RU-PRE vs. UD-late: $t_{17} = -2.47$, $p = 0.02$) of the sixteen-block sequence. Moreover, it decreased significantly across UD blocks (UD-early vs. UD-late: $t_{17} = 5.55$, $p < 0.001$). However, we found no significant difference between the RU-PRE safety margin and the UD safety margin, although the safety margin decreased significantly across UD blocks (UD-early vs. UD-late: $t_{17} = 2.58$, $p = 0.02$). As in Experiment 1, the increased GF offset in the upside-down posture compensated an increased in the peak SF (RU vs. UD: $t_{17} = -2.87$,

$p = 0.01$) that was due to an unequal distribution of the load force on the two fingers and to a smaller coefficient of friction for the index finger in the upside-down posture relative to the right-side-up posture (RU vs. UD: $t_{17} = 4.21$, $p < 0.001$).

We now compare the RU-PRE condition with the RU-POST condition to test whether repeated practice in an upside-down posture has an impact on the control of grip force in movements performed subsequently in a right-side-up posture. The typical traces in Figure 3.4 depict very similar temporal coupling between the first block of the RU-POST condition and the last block of the RU-PRE condition. The averaged data depicted in Figure 3.5A-C confirm this observation. We found no significant difference between the first blocks of the RU-POST condition and the mean of the RU-PRE blocks in terms of GF-LF correlation (Fig. 3.5A), GF offset, GF gain (Fig. 3.5B), safety margin (Fig. 3.5C) and GF lag (RU-PRE vs. RU-POST-early; $p > 0.2$ for all comparisons). In terms of GF dynamics, participants were therefore able to switch back rapidly to the "right-side-up" LF model after the 16 blocks in the upside-down posture. We show hereafter that the movement kinematics tell a different story.

3.3.4 Movement kinematics in right-side-up orientation after repeated practice in upside-down orientation

The kinematics observed in Experiment 2 were consistent with the results of Experiment 1 (Figure 3.5D). In the UD condition, ΔPV was initially similar to the RU-PRE condition from an egocentric point-of-view (RU-PRE vs. UD-early: $t_{17} = 0.59$, $p = 0.56$), but then decreased significantly across blocks (UD-early vs. UD-late: $t_{17} = 3.52$, $p = 0.003$). In contrast to Experiment 1, ΔPV actually reversed with respect to the RU asymmetry after some practice. Importantly, the RU-POST condition allowed us to detect the presence of after-effects induced by the adaptation to the upside-down posture. Indeed, ΔPV at the beginning of the RU-POST condition was significantly smaller than during the RU-PRE condition (RU-PRE vs. RU-POST-early: $t_{17} = -2.76$, $p = 0.01$). In contrast, the difference between the first blocks of the RU-POST condition and last blocks of the UD condition was smaller and not significant (UD-late vs. RU-POST-early: $t_{17} = -1.52$, $p = 0.15$). ΔPV then increased significantly (decreased in absolute value) with more practice in the right-side-up posture (RU-POST-early vs. RU-POST-late: $t_{17} = -2.45$, $p = 0.02$) and returned to baseline (RU-PRE vs. RU-POST-late: $t_{17} = 1.31$, $p = 0.21$).

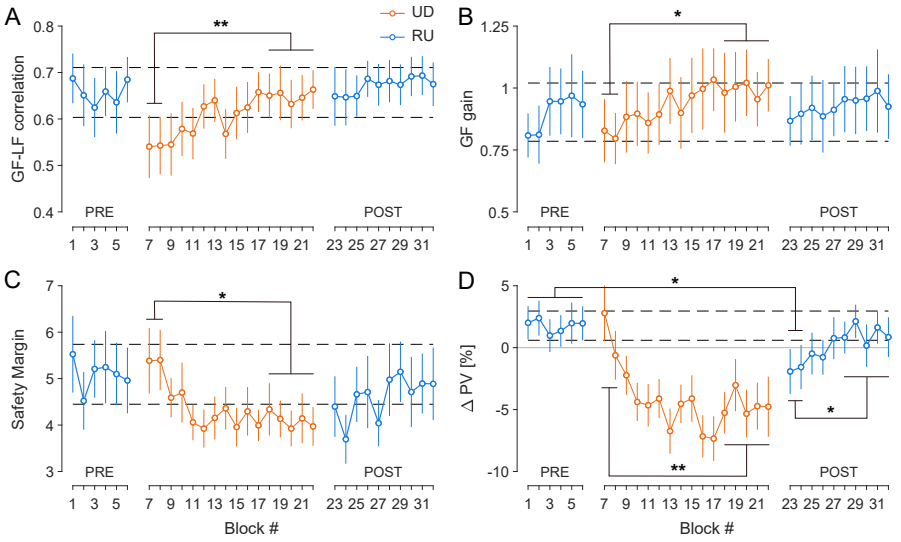

Figure 3.5 – Experiment 2: Arm kinematics, but not grip dynamics, are affected after practice in an upside-down posture. A: GF-LF correlation; B: GF gain; C: GF safety margin; D: ΔPV across blocks (mean ± standard error). Dashed horizontal lines representing the mean of the RU-PRE condition ± standard error were plotted to facilitate the comparison between the RU-PRE and RU-POST conditions. $^{*}p < 0.05$; $^{**}p < 0.01$; $^{***}p < 0.001$.

3.4 Discussion

In the present study, we challenged the ability of the brain to use an internal estimate of the gravitational force for GF and kinematics programming by asking participants to perform rhythmic arm movements in an upside-down posture, while holding an object in precision grip. Our main goal was to investigate the reference frame in which the control of grip force and arm movement operates in upside-down condition: is it a body-centered (egocentric) reference frame, or an Earth-centered (allocentric) reference frame?

3.4.1 GF-LF coupling reflects an allocentric control of grip force

A particular attention was given to the quality of the GF-LF coupling, characterized firstly by the correlation coefficient and the time lag between the two forces. For most participants, we found very similar correlation coefficients and time lags in both body orientations, even when focusing on the first cycles

performed in each condition. These observations indicate that the mechanism responsible for GF-LF coordination operates in an allocentric reference frame in which gravity defines "up" and "down". If GF was planned in an egocentric reference frame, we would have observed a negative GF-LF correlation coefficient (180° phase-shift) for the first movements performed upside-down, or at least a high time lag between GF and LF reflecting a dominant feedback control. Previous work has emphasized flexible coordination patterns across conditions of loading and movement kinematics (White, 2015; Zatsiorsky et al., 2005). Here we provide evidence that this flexibility also enables humans to fine-tune grip-load coupling when the body configuration changes relative to gravity. Because the muscles involved in the generation of single-joint, vertical arm movements in the upside-down body orientation (predominantly the latissimus dorsi, teres major and posterior deltoid) are very different from those involved in the right-side-up body orientation (predominantly the pectoralis major and anterior deltoid), the hypothesis that GF-LF coupling would stem from an automatic activation of the finger muscles (in particular, the FDI muscle) following activation of the arm muscle is not plausible. We suggest instead, as it has been suggested by several authors in the past (Augurelle et al., 2003a; Blakemore et al., 1998; Crevecoeur et al., 2009a; Flanagan and Wing, 1997; White et al., 2005), that the robustness of the GF-LF coupling is due to the existence of a flexible internal model of LF that accounts for gravity. We hypothesize that the flexibility of these predictive mechanisms has arisen from the necessity for the CNS to coordinate fingers force and arm movement along various movement directions and in various body postures. This could be accomplished with the help of an Earth-centered parametric forward model (McNamee and Wolpert, 2019; White et al., 2020) where the value of the gravitational force along the movement axis can be adjusted according to movement direction. As a by-product, such internal parametric model would allow for a fast adaptation of sensorimotor coordination to altered-gravity environments (White et al., 2020). Very fast adaptation of GF control has indeed been observed in parabolic flights in microgravity (Augurelle et al., 2003a; Crevecoeur et al., 2009a; Hermsdörfer et al., 2000), partial gravity (Opsomer et al., 2018) and hyper-gravity (Augurelle et al., 2003a; Crevecoeur et al., 2010b) as well as in the hyper-gravity environment of human centrifuges (Barbiero et al., 2017; White et al., 2018). In contrast, feedforward control of GF needs time to adapt when moving objects with unfamiliar dynamics such as elastic or viscous loads (Danion et al., 2013; Danion and Sarlegna, 2007; Diamond et al., 2015; Hadjiosif and Smith, 2015).

Interestingly, not all participants showed equal grip force adaptation to inverted body orientation. As emphasized in Experiment 2, some participants showed in the UD condition a substantial decrease in the GF-LF correlation, mainly due to a decrease in the amplitude of the GF modulation and, in some rare cases, to a substantial increase in the temporal delay between GF and LF. This is a strong indication that sensory feedback informing about the amplitude and direction of the tangential load at the fingertip, already available before the beginning of the movement, is not sufficient in itself to allow for an efficient coupling between GF and LF for these participants. Rather, this sensory feedback must be complemented with accurate predictive mechanisms. Particularly noteworthy is the fact that the GF-LF correlation improved significantly with practice and returned to baseline on average (see Figure 3.5A), showing that an initially poor prediction of LF can become rapidly more accurate. Such signs of initial impairment of the GF-LF coupling followed by rapid adaptation were observed during rhythmic and discrete arm movements performed in parabolic flights (Augurelle et al., 2003a; Crevecoeur et al., 2010a; Opsomer et al., 2018), in short-arm human centrifuges (Barbiero et al., 2017) and in rotating chambers (Nowak et al., 2004b). The latter is however a particular case, as rotating environments induce inertial centrifugal and Coriolis forces that vary as a function of hand position and speed and thus differ greatly from the constant action of gravity. Sensorimotor adaptation to a rotating environment can actually lead to observable after-effects in the GF-LF coupling (Nowak et al., 2004b). The fact that we did not observe any after-effects in the GF-LF coupling in right-side-up orientation after practice in upside-down orientation (Experiment 2) suggests once again that an internal estimate of gravity allows switching from one posture to the next, without the need to activate or generate a new internal model of LF.

Another similarity observed between our results in the inversion chair and parabolic flight results was the greater GF offset observed in the upside-down relatively to the right-side-up condition and the progressive reduction of this offset following practice (Augurelle et al., 2003a; Crevecoeur et al., 2009a, 2010a; Opsomer et al., 2018). It has been proposed that increasing the grip force could be a simple strategy to cope with an elevated uncertainty surrounding LF prediction (Crevecoeur et al., 2010a; Hadjiosif and Smith, 2015), even if the prediction is actually correct. Note that the difference in adaptation times observed between the static component (GF offset) and the dynamic component (GF gain) of the grip force was also observed in some parabolic flights studies (Crevecoeur et al., 2009a; Opsomer et al., 2018).

To sum up, the analysis of the grip dynamics strongly indicates that the predictive mechanism used by the CNS to anticipate changes in tangential loads at the fingertips operates in an Earth-centered allocentric reference frame, in agreement with the hypothesis that an internal representation of gravity is used for predictive control. Interestingly, we discuss hereafter the control of the kinematics of the arm that in contrast appears to operate in a more egocentric reference frame.

3.4.2 Arm kinematics reflect an egocentric planning of movement trajectory

In the right-side-up posture, the vertical velocity of the arm was characterized by a dependency of the velocity peaks on movement direction. More specifically, velocity peaks were more elevated in the upward direction than in the downward direction. Although direction-dependent kinematics have been reported extensively in the literature for discrete arm movements (Gaveau et al., 2016; Gentili et al., 2007; Papaxanthis et al., 1998b; Le Séac'h and McIntyre, 2007), we found no previous report documenting this kind of asymmetry for rhythmic arm movements. Model simulations in optimal control theory have shown that selecting different velocity profiles for upward versus downward movements optimizes effort-related motor costs (Berret et al., 2008; Crevecoeur et al., 2009b; Gaveau et al., 2016, 2014). Importantly, the dependency on movement direction has been reported to disappear in the horizontal plane (Gentili et al., 2007; Le Séac'h and McIntyre, 2007) but to persist temporarily in a weightless environment (Gaveau et al., 2016; Papaxanthis et al., 1998a), which strongly indicates that the action of gravity is anticipated by the CNS and incorporated into the planning process underlying arm movements. Interestingly, we also observed a persistence of this velocity asymmetry during the first blocks performed in the upside-down posture, from an egocentric perspective. This is in line with the hypothesis that the orientation of the body with respect to gravity can bias the planning of arm movements (Le Séac'h and McIntyre, 2007) and suggests that the kinematics of the arm are preferentially planned in an egocentric reference frame. It is important to stress out, however, that reproducing the same velocity asymmetry as in the right-side-up posture while inverted would still require accurate predictions of gravity's effect, because the muscle groups involved are different in the two body orientations. In other words, to reproduce the kinematics of the right-side-up posture, prediction must precede control (Flanagan et al., 2003). Thereby, shoulder dynamics were able to adapt very quickly to

the upside-down posture in order to reproduce the right-side-up kinematics, a result that can be compared to previous results obtained in microgravity (Papaxanthis et al., 2005).

3.4.3 Arm kinematics are progressively re-adjusted in the upside-down posture

Strikingly, with practice in the upside-down posture, the difference in velocity peaks between the HEAD and FEET directions decreased progressively, and even reversed in Experiment 2, tending towards the same difference as in the right-side-up posture from an allocentric perspective. In the same vein, Gaveau et al. (2016) observed a progressive adaptation of the velocity profile to microgravity towards a new velocity profile that minimizes movement effort in a weightless environment. More generally, a re-optimization process is thought to underlie the kinematic adaptation to novel limbs or environmental dynamics (Izawa et al., 2008; Crevecoeur et al., 2009b). Here, the progressive kinematics tuning observed in the upside-down posture could potentially be explained by a similar re-optimization of the control policy, although model simulations beyond the scope of this paper are required to support this hypothesis. The reproduction of the kinematics of the right-side-up posture during the first block in the upside-down posture, as well as the unimpaired and stable coupling between GF and LF in that same posture, indicate that gravity's effects were predicted accurately. Therefore, the kinematic adaptation does probably not stem from an adaptation of state prediction. Nonetheless, distinct internal models could underlie the control of grip force and the control of arm kinematics (Flanagan and Lolley, 2001; Danion et al., 2013).

3.4.4 Kinematic adaptation to upside-down body orientation induces after-effects

Importantly, this adaptation to the upside-down body orientation induced significant after-effects observable in the velocity profile of subsequent movements performed in right-side-up posture (see Experiment 2). This is very interesting, because all sensory signals indicated to the participants that they were in the right-side-up posture again, long before performing the movements. Once again, these findings suggest that the movement kinematics are planned preferentially in an egocentric reference frame. The transition from one posture to the next would then require an internal rotation of the frame of reference,

which took a few trials.

3.4.5 Verticality perception in the upside-down posture

Predictive control of grip force and arm trajectory requires an estimate of the movement direction with respect to gravity. Furthermore, transforming sensory signals from different modalities into a common, allocentric reference frame also requires an internal representation of body orientation. Therefore, verticality perception is an important parameter to consider. Verticality perception is built by integrating vestibular, visual and somatosensory signals as well as prior expectations. Vestibular signals are integrated with signals from other sensory modalities already in the vestibular nuclei and in the cerebellum (Barmack, 2003; Jian et al., 2002; Angelaki and Cullen, 2008; Green and Angelaki, 2010) and higher in the thalamus (Barra et al., 2010; Pérennou et al., 2008). From there, the resulting signals are sent to various cortical areas, including the parieto-insular area often referred to as the vestibular cortex (Brandt and Dieterich, 1999). Interestingly, fMRI data showed brain activity within that same area to be consistent with a central representation of gravitational motion (Indovina et al., 2005). An estimate of body orientation combined with an internal model of gravity's effect could be used to predict load force changes induced by arm movements. Previous studies have shown that when the body is upside-down, the perceived visual vertical is unbiased but shows greater inter- and intra-subject variability than when the body is upright (Kaptein and Van Gisbergen, 2004; Schöne, 1964; Tarnutzer et al., 2009; Udo De Haes, 1970). This greater variability in the estimation of the vertical axis when upside-down could be linked to the hypothetical inability of the otolith organs to distinguish between the right-side-up and upside-down head orientations (Bortolami et al., 2006b; Graybiel and Patterson, 1955). It could be one factor explaining the reduced GF-LF coordination and the increased GF lag observed in some participants, if the perceived orientation of gravity relative to movement direction is used to predict the amplitude and timing of the load force. Future studies investigating the effect of verticality misperception on grip-load forces coordination could provide additional support to the hypothesis that the CNS uses of an internal estimate of gravity for predictive grip control.

3.5 Conclusion

This study was performed to investigate whether predictive mechanisms of movement dynamics are flexible enough to allow for accurate predictions of the consequences of arm motor commands when the human body is in the uncommon, upside-down posture. By investigating the coordination between the grip force and the load force during rhythmic arm movements performed in an upside-down posture, we showed that it is generally indeed the case: the predictions of sensory feedback that sub-serve the tight coupling between the grip force and the movements of the arm is still accurate in an upside-down body posture. In other words, our results indicate that grip-force control is performed in an allocentric (gravity-centered) reference frame. By contrast, time for adaptation was required in the upside-down posture for the kinematics to retrieve the "right-side-up" profile (as seen from an allocentric perspective) and induced an after-effect upon return to right-side-up posture, which is consistent with an egocentric (body-centered) planning of movement kinematics. Our results therefore highlight distinct processes underlying the adaptation of grip dynamics and movement kinematics to the unusual upside-down body orientation with respect to gravity. Moreover, the similarities observed between our study and previous parabolic flight studies suggest that a common mechanism could underlie sensorimotor adaptation to altered gravity environments and sensorimotor adaptation to unfamiliar body orientations.

Chapter 4

Grip dynamics during rhythmic arm movements in Space

As seen in the previous chapters, the tight temporal coupling between the grip force and the load force during object manipulation is maintained across different gravitational contexts. When confronted to novel environments, participants nevertheless increase the grip-load force ratio, probably to increase the safety margin against accidental slips. But what are the characteristics of the grip-load force coupling in microgravity after *long-term* adaptation, i.e. when this environment is not novel anymore? Do astronauts tune the grip force to the object mass and movement-induced inertial loads with the same accuracy as they do on Earth? To address this question, we asked six astronauts to perform rhythmic arm movements with an object held in precision grip, both on Earth and on the International Space Station. Various masses were used, as well as various frequencies. Corroborating the results from previous studies, a steady grip-load force coupling was rapidly acquired, both on the ground and in Space. Strikingly, the grip-load force ratio at the time of maximum load was independent from object mass, movement frequency or gravity level. This constant force ratio was achieved by offsetting the grip force as a function of load force range. This suggests that tactile and proprioceptive feedback are integrated quickly to update the anticipatory control of the grip force.

4.1 Introduction

Object manipulation is as frequent and essential on the International Space Station (ISS) as it is on Earth. Yet, although the grip-load force coupling has been studied extensively on the ground since the seminal studies of Johansson and Westling (1984, 1987a, 1988a), the same topic has received little attention in Space. The long-term adaptation of grip control to microgravity has for instance never been studied. One reason could simply be that free-floating astronauts seemingly manipulate objects just fine. Furthermore, experiments conducted in parabolic flights have usually reported a quick adaptation of the grip-load force coordination to microgravity (see Chapters 1 and 2 and White et al. 2020 for a review). Still, subtle differences relative to 1-g performance have also been noted and better characterizing these differences could provide new insights on the mechanisms underlying the GF-LF coordination.

For instance, we saw in Chapter 2 that the grip-load force ratio at the times of peak LF remained slightly more elevated in 0-g than in 1-g. Besides, the ability to reproduce imposed isometric forces with the arm has been shown to be impaired during short exposure to microgravity (Mierau et al., 2008), as was the ability to discriminate masses during a short mission in Space (Ross et al., 1986). These two abilities are crucial to accurately adjust GF as a function of LF. Two studies focusing on the hyper-gravity phases of parabolic flight maneuvers have furthermore suggested that the increase in weight of the manipulated object caused by the increased gravitational level might be erroneously attributed to a change in mass (Crevecoeur et al., 2010b, 2014). The authors suggested that uncertainty about object mass could also explain the excessive grip force often applied during early exposure to microgravity (Crevecoeur et al., 2010b,a). Studying the GF-LF coupling during spaceflight and upon return to Earth could allow us to see if those "impairments" observed in short time windows persist on the long run and impact object manipulation.

Several studies have investigated how GF modulations change, on Earth, as a function of movement frequency and object weight during rhythmic arm movements. A consistent observation across studies was that an increase in movement frequency or object weight induced an increase in the GF offset (White et al., 2005; White, 2015; Zatsiorsky et al., 2005; Flanagan et al., 1993). In other words, if one models the GF-LF relationship by the linear regression $GF = \alpha LF + \beta$, increasing movement frequency or object weight (hence LF range), produces an increase in the intercept β. The effects of movement frequency and object weight on α, the GF gain, are by contrast not very consistent

across studies. Zatsiorsky et al. (2005) reported a decrease in α with movement frequency (also observed by Flanagan et al. 1993) and an increase with object weight, while White (2015) observed very little change of GF gain across frequency and weight conditions. When object weight was varied by varying the gravito-inertial level instead of the object mass, contradictory results were obtained. Augurelle et al. (2003a) observed a continiuous GF-LF relationship across gravity levels after adaptation, while White (2015) observed a dependence of the GF offset on gravity level. In microgravity, White et al. (2005) observed a decrease in GF gain relative to normal gravity. However, in 0-g the vertical component of the load alternates between positive and negative values, which was not taken into account to compute the gain, despite the possibility that the CNS could theoretically adjust GF differently depending on the direction of the load[1]. Therefore, it appears that additional studies are required to decipher how the GF modulations are adjusted by the CNS as a function of inertial and gravitational loads.

To further investigate how grip force is tuned to movement frequency, object mass and gravity on the long run, we decided to conduct an experiment on the ISS focused on the study of the GF-LF coupling during rhythmic arm movements. Six astronauts performed vertical arm oscillations with an object held in precision grip, at various movement frequencies and with various object masses. The experiment was performed two times before flight, three times during the course of a long-duration inflight mission and two times post-flight[2]. A detailed analysis of the GF-LF coupling was performed by extracting several parameters, including the GF-LF correlation, the GF gain, the GF/LF ratio at the times of peak load and the normal and tangential forces at each fingertip. We compared these parameters between task conditions and between pre-flight and inflight sessions. We furthermore examined these parameters during the first days after return to Earth to highlight potential impairments of the GF-LF coupling.

[1] We have for instance observed a higher GF gain in the upside-down posture than in the right-side-up posture in Experiment 1 of Chapter 3.

[2] The study presented in this chapter is ongoing. In total, the protocol includes four post-flight sessions, but only the first two post-flight sessions were performed by at least five astronauts so far.

4.2 Materials and Methods

4.2.1 Participants

Six male astronauts, aged 41-51 at the time of their first pre-flight session, participated in this study. These astronauts were tested during ISS expeditions 56/57, 60/61, 64/65 and 65/66. Two of them were first-time fliers. All astronauts were engaged in long-duration missions lasting at least 168 days. All participants provided written informed consent prior to testing. The experimental protocol was approved by the Medical Board of the European Space Agency, the Institutional Review Board of the National Aeronautics and Space Administration and the Human Research Multilateral Review Board.

4.2.2 Setup

The participants were sitting upright in a chair in front of a utility box (Fig. 4.1A). The utility box comprised a graphical user interface in the form of a touch-screen (thanks to which the participant could navigate autonomously through the experimental tasks), a vertical target frame with 13 LED's spaced by 5 cm and three cradles storing additional masses. The vertical and horizontal position of the utility box could be adjusted so that it was always 1 to 5 cm above the legs of the participant and 1 to 5 cm in front of the abdomen. In Space, shoulder and waist belts as well as foot straps were used to restrain the participant. During the tasks, participants moved an instrumented manipulandum (Fig. 4.1B) equipped with force and inertial sensors, infrared markers and moisture sensors covering the force sensors. The mass of the manipulandum could be changed by means of additional masses composed of aluminum covers loaded with ballasts. Three different masses were used for this study, all sharing the same dimensions and made of the same material with the same surface treatment. These additional masses were mounted and dismounted easily by the participant himself. Depending on the mass in place, the total mass of the manipulandum could reach 400, 600 or 800 g. In addition, a bracelet equipped with additional markers (not used in this study) was attached on the wrist of the participant. The cable of the manipulandum was fixed on the participant's arm by means of straps.

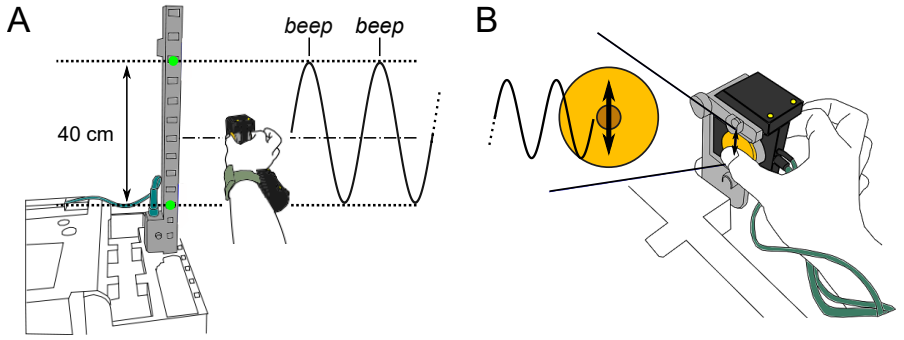

Figure 4.1 – Experimental procedure. (A) Illustration of the oscillation task. Participants performed vertical arm oscillations with a manipulandum held in precision grip. (B) Illustration of the friction task, performed before and after the oscillation tasks to estimate the static coefficient of friction.

4.2.3 Procedure

The experimental task consisted of rhythmic arm oscillations performed along the vertical axis with the manipulandum held in precision grip (Fig. 4.1A). All participants performed the task with their (dominant) right arm. The arm was extended (while keeping a small flexion of the elbow) to bring the hand to the right of the vertical target frame and the movements were mainly executed by rotating the arm around the shoulder, although small wrist and elbow rotations were allowed. At the beginning of a block of oscillations, the participant was instructed to pick up the manipulandum at the center of the moisture sensors using the thumb and index fingers and to move it next to the blinking target LED (located at the level of the dashed-dotted line in Fig. 4.1A). Once the manipulandum was positioned correctly, the LED turned off and two other target LED's turned on, located 20 cm above and below the initial LED on the target mast, delimiting movement amplitude[3]. Simultaneously, the metronome started, signaling the beginning of the oscillation task. The participant was instructed to oscillate between the lit targets and to execute one full cycle per beep. The rhythmic beeps stopped after ten seconds but the participant was instructed to continue the oscillations until the end of the block, which lasted 31 seconds.

On the ground (pre-flight and post-flight sessions), the mass of the manipulandum was kept to a constant value of 400 g and three movement frequencies

[3]The lit targets were always the same for a given participant, but could be changed across participants to adapt to each participant's size. Movement amplitude was always 40 cm.

were tested per session: 0.66 Hz, 1 Hz and 1.33 Hz. Participants performed six blocks (two series of three blocks) per session: blocks 1 and 4 were performed at 1 Hz; blocks 2 and 5 at 1.33 Hz; and blocks 3 and 6 at 0.66 Hz. A break lasting around fifteen minutes was inserted between the two series (i.e. between blocks 3 and 4), during which the participants performed point-to-point arm movements related to another study. on the ISS (inflight sessions), in addition to the three different frequencies, three different manipulandum masses were tested per session: 400 g, 600 g and 800 g. Participants performed ten blocks (two series of five blocks) in each inflight session. They first performed one block with the 800-g mass, one block with the 400-g mass and one block with the 600-g mass, in that specific order and at the 1-Hz pace. Then, they performed one block at the 1.33-Hz pace and one block at the 0.66-Hz pace with the 600-g mass. This sequence of five blocks was repeated one time after a break of around fifteen minutes during which the participant performed the point-to-point movements.

In addition to the oscillation task described above, the participants also performed a friction task in order to estimate the static coefficient of friction at the finger-object interface. During a friction task (illustrated in Fig. 4.1B), the manipulandum was locked on the utility box in a retainer. The participant was instructed to pinch the manipulandum at the center of the moisture sensors between the thumb and index finger and to squeeze either lightly, moderately or firmly. They were then instructed to rub the fingers up and down on the moisture sensors for fifteen seconds, while trying to maintain pinch force. During each session, participants performed the three blocks of the friction task before and after the oscillation tasks.

Sessions were organized as follows. Each subject was tested two times on the ground during the year preceding launch. Onboard the ISS, subjects were tested during three sessions: one Early session before Flight Day (FD) 14; one Middle session on FD 85($\pm$15); and one Late session on FD 145($\pm$10). Upon return to Earth, they were tested on R+1 and on R+12($\pm$3)[4]. All sessions were organized as described above, except the R+1 session during which only three oscillation blocks were performed, all at the 1-Hz pace. Five astronauts completed all these sessions and one astronaut completed the two pre-flight sessions and the Early inflight session.

[4] Additional sessions are planned after R+30, but they are not presented here because the amount of data for these sessions is not sufficient yet.

4.2.4 Data acquisition and processing

The position and orientation of the manipulandum were measured with a tri-dimensional (3-d) motion tracking system composed of two CODA CX-1 units (Codamotion, Charnwood Dynamics) tracking the position of eight infrared markers located on the manipulandum shell. The position of the markers were acquired at a sampling rate of 200 Hz. The position of the center of mass of the manipulandum was reconstructed from the position of the markers using custom routines in Matlab. This position signal was then filtered using a dual-pass Butterworth low-pass filter of order four with a cut-off frequency of 7 Hz. The 3-d velocity and acceleration of the manipulandum were then computed by numerical differentiation of the position signal. Furthermore, embedded inertial sensors (one accelerometer and one gyroscope) allowed measuring the acceleration and angular velocity of the manipulandum in 3-d. They were used to reconstruct the position of the manipulandum in some rare cases (3% of the trials) when the markers were occluded from the motion-tracking cameras for short periods of time (never longer than a few hundred milliseconds). Two 3-d force/torque sensors (Mini 40 F/T transducers, ATI Industrial Automation, NC) recorded the forces and torques exerted by the fingers on the object. Finally, skin moisture of the thumb and index fingerpads was measured by two moisture sensors at each finger contact surface. These moisture sensors were formed by a circle printed circuit board of 40 mm in diameter covering each force sensors, with sensing electrodes located in a 10 mm-diameter circle at its center. They could distinguish between five levels of humidity. Accelerometer and gyroscope data, forces, torques and finger moisture were all acquired at a sampling rate of 1000 Hz and were filtered during post-processing using a dual-pass Butterworth low-pass filter of order four with a cut-off frequency of 50 Hz.

4.2.5 Data analysis

All analyses were performed using Matlab R2018a. The load force (LF) was defined as the norm of the force applied tangentially by the fingers on the object, computed as the vector sum of the tangential forces (TF) measured by the left and right sensors. The grip force (GF) was defined as the force applied by the fingers normally to the contact surfaces and was computed as the average of the normal forces (NF) measured by the two sensors.

Individual oscillation cycles were delimited using the positive peaks of the

vertical component of the manipulandum velocity. Within each cycle, we computed the minimum value of the vertical component of the acceleration (the negative peak occurring at the top of the trajectory) and the maximum value of the vertical component of the acceleration (the positive peak occurring at the bottom of the trajectory). We then computed the values of GF and LF at the times of these acceleration peaks, as well as the normal and tangential forces at each finger. To assess the quality of the GF tuning to the load force, we computed the ratio between GF and LF at those times, as well as the safety margin (SM), which was defined in the same way as in Section 3.2.5. The parameters of the relationship between the slip force (SF) and TF ($SF = (TF/k)^{1/n}$; see Section 3.2.3) was estimated thanks to the friction tasks. Friction data from all sessions were assembled and sorted according the participant and average humidity of the fingers measured on the day of the experiment. In that way, the k and n parameters could be estimated for each participant, load direction (radial and ulnar), finger and humidity level[5].

To quantify the correlation between GF and LF, the R-squared coefficient between the two signals was computed within each block. This coefficient was computed separately for positive (R_p^2) and negative (R_n^2) values of the vertical component of hand acceleration. Additionally, the GF gain was computed as the slope α of the linear regression that best fitted the GF-LF relationship in the least-square sense. This gain was also computed separately for positive (α_p) and negative (α_n) values of vertical hand acceleration.

4.2.6 Statistical analysis

To study the evolution of the dynamics of precision grip across the blocks of the first pre-flight and inflight sessions, we used a 2-way, repeated-measures analysis of variance (rm-anova) to compare the two series of blocks performed during these sessions. The two factors of the rm-anova were *Condition* (3 levels on the ground, 5 levels in flight) and *Series* (2 levels).

Because adaptation effects were found during the first pre-flight and inflight sessions (see below) but not later, all pre-flight blocks except the first series of the first pre-flight session were grouped by participant and condition and averaged together, and so were all inflight blocks except the first series of the Early session. We then tested the effect of *Condition* and acceleration *Direction* (to compare the grip dynamics at the top and bottom of the trajectory, as well

[5]The number of humidity levels varied between 1 and 5 depending on the participant and the finger.

as the GF-LF correlation for positive and negative values of acceleration) during the pre-flight and inflight sessions using a 2-way rm-anova. To compare sessions, we used a 2-way rm-anova with factors *Session* and *Condition* separately for the two directions. Paired t-tests were used to break significant interaction effects and for post-how pairwise comparisons. Bonferroni corrections were used when necessary. All significance levels were set to 0.05.

4.3 Results

Example traces of GF as a function of LF are displayed in Fig. 4.2. The vertical component LF_v of the load force has been considered here, so that the direction of the load is represented by the sign of LF_v: when $LF_v > 0$, the vertical component of LF points upward (toward participant's head). On the ground (Fig. 4.2A), LF_v was mostly positive to counteract the gravitational force. Only at high oscillations frequencies, when hand acceleration exceeded the gravitational acceleration, did the load become briefly negative at the top of the trajectory (see red traces showing oscillations at 1.33 Hz). GF was correlated with LF, as has been documented extensively, and its offset was scaled as a function of LF range. In the three speed conditions, GF was well above the slip force. In flight (Fig. 4.2B), LF_v was symmetrically distributed around zero, the gravitational component of the load being equal to zero. GF increased as a function of the absolute value of LF_v and its offset was scaled as a function of LF range, as on the ground, so that GF was always above SF. Interestingly, it can be observed that the distance between GF and SF (the dotted lines in Fig. 4.2) was larger when $LF_v < 0$ than when $LF_v > 0$; similarly, the GF gain was globally larger when $LF_v < 0$ than when $LF_v > 0$.

The traces displayed in Fig. 4.2B were taken from the Early inflight session of a typical participant, suggesting that a seemingly adequate grip-load force coupling is achieved rather quickly. To quantify this, we first investigated the evolution of the R^2 coefficient between GF and LF across the different blocks of the first pre-flight and inflight sessions. On the ground, the correlation between GF and LF was higher when acceleration was positive, i.e. when LF was the highest, in all conditions (Fig. 4.3A,C). During the second series of blocks (blocks 4-6), R_p^2 was a bit higher than during the first blocks, although not significantly (main effect of *Series*: $F_{1,5} = 4.60$, $p = 0.085$) and there was also a marginal effect of *Condition* on R_p^2 ($F_{2,5} = 4.02$, $p = 0.052$; no significant interaction between *Condition* and *Series*). The marginal effect of

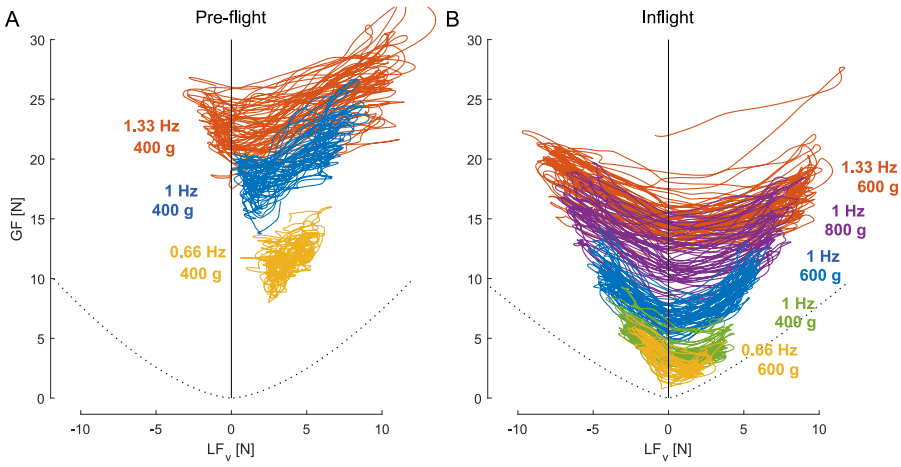

Figure 4.2 – GF versus the vertical component of LF from a typical participant in the different experimental conditions. A: Pre-flight example traces in the three speed conditions (from the first pre-flight session of this participant). B: Inflight example traces in the five inflight experimental conditions (from the first inflight session of this participant). The dotted lines show an estimation of SF.

Series disappeared during the second pre-flight session ($F_{1,5} < 0.01$, $p > 0.90$). During the first inflight session, this time R_n^2 tended to be larger than R_p^2 and was on average similar to R_p^2 on Earth. Importantly, while R_p^2 did not significantly change between the first and second series ($F_{1,5} < 0.1$, $p > 0.99$), R_n^2 increased significantly in all conditions ($F_{1,5} = 15.1$, $p = 0.011$). There was also a significant main effect of *Condition* ($F_{4,5} = 3.80$, $p = 0.019$), but no significant *Condition*×*Series* interaction ($F_{1,5} = 0.41$, $p = 0.80$). The increase of R_n^2 across series disappeared during the second and third inflight sessions ($p > 0.3$ in both sessions), but the significant effect of *Condition* persisted ($p < 0.05$). Moreover, there was no main effect of *Session* (Early vs. Middle vs. Late) on R_n^2 after removing the first series from the Early session ($F_{2,8} = 1.34$, $p = 0.32$).

We next averaged the two pre-flight sessions together and the three inflight sessions together, not including the first series from the first pre-flight and first inflight sessions during which learning effects were observed (these blocks were excluded for all analyses below). After excluding these first series, all variables studied here were very stable across pre-flight sessions and across inflight sessions (no significant effect of *Session* was found prior to flight and in flight). Figure 4.4 shows the R^2-coefficient and the GF gain α on the ground and on the ISS for positive and negative values of hand acceleration (conditions

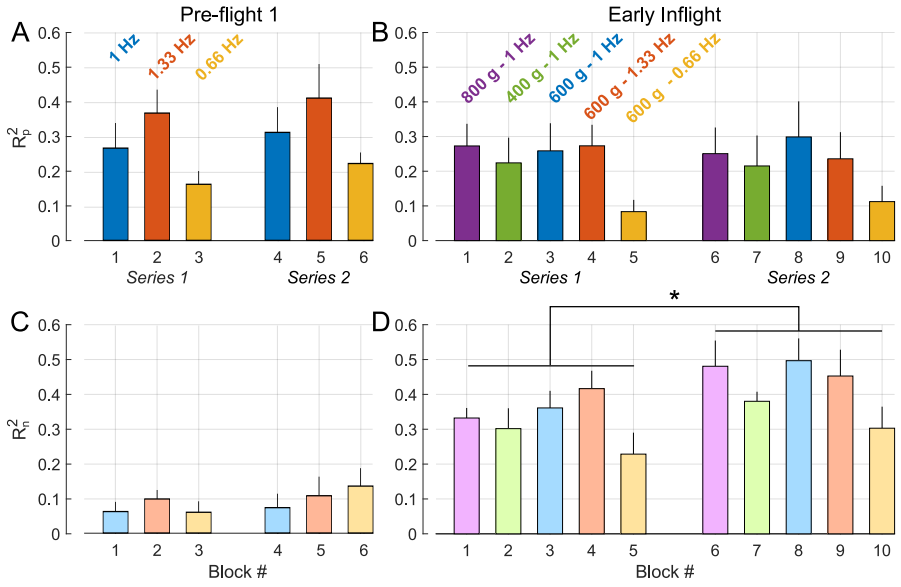

Figure 4.3 – Mean grip-load force correlation across the 6 blocks of the first pre-flight session (A,C) and the 10 blocks of the first inflight session (B,D). A,B: R-squared coefficient between GF and LF when object acceleration is positive (R^2_p). C,D: R-squared coefficient between GF and LF when object acceleration is negative (R^2_n). Acceleration is positive along the vertical axis when pointing upward, i.e. in the lower part of the trajectory. The block numbers on the horizontal axes denote the order in which the blocks were performed (same order in all sessions). The asterisk shows the significant difference between series (2-way rm-anova; $^*p < 0.05$). Error bars show the standard error.

were sorted by LF range). On the ground, both R^2 and α were significantly higher when acceleration was positive, i.e. when acceleration opposed gravity. Frequency condition also impacted these parameters, although not significantly for R^2. In flight, both R^2 and α were larger when acceleration was in the negative direction than when it was in the positive direction (R^2: $F_{1,5} = 6.89$, $p = 0.047$; α: $F_{1,5} = 18.3$, $p = 0.008$). R^2 was significantly influenced by the condition (main effect of *Condition*:$F_{4,20} = 6.23$, $p = 0.002$) but not the GF gain ($F_{4,20} = 0.77$, $p = 0.55$). Interaction effects between *Condition* and *Direction* were not significant.

Acceleration peaks were used to determine the top and bottom of the trajectories, a peak positive value corresponding to the bottom of the trajectory and a peak negative value corresponding to the top of the trajectory. We computed the absolute value of the acceleration, LF, GF and the ratio be-

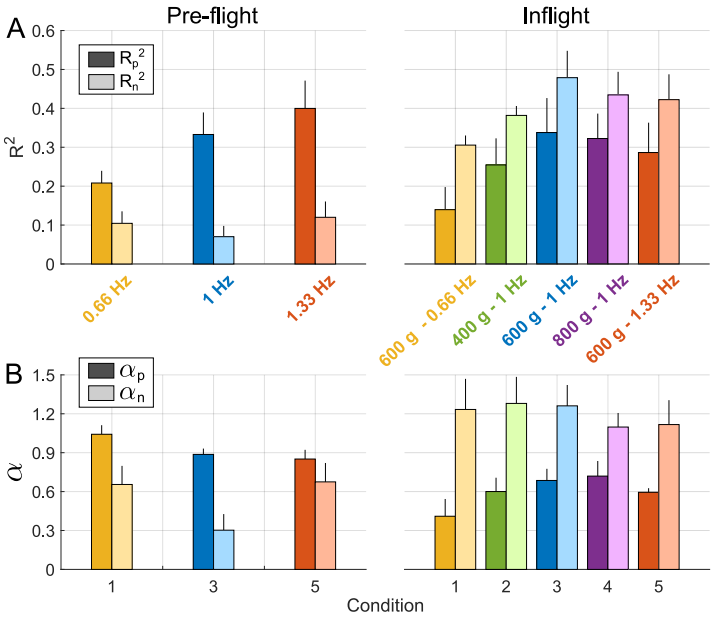

Figure 4.4 – Grip-load force correlation during the pre-flight and inflight sessions. The first series of the first pre-flight and first inflight session were not included. A: R^2-coefficient between GF and LF. B: the GF gain α, computed as the slope of the linear regression that best fits the GF-LF relationship. Both R^2 and α were computed for positive (dark bars, R_p^2 and α_p) and negative (light bars, R_n^2 and α_n) values of the acceleration. Conditions are sorted by LF range. Error bars show the standard error.

tween GF and LF at these acceleration peaks within each cycle. The mean values of each participant are reported for each condition in Fig. 4.5 and the means across participants are reported in Fig. 4.6. As expected, on the ground both negative and positive acceleration peaks increased in absolute value with oscillation frequency (Fig. 4.5A; main effect of *Condition*: $F_{2,10} = 240.0$, $p < 0.001$). More interestingly, the absolute value of the acceleration was greater at the bottom of the trajectory than at the top (main effect of *Direction*: $F_{1,5} = 12.2$, $p = 0.017$) but the effect of direction depended on movement frequency (*Condition*×*Direction*: $F_{2,10} = 8.70$, $p = 0.006$). Paired t-tests nevertheless showed significant differences between *Bottom* and *Top* in the three conditions ($t_5 > 2.9$, $p < 0.05$). Logically, LF was substantially greater at the bottom than at the top and the maximum value of LF increased with movement frequency (Fig. 4.5C). GF also increased significantly with movement frequency (Fig. 4.5E; $F_{2,10} = 38.7$, $p < 0.001$) and was larger at the bottom

than at the top ($F_{1,5} = 44.4$, $p = 0.001$). This difference was larger at higher frequencies, as reflected by the significant interaction effect between *Condition* and *Direction* ($F_{2,10} = 4.37$, $p = 0.043$). Note that GF at the top of the trajectory also increased with movement frequency, contrary to LF, reflecting the fact that the increase in LF range was coped with mainly by increasing GF offset rather than GF modulation. Consequently, the GF/LF ratio at the top of the trajectory was very high and variable (not shown in Fig. 4.5E). In contrast, this ratio was much more stable at the bottom of the trajectory and not significantly influenced by the frequency condition ($F_{2,10} = 1.70$, $p = 0.23$).

In flight, acceleration peaks were more symmetrical than prior to flight, although a slight asymmetry persisted (marginal main effect of *Direction*: $F_{4,20} = 4.56$, $p = 0.086$; no significant interaction effect: $F_{2,10} = 2.05$, $p = 0.13$). LF was larger at the bottom than at the top ($F_{1,5} = 49.3$, $p < 0.001$) despite the absence of gravitational load. GF increased monotically with LF (main effect of *Condition*: $F_{2,10} = 29.5$, $p < 0.001$) but was slightly more elevated at the top of the trajectory than at the bottom, contrary to LF (marginal main effect of *Direction*: $F_{1,5} = 6.04$, $p = 0.057$). Consequently, there was a significant main effect of *Direction* on the GF/LF ratio ($F_{1,5} = 20.8$, $p = 0.006$) and a significant *Condition*×*Direction* interaction ($F_{4,20} = 7.49$, $p < 0.001$). The GF/LF ratio at the bottom of the trajectory was strikingly unaffected by the condition ($F_{4,5} = 0.75$, $p = 0.57$), in contrast to the GF/LF ratio at the top ($F_{4,5} = 3.38$, $p = 0.029$). Moreover, for conditions 1, 3 and 5 that were performed both on the ground and in flight, no significant difference in GF/LF ratio at the bottom of the trajectory was found between the pre-flight and inflight sessions (uncorrected paired t-tests: $p > 0.4$ in the three conditions).

To further investigate the asymmetry in GF/LF ratio observed during the three inflight sessions, we looked at the normal (NF) and tangential (TF) forces at the thumb and index fingers separately. In flight, at the bottom of the trajectory there was no difference in tangential forces between the two fingers ($F_{1,5} = 0.70$, $p = 0.44$), which means that the load force was distributed equally between the two fingers. By contrast, at the top of the trajectory TF was significantly larger on the index than on the thumb side ($F_{1,5} = 27.4$, $p = 0.003$), independently from task condition. This was caused by a misalignment of the center of pressure that was on average more pronounced when the load was in the feetward direction. This explains, at least in part, why the GF/LF ratio was larger at the top of the trajectory. Indeed, this ratio does not take into account unequal distributions of TF between the two fingers. When looking at the NF/TF ratios for each finger individually (Fig. 4.7), it can be seen

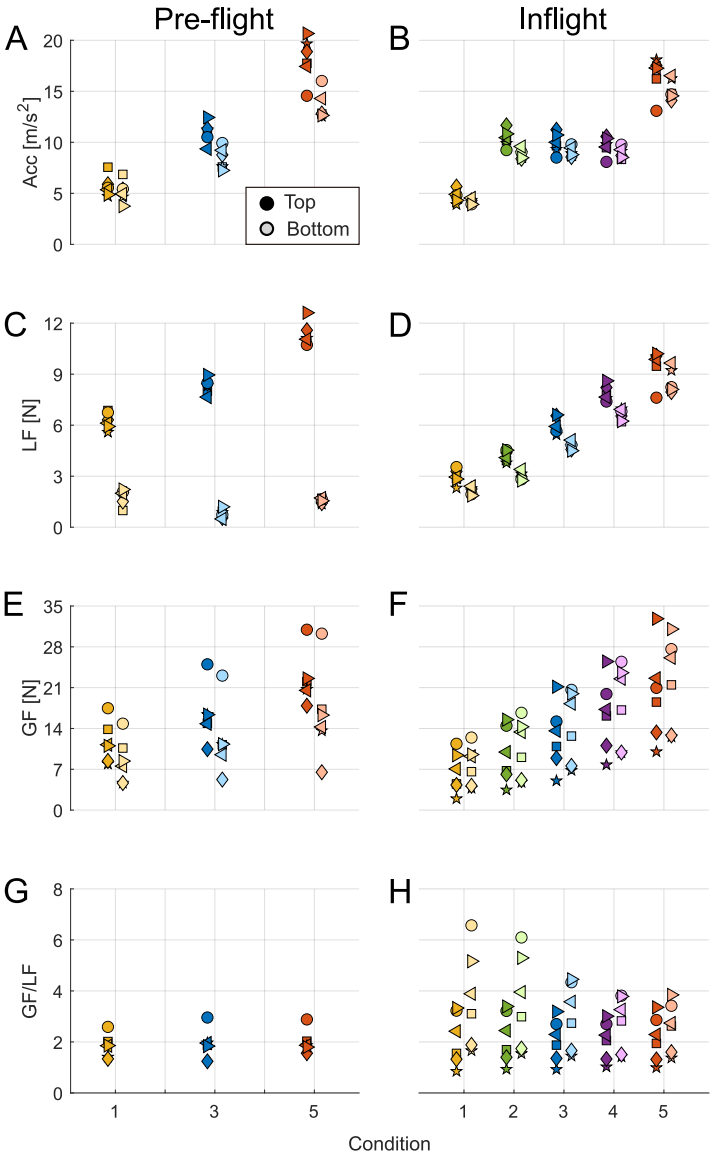

Figure 4.5 – Acceleration, LF, GF and GF/LF ratio at peak accelerations (top and bottom of the trajectory) during pre-flight (left panels) and inflight (right panels) sessions, in the different experimental conditions. Each symbol represents the mean for one participant ($N = 6$). The bottom of the trajectories (dark colors) corresponds to acceleration maxima, while the top of the trajectories (light colors) corresponds to acceleration minima. The GF/LF ratio at the top of the trajectories on the ground are out of axis range due to the very small values of LF at these times.

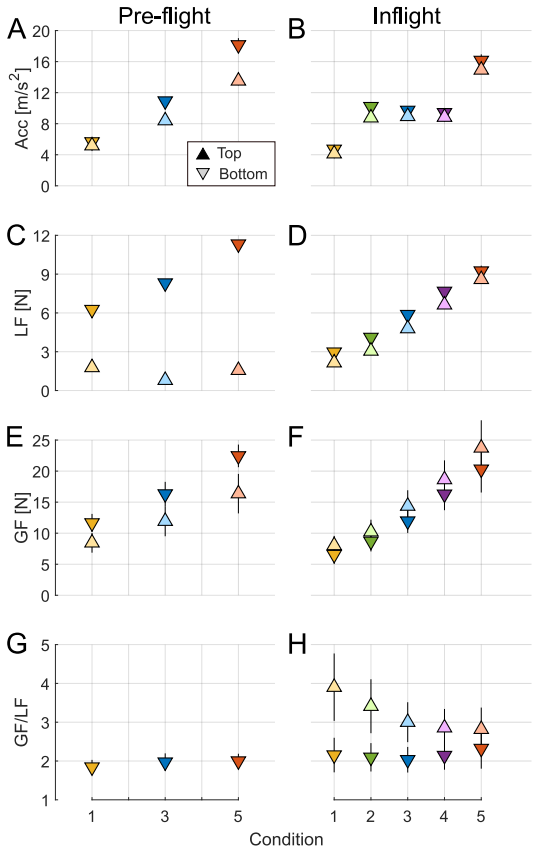

Figure 4.6 – Data from Fig. 4.5 averaged across participants. The bottom of the trajectories (triangles pointing down) corresponds to acceleration maxima, while the top of the trajectories (triangles pointing up) corresponds to acceleration minima. Error bars show the standard errors.

that the difference between the top and the bottom of the trajectory was much smaller for the index finger than for the thumb. Moreover, the NF/TF ratio for the index finger was constant across conditions (no significant main effect of *Condition*: $F_{4,20} = 0.56$, $p = 0.69$; and no interaction effect between *Condition* and *Direction*: $F_{4,20} = 0.88$, $p = 0.50$). However, a small main effect of *Direction* was still present ($F_{1,5} = 13.3$, $p = 0.015$). The safety margin, which takes into account the variations of the coefficient of friction as a function of normal force, load direction and finger (see section 4.2.5), was however not significantly different between the top of the trajectory and the bottom ($F_{1,5} = 1.65$, $p = 0.26$) but was significantly impacted by the task condition ($F_{4,20} = 9.20$, $p < 0.001$), decreasing as the LF range increased.

Finally, we analyzed the grip-load force coupling on return to Earth at R+1 and R+12 (Fig. 4.8). We focused our analyses on the GF/LF ratio at the time of peak acceleration, on the R^2 coefficient and on the GF gain

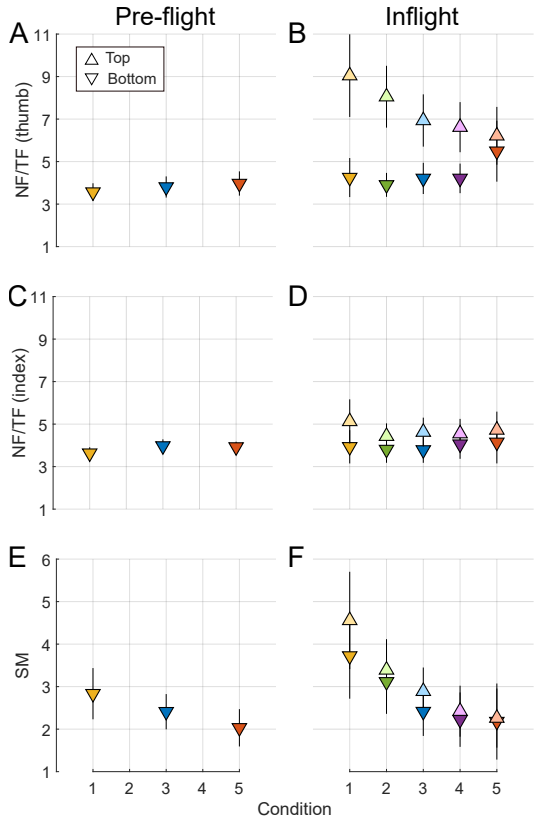

Figure 4.7 – Force ratios and safety margins for thumb and index fingers during pre-flight (left panels) and inflight (right panels) sessions. A: NF/TF ratio at the thumb finger; B: NF/TF ratio at the index finger; D: Safety margin. The ratios at the top of the trajectories are not shown for the pre-flight sessions, as the low tangential forces at these times yields very high force ratios. Error bars show the standard error.

α. At R+1, none of these variables changed significantly across the 3 blocks of condition 3 (the only condition performed at R+1). These 3 blocks were therefore averaged together. Comparing condition 3 between pre-flight, R+1 and R+12 with a 1-way rm-anova, we found no significant effect of *Session* on the GF/LF ratio ($F_{2,4} = 0.02$, $p = 0.98$), a significant effect on R_p^2 ($F_{2,4} = 4.62$, $p = 0.046$) and marginal effects on R_n^2 ($F_{2,4} = 3.65$, $p = 0.075$), α_p ($F_{2,4} = 3.57$, $p = 0.078$) and α_n ($F_{2,4} = 4.45$, $p = 0.050$). Differences were mainly observed between the R+12 session and the pre-flight and R+1 sessions, not between the pre-flight and R+1 sessions (but no effect survived the corrections for multiple comparisons following the post-hoc pairwise t-tests). Comparing all conditions between the pre-flight and R+12 sessions with a 2-way rm-anova yielded a significant main effect of *Session* on R_p^2 ($F_{1,4} = 34.6$, $p = 0.004$) and no significant *Condition*×*Session* interaction effect ($F_{2,4} = 0.26$, $p = 0.78$). The GF gain was also slightly more elevated in the R+12 post-flight session relative to pre-flight, but not significantly.

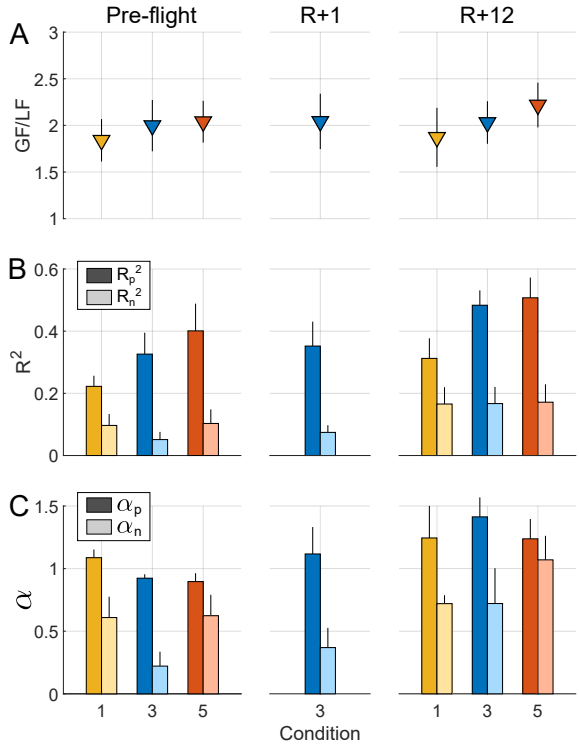

Figure 4.8 – Grip-load force coupling upon return to Earth (at R+1 and R+12(±3)) relative to pre-flight. A: GF/LF ratio at peak positive acceleration. B: R^2 coefficient. C: α. Error bars the standard error.

4.4 Discussion

This study investigated the coupling between the grip force and the load force during rhythmic arm movements in six astronauts engaged in long-duration spaceflight missions. The movements were performed at various paces and with various masses. Results showed a fast adaptation of the GF-LF coupling to microgravity, a fast re-adaptation to Earth gravity and a finely tuned grip-load force ratio that depended very little on the object weight or the movement frequency.

4.4.1 Rapid adaptation to microgravity

Signs of improvement in the GF-LF correlation were found only during the first pre-flight session and the first inflight session. This means that an adequate

GF-LF coupling is acquired quickly, i.e. after at most 30-s of practice of each condition, and as quickly in microgravity as in normal gravity in astronauts highly trained to the 0-g environment. This did not come as a big surprise, given the rapid adaptation of the GF-LF coupling observed in parabolic flights in participants experiencing microgravity for the first time (Chapter 2; Augurelle et al. 2003a; Hermsdörfer et al. 2000). Signs of incomplete adaptation, reflected by an increased GF/LF ratio in microgravity, have however been reported in parabolic-flight studies (Chapter 2; Augurelle et al. 2003a). The present results indicate that GF/LF ratios similar to those measured on Earth can be achieved with enough training in microgravity. An important caveat to acknowledge, however, is that the small sample size limits our ability to detect small differences between sessions and between movement conditions.

4.4.2 Fine tuning of the grip-load force ratio

Theoretically, one can achieve the same GF/LF ratio at the time of maximum load across different conditions of arm speed or object weight by maintaining the same GF offset and the same GF gain in all conditions. This was not the strategy used by the astronauts in this study. Instead, they increased GF offset proportionally to the LF range. This result is consistent with the results of previous studies conducted on the ground (Flanagan and Wing, 1995; White, 2015; Zatsiorsky et al., 2005). The variations in GF gain as a function of object weight and movement frequency are less consistent across studies and are globally less salient than the variations in GF offset. This has been interpreted as evidence that the source of the load (inertial or gravitational) is taken into account by the CNS to adjust GF (White, 2015; Zatsiorsky et al., 2005). Another explanation, which would be consistent with the results of this study, is that the CNS could use a simple strategy consisting in modulating GF offset as a function of LF variance in order to maintain a constant GF/LF ratio at the times of peak LF. This would be consistent with results from Hadjiosif and Smith (2015) showing that the GF safety margin is more sensitive to LF variability than to LF mean, as well as with the observation that the GF/LF ratio is independent of the arm motor command (White et al., 2005; Descoins et al., 2006). Because the LF profile was more or less the same across all cycles of a given condition, an estimate of the LF range for that condition could be acquired very quickly and transferred across cycles, series and sessions.

An interesting characteristics of the rhythmic movements in Space was that the GF/LF ratio was greater at the top than at the bottom of the trajectory.

We saw that it could be partially explained by an unequal distribution of LF between the two fingers when the load was negative (feetward direction). The tangential force was on average larger on the index finger than on the thumb at the top of the trajectory, because of a misalignment of the centers of pressure. Such asymmetry was also observed in Chapter 3 in the upside-down posture, where LF was mostly in the feetward direction due to the presence of gravity. The safety margin, computed as the minimum of the safety margins at each finger, was not statistically more elevated at the top than at the bottom, although a slight asymmetry persisted. Such fine adjustments of the grip force is most probably made possible by a very rapid integration of tactile feedback in the motor plan (Witney et al., 2004). Note however that the safety margin was not constant across frequency and mass conditions, increasing when LF range decreased. This might indicate that the dependence of the static coefficient of friction on the normal force (André et al., 2009; Comaish and Bottoms, 1971) is not taken into account by the CNS. Indeed, if the influence of grip force on the static coefficient of friction is neglected, then the constancy of the safety margin only depends on the constancy of the grip-load force ratio. Our results however indicate the this influence is not negligible.

4.4.3 Re-adaptation to Earth gravity

Upon return to Earth, the grip-load force coupling was surprisingly similar to pre-flight on R+1, despite verbal comments from the astronauts emphasizing how heavy their arm and the objects felt. It would suggest that tactile and proprioceptive information about load forces were intact and interpreted correctly in the context of grip control. We noted however some differences in GF gain and GF-LF correlation between R+1 and R+12 and between pre-flight and R+12. This may indicate an interference between the adaptation or habituation to the task itself and the re-adaptation the Earth gravity.

4.4.4 Changes of movement kinematics in Space

Finally, we found an asymmetry in the acceleration profiles on Earth (positive peaks being larger than negative ones, in absolute value) which was reduced in flight, indicating that the kinematic asymmetry in normal gravity is due to the presence of the gravitational force. This is consistent with the adaptation of the asymmetry of the velocity profiles of discrete arm movements observed in parabolic flights (Gaveau et al., 2016; Papaxanthis et al., 2005).

4.4.5 Conclusion

The present work highlights the complementary roles played by sensory feedback and predictive mechanisms in coordinating grip and load forces adequately in very different circumstances (Witney et al., 2004). Independently from the gravitational context, GF was finely tuned in each condition to take into account the LF range during the task, the load distribution between the thumb and index finger and the load direction. This corroborates the results presented in the previous chapters emphasizing the robustness of the GF-LF coupling during object manipulation.

Chapter 5

Reaching arm movements in Space

Our brain is used to the constant gravitational force acting on our body and has evolved to use it to its advantage. One of the great functions of gravity perception is spatial orientation. Although the role played by gravity in verticality perception has been studied extensively, the implications for arm movement control have not been deeply investigated. More specifically, the interaction effects of visual, gravitational and proprioceptive cues on the accuracy of reaching arm movements have received little attention. In this chapter, we report preliminary results from a spaceflight experiment that was conducted precisely to fill this gap. Reaching movements performed in the sagittal plane with a hand-held object were studied in six astronauts on Earth and during the course of a long-duration ($>$ 5 months) spaceflight. Movements were performed along two different axes in a seated or supine posture, with eyes open or with eyes closed. Results demonstrate that gravitational cues are necessary for maintaining directional accuracy when performing repeated reaching movements without visual feedback. In Space, hand paths of movements performed without vision were almost systematically tilted in the same direction. Interestingly, this tilt increased linearly through the repetitions of the movements while eyes remained closed. The same behavior was observed on Earth in the supine posture for longitudinal movements. We discuss the possibility that these results reflect a biased proprioceptive drift or a progressive rotation of the internal representation of the orientation of the body.

5.1 Introduction

When reaching for an object or aiming at a target, one of the first things the CNS must do before planning and executing the movement is to estimate to position of the target with respect to the body. Vision is arguably the dominant sense for achieving such tasks with precision and accuracy. However, other senses contribute as well, and can even substitute vision successfully when the latter is not available. If you close your eyes now, you should still be able to reach for your cup of coffee, your mouse or your pen with relative ease, even though your movements will probably be substantially slowed down and clumsy. Previous studies, as well as the present one, suggest however that this task would be more difficult if you were lying down and more difficult still if you were an astronaut reading these pages onbard the International Space Station (ISS). Gravity, not surprisingly, appears to play a key role in spatial orientation.

On Earth, the constant gravitational background indeed provides a clear, ubiquitous direction for the vertical axis. When human subjects are asked to align a luminous line with the perceived vertical axis while sitting upright in the dark, they do so very accurately (i.e., with very little bias) and with a high precision (i.e., with low variability). This is because a large number of sensory cues other than visual ones inform about the direction of gravity, in particular from the vestibular and somatosensory systems (see Section 1.2). If the same task is performed while the body is tilted relative to the gravitational axis, however, larger errors and variability are usually observed (Asch and Witkin, 1948; Aubert, 1861; Mittelstaedt, 1983; Bortolami et al., 2006a; Schöne and De Haes, 1968; Kaptein and Van Gisbergen, 2004). In particular, at backward body tilts close to 90° (supine position), there is a tendency to overestimate the angle of tilt of the body (Bortolami et al., 2006a; Ebenholtz, 1970).

The possible role of gravity as a reference axis during arm motor planning and control has been recognized in particular after it was observed that arm kinematics depend on the direction of the movement relative to gravity (Papaxanthis et al., 1998a,c). This hypothesis was further tested by asking participants to perform vertical and horizontal pointing arm movements in a seated and lying down posture with eyes open and with eyes closed (Le Séac'h and McIntyre, 2007). This experiment allowed to confirm that a gravitational, allocentric reference frame was used to plan movement kinematics. Interestingly though, an egocentric reference also appeared to play a role, especially when eyes were closed. In addition, during short-term exposure to micrograv-

ity, the asymmetry of vertical movements initially persists, before progressively decreasing with practice (Papaxanthis et al., 2005; Gaveau et al., 2016). This indicates that an internal representation of the vertical axis is still used during motor planning in microgravity. These works motivated the design of the present experiment for studying the influence of visual, gravitational and egocentric cues on arm kinematics.

In microgravity, gravitational loads acting on the limbs, on the otolith organs and on internal organs cannot be used anymore to infer the direction of the vertical. Consequently, a strong sense of disorientation is often experienced (Lackner and Graybiel, 1979; Kornilova, 1997). For instance, the lack of gravitational pull often leads to the illusion of being upside-down, whether during parabolic flight maneuvers (Lackner and DiZio, 1993; Lackner and Graybiel, 1979; Graybiel and Kellogg, 1967) or in Space (Mittelstaedt and Glasauer, 1993; Clément, 2007). This shows that the notion of "up" and "down" becomes a much more ambiguous concept in microgravity. Furthermore, the abilities to accurately perceive the direction of the body midline (Clément et al., 2007), the postural vertical (Clément et al., 1984) and the subjective horizon (Carriot et al., 2004) have also been reported to be impaired in microgravity. But other studies have also provided indications that proprioceptive information originating from muscle receptors might be impaired as well in microgravity, or at least require some sort of re-calibration (Lackner et al., 1992; Fisk et al., 1993; Lackner and Graybiel, 1981; Roll et al., 1998). For instance, when participants were asked to reproduce, with eyes closed, well-practiced movements of imposed amplitude, the amplitude of slow (but not fast) movements was significantly reduced in 0-g relative to 1-g (Fisk et al., 1993). The authors interpreted this result as a reduction in the sensitivity of the muscle spindles in the absence of gravitational load.

The above results suggest that both body posture relative to gravity and gravity level could potentially impact the end-point accuracy of reaching arm movements, in particular when eyes are closed. Consistent with this hypothesis, larger errors during pointing to remembered target locations were observed when subjects were in a supine and prone posture (Smetanin, 1997) or in an inverted posture (Hondzinski et al., 2016) than when they were in an upright posture. Errors were also more variable in the supine and inverted postures. Pointing movement errors to remembered targets have also been reported to increase during the microgravity and hypergravity phases of parabolic flight maneuvers (Bock et al., 1992; Whiteside, 1961) as well as during spaceflight (Watt, 1997), but results have been rather scarce and contradictory (Bock,

1998). To our knowledge, no studies have investigated the accuracy of reaching arm movements after long-term adaptation to microgravity, neither the combined effects of posture and gravity level on end-point accuracy.

The goal of the present experiment was thus to fill this gap by studying the combined effects of vision, body posture and gravity on the accuracy of reaching arm movements and the long-term adaptation of these movements to spaceflight, as well as the re-adaptation to 1-g gravity upon return to Earth. To that end, six astronauts performed reaching arm movements in the sagittal plane in a seated and supine posture, prior to flight then several times during the course of a long-duration mission onboard the ISS, and finally multiple times after their return on the ground. We investigated how visual and gravitational cues affected movement amplitude, hand-path tilt relative to the target axis and end-point variability.

5.2 Materials and Methods

5.2.1 Participants

Six male astronauts, aged 41-51 at the time of their respecitve first pre-flight session, participated in the study. All astronauts were right-handed. The astronauts were tested onboard the International Space Station (ISS) during expeditions 56/57, 60/61, 64/65 and 65/66, which all lasted at least 168 days. All participants provided written informed consent prior to testing. The experimental protocol was approved by the Medical Board of the European Space Agency, the Institutional Review Board of the National Aeronautics and Space Administration and the Human Research Multilateral Review Board.

5.2.2 Setup

The participants were either sitting upright on a chair (Fig. 5.1A) or lying supine on a mattress (Fig. 5.1B) in front of a utility box. The utility box comprised a graphical user interface in the form of a touch-screen (thanks to which the participant could navigate autonomously through the experimental tasks) as well as LED's located on a mast and on the side of the utility box that served as targets during the movements and defined the z- and y-axis, respectively. The x-axis was normal to the yz-plane and pointed towards the right-hand side. In both postures, arm movements were performed in the sagittal plane, either on the right of the mast and parallel to the z-axis (Head-Feet

movements, Fig. 5.1C), or on the right of the utility box and parallel to the y-axis (Front-Back movements, Fig. 5.1D). Head-Feet movements were executed mainly by rotating the arm around the shoulder, although wrist and elbow rotations were allowed. Front-Back movements were performed by extending the arm forward or flexing it backward. The depth and height of the utility box could be adjusted so that it was always 1 to 5 cm above the legs in the seated posture and 1 to 5 cm in front of the abdomen in the seated and supine postures. Furthermore, the location of the targets was chosen for each participant so that the posture was comfortable and the arm was never fully extended, but was always the same for a given participant. In space, belts and straps were used to restrain the participant. Shoulder and waist belts as well as foot straps were used for the upright posture, while shoulder, waist and thigh straps were used for the supine posture. On Earth, for comfort the head of the participant was lying on a small cushion when in supine posture. During the tasks, participants moved an instrumented manipulandum (Fig. 5.1C,D). The position and orientation of the manipulandum were measured with a motion-tracking system composed of two CODA CX-1 units (Codamotion, Charnwood Dynamics) tracking the position of eight infrared markers located on the manipulandum shell. Furthermore, embedded inertial sensors (one accelerometer and one gyroscope) allowed measuring the acceleration and angular velocity of the manipulandum. The total mass of the manipulandum was 405 g. In addition, a bracelet equipped with additional markers (not used in this study) was attached on the wrist of the participant. The cable of the manipulandum was fixed on the participant's arm by means of straps.

5.2.3 Procedure

The experimental task consisted of reaching (point-to-point) movements of the right arm performed with the manipulandum held in precision grip. There were four different movement configurations: Seated Head-Feet, Seated Front-Back, Supine Head-Feet and Supine Front-Back; and correspondingly four movement directions in each posture: headward, feetward, forward and backward. In addition, there were two different vision conditions: each movement was performed with eyes open and with eyes closed. Each movement configuration $\times$ vision condition was performed in a separate block. At the beginning of each block, the participant was instructed to pick up the manipulandum using the thumb and index fingers and to move it next to the start target (the lowest of the two targets for Head-Feet movements and the closest of the two targets for

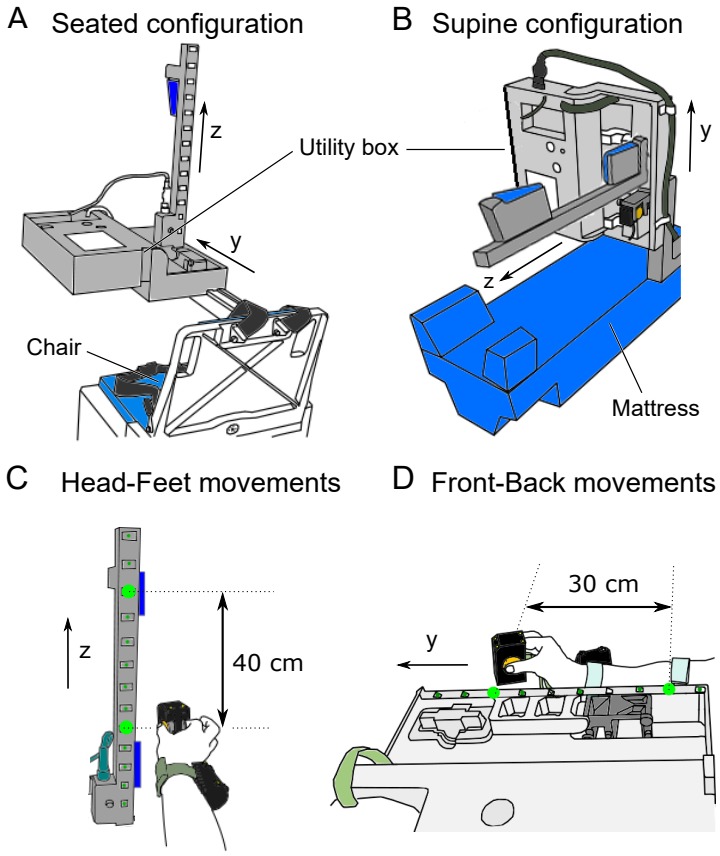

Figure 5.1 – Experimental setup. (A) Configuration of the chair and utility box for the seated posture; (B) Configuration of the mattress and utility box for the supine posture; (C) Target frame for vertical movements; (D) Target frame for horizontal movements.

Front-Back movements). Movement amplitude was delimited by the two targets (40 cm for Head-Feet movements and 30 cm for Front-Back movements). Once the manipulandum was positioned correctly, the participant was either instructed to keep his eyes open or to close them until the end of the block, depending on the vision condition. Task instructions were then to move the manipulandum quickly and accurately to the other lit target at the sound of each beep, to mark a full stop at the target and to wait for the next beep to perform the next movement in the opposite direction. A complete block consisted of 18 trials, always alternating between headward (forward) and feet-

ward (backward) movements in the case of Head-Feet (Front-Back) movements. All Head-Feet blocks started with a headward movements and all Front-Back movements started with a forward movements. The delay between two consecutive trials was chosen randomly between 1.0 , 1.3 , 1.6 and 1.9 s and one block lasted 25 s.

Each experimental session was broken down into two sub-sessions of 8 blocks each, one sub-session for each posture. The order of the sub-sessions was not imposed and could vary across participants and across sessions. Each sub-session started with four blocks of Head-Feet movements and ended with four blocks of Front-Back movements. In each movement configuration, the first and third blocks were always performed with eyes open, while the second and fourth blocks were always performed with eyes closed. Sessions were organized as follows. Each participant was tested two times on the ground during the year preceding launch. Onboard the ISS, subjects were tested during three sessions: one Early inflight session between Flight Day (FD) 4 and FD 10; one Middle inflight session between FD 73 and FD 87; and one Late inflight session between FD 135 and FD 146. Upon return to Earth, they were tested the day after their return (R+1), then on R+5($\pm$1) and on R+12($\pm$2)[1]. All sessions were identical in terms of number of trials and conditions, except the R+1 session during which only the seated posture was tested. Five astronauts completed all sessions and one astronaut completed the pre-flight sessions and the Early inflight session.

5.2.4 Data acquisition and processing

The position of the manipulandum markers were acquired at a sampling rate of 200 Hz. The position of the center of mass of the manipulandum was reconstructed from the position of the markers using custom routines in Matlab. This position signal was then filtered using a dual-pass Butterworth low-pass filter of order four with a cut-off frequency of 7 Hz. The tridimensinal velocity and acceleration of the manipulandum were then computed by numerical differentiation of the position signal. Accelerometer and gyroscope data were acquired at a sampling rate of 1000 Hz and were filtered during post-processing using a dual-pass Butterworth low-pass filter of order four with a cut-off frequency of 50 Hz. These data were used to reconstruct the position of the manipulandum in some rare cases (1% of the trials) when the infrared markers tracked by

[1] Additional sessions are planned after R+30, but they are not presented here because the amount of data for these sessions is not sufficient yet.

the cameras were occluded for short periods of time (always shorter than 2.5 seconds).

5.2.5 Data analysis

For each trial, movement onset and offset were determined using the component of the velocity along the target axis (z-axis for Head-Feet movements, y-axis for Front-Back movements) and a method similar to the one described in Crevecoeur et al. 2009b. They were defined as the intersection between the zero-velocity axis and the tangents to the velocity profile at the times of 15 % of peak velocity.

Trials that did not respect certain criteria were automatically rejected (<1% of the trials). These criteria ensured that movements were sufficiently fast (<2 s), did not anticipate the beep and came to a full stop between two consecutive movements.

Hand path was characterized by means of three variables: movement amplitude, hand-path tilt in the sagittal plane and end-point variability. Movement amplitude was computed as the distance between the position of the center of the manipulandum at the starting point and its position at the end point. Hand-path tilt was computed as the angle between a line connecting the starting and end points projected on the sagittal plane and the main movement axis (y- or z-axis). A positive angle of tilt denotes a counter-clockwise rotation of the path in the sagittal plane when the x-axis points towards the observer. End-point variability was computed within each block as the square root of the largest eigenvalue of the covariance matrix of the end-point positions in the sagittal plane. This corresponds to the standard deviation of the position along the axis of maximum variability.

We also computed the angle between the tangential velocity vector and the target axis in the sagittal plane at 100 time points equally distributed between movement onset and movement offset. This was performed to find the moment from which hand path started to statistically differ between the two vision conditions. First, for each trial the y- and z-components of hand velocity were re-sampled using 100 equally-spaced time points. Then, the angle between the tangential velocity vector and the target axis was computed, at each of these time points, as the arctangent of the y- and z-components of the velocity vector. Finally, all trials pertaining to the same participant and movement condition were averaged together. Note that for this analysis, only the last four trials of each block performed with eyes closed were considered, because hand-path

tilt was maximal during these trials. For the blocks performed with eyes open, all trials were included. For each movement configuration and each movement direction, we compared the angle of the tangential velocity vector between the eyes-open and eyes-closed condition at each time point using paired t-tests and looked for the first sample beyond which the angular difference was significant at the 0.05 level and remained significant for at least 300 ms. The index of this sample was multiplied by the average movement duration to find an estimate, in milliseconds, of the time from movement onset beyond which the direction of the velocity vector started to statistically differ between the eyes-open and eyes-closed conditions. This analysis was performed separately for the pre-flight and inflight data.

5.2.6 Statistical analysis

For the statistical analyses, the two blocks performed in each condition by each participant were averaged together, as well as the two pre-flight sessions. A 2-way repeated-measure anova (rm-anova) was used to test the effects of movement *Configuration* (Seated Head-Feet vs. Seated Front-Back vs. Supine Head-Feet vs. Supine Front-Back) and *Vision* (eyes open vs. eyes closed) on mean amplitude and hand-path tilt. The same 2-way rm-anova was used to test the effect of movement configuration and vision on the *drift* of amplitude and hand-path tilt across trials. To compute this drift, within each block a linear regression was used to fit (in the least-square sense) the evolution of the variable of interest across trials. The total drift during a block was computed as the slope of the linear regression multiplied by the number of trials. Additionally, we used one-sample t-tests separately for each condition to determine if the drifts were significantly different from zero. To compare the drift in the eyes-closed condition between the different inflight sessions, a separate 1-way rm-anova was used for each movement configuration.

The effects of *Vision* and movement *Direction* on end-point variability were tested by using a separate 2-way rm-anova for each movement configuration.

For all tests, a significance threshold of 0.05 was chosen.

5.3 Results

Figure 5.2 shows the mean paths travelled by the manipulandum in the sagittal plane in the four movement configurations, both pre-flight and during the Early

inflight session (averaged across the six participants). As will be detailed below, in some conditions the amplitude and the angle of tilt drifted across trials performed with eyes closed. Therefore, for that vision condition, only the last six trials of each block were included in the average traces.

On Earth (Fig. 5.2A), participants had no trouble in making movements parallel to the target axis when the latter was parallel to gravity (Seated Head-Feet and Supine Front-Back movements), even with eyes closed. In contrast, hand paths were tilted relative to the target axis when the latter was perpendicular to gravity (Seated Front-Back and Supine Head-Feet movements) when eyes were closed. Front-Back movements performed in a seated posture presented a small positive angle of tilt (counter-clockwise rotation in the sagittal plane), while Head-Feet movements performed in a supine posture presented a pronounced negative angle of tilt (clockwise rotation).

In the weightless condition of the ISS, the participants had much more difficulties in maintaining paths parallel to the target axes when their eyes were closed, whatever the movement direction and the posture of the body. As depicted in Fig. 5.2B, when no vision was allowed, at the end of each block hand paths were substantially tilted clockwise relative to the corresponding hand paths performed with eyes open. Moreover, movement amplitude was reduced relative to trials performed with eyes open, especially in the case of Head-Feet movements.

5.3.1 Hand-path tilt

Figure 5.3 presents the average evolution of hand-path tilt during the course of each block in the different conditions, both on the ground and during the Early inflight session. Prior to flight (Fig. 5.3A), there was a significant main effect of movement configuration on hand-path tilt ($F_{3,15} = 14.0$, $p < 0.001$), a non-significant main effect of *Vision* ($F_{1,5} = 6.32$, $p = 0.054$) and a significant *Configuration*$\times$*Vision* interaction ($F_{3,15} = 8.42$, $p = 0.002$). The angle of tilt was significantly positive in the Seated Front-Back configuration (t-test, all trials averaged: Eyes open: $t_5 = 4.07$, $p < 0.01$; Eyes closed: $t_5 = 2.74$, $p = 0.041$), but the difference between vision conditions was not significant ($t_5 = -1.94$, $p = 0.11$). In the Supine Head-Feet configuration, the angle of tilt was significantly negative when eyes were closed ($t_5 = -4.82$, $p = 0.005$). The angle of tilt was not significantly different from zero in the other conditions. Strikingly, the total drift of the angle of tilt during a block was influenced by movement configuration ($F_{3,15} = 6.68$, $p = 0.004$) and vision ($F_{1,5} = 8.72$,

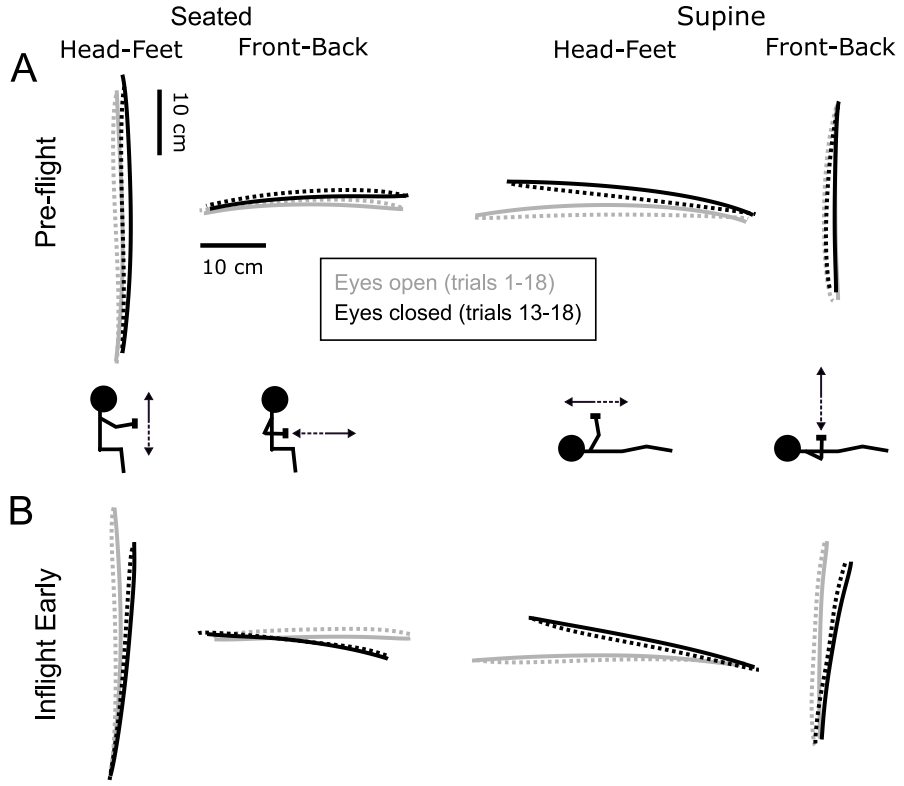

Figure 5.2 – Average hand paths during the pre-flight sessions (A) and the Early inflight session (B). Traces show the mean paths across participants in each movement configuration and vision condition. For the Eyes-closed condition (black traces), only the last six trials of each blocks were included. For the Eyes-open condition (grey traces), all trials were included. Plain lines, headward and forward movements; dashed lines, feetward and backward movements.

$p = 0.03$) and the effect of vision depended on the movement configuration (*Configuration*$\times$*Vision*: $F_{3,15} = 4.78$, $p = 0.016$). Actually, hand-path tilt was very stable across trials in all movement configurations except in the Supine Head-Feet condition with eyes closed. In that condition, the angle of tilt decreased linearly across trials, becoming increasingly negative (t-test on the drift: $t_5 = -4.92$, $p = 0.004$). The average drift of the angle of tilt across the 18 trials was equal to $-5.1°\pm2.5$ (mean $\pm$ standard deviation across participants). Consequently, hand path was significantly more tilted with eyes closed than with open in that configuration (all trials averaged: $t_5 = 4.46$, $p = 0.007$). The drift was not significantly different from zero in the other conditions ($p > 0.10$).

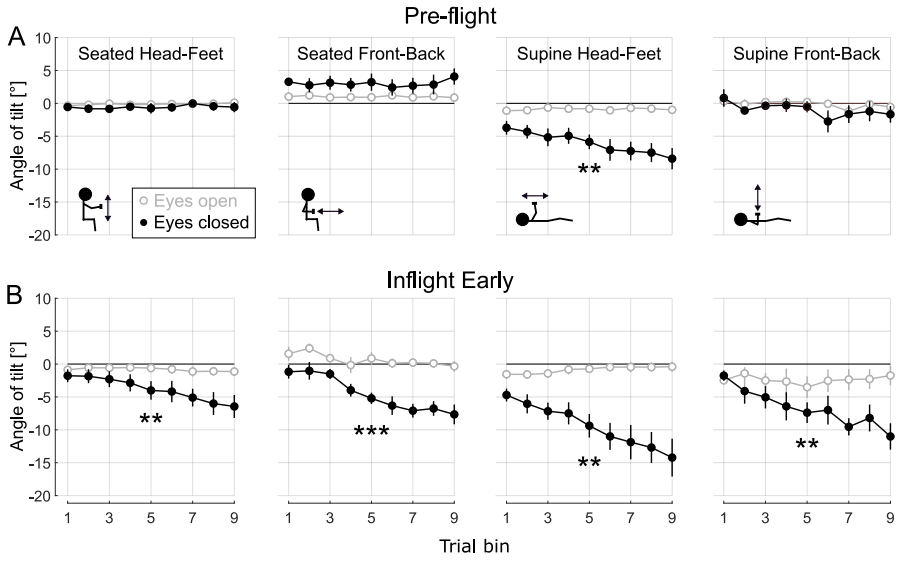

Figure 5.3 – Hand-path tilt in the sagittal plane in all movement configurations during the pre-flight sessions (A) and during the Early inflight session (B). Each panel shows the evolution of the angle of tilt across trials performed with eyes open (grey lines) and with eyes closed (black lines) in a specific movement configuration. Each bin shows the mean of two consecutive trials (one in each direction) × two blocks × the number of sessions (two pre-flight sessions, one Early inflight session). Circles and error bars show mean ± standard error. Asterisks show slopes that are significantly different from zero ($^{**}p < 0.01$; $^{***}p < 0.001$).

During the Early inflight session, hand paths rotated progressively in the clockwise direction across trials performed with eyes closed, in the four movement configurations (Fig. 5.3B). There was no main effect of *Configuration* on tilt drift ($F_{3,15} = 0.97$, $p = 0.43$) but a significant main effect of *Vision* ($F_{1,5} = 95.3$, $p < 0.001$). The interaction effect between the two factors was not significant ($F_{3,15} = 2.54$, $p = 0.096$). The total drift across the 18 trials was equal to $-5.7°\pm3.5$, $-8.1°\pm2.4$, $-9.9°\pm5.3$ and $-8.4°\pm3.5$ in the Seated Head-Feet, Seated Front-Back, Supine Head-Feet and Supine Front-Back configurations, respectively (mean ± standard deviation across participants). The drifts were significantly negative in the four movement configurations when eyes were closed ($t_5 < -4.0$, $p < 0.01$) but not significantly different from zero when eyes were open ($p > 0.05$). Consequently, hand paths were on average more tilted with eyes closed than with eyes open in all movement configurations ($t_5 > 3.2$, $p < 0.05$). Note that the angle of tilt was furthermore not significantly different from zero when eyes were open ($p > 0.10$).

To determine at what time, during the movement, hand path started to differ between the two vision conditions, we compared the temporal evolution of the orientation of the tangential velocity vector in the two vision conditions from movement onset to movement end (see Methods). Here, we compare the average of all trials performed with eyes open with the average of the last two trials of each block performed with eyes closed. Prior to flight, in the Supine Head-Feet configuration the direction of the tangential velocity vector started to statistically differ between the two vision conditions 80 ms after movement onset for headward movements and 33 ms after movement onset for feetward movements. In flight, this time ranged between 11 and 210 ms depending on the movement configuration (all times are reported in Table 5.1). Therefore, hand-path tilt was not due to movement corrections occurring at the end of the movement.

Session	Posture	Direction			
		Headward	Feetward	Forward	Backward
Pre-flight	Supine	80	33	-	-
Inflight Early	Seated	64	111	107	36
	Supine	11	18	41	210

Table 5.1 – Times from movement onset (in ms) beyond which the direction of the tangential velocity vector starts to significantly differ between the eyes-open blocks (all trials) and the eyes-closed blocks (last two trials of each block).

We next investigated whether the drift of hand-path tilt changed during the Middle and Late inflight sessions relative to the Early session. Figure 5.4 shows that the tilt drift decreased on average across inflight sessions in all configurations. However, the inter-subject variability of the change across sessions was quite high and the main effect of *Session* (Early vs. Middle vs. Late) was significant only for Head-Feet movements in the Seated posture ($F_{2,8} = 5.34$, $p = 0.034$). The slopes characterizing the drift remained negative in all inflight sessions in almost all participants. We found no significant change of drift across the two pre-flight sessions and across the post-flight sessions. Moreover, we found no significant differences in hand-path tilt between the pre-flight and R+1 sessions for the Seated posture nor between the pre-flight and R+5 sessions for the Supine posture. Interestingly though, there was a significant change in mean hand-path tilt across post-flight sessions for vertical movements (Seated Head-Feet and Supine Front-Back) with eyes closed (1-way rm-anova, effect of *Session* on mean hand-path tilt: Seated Head-Feet: $F_{2,8} = 5.33$, $p = 0.034$; Supine Front-Back: $F_{1,4} = 13.3$, $p = 0.022$). In these two movement configu-

rations, the angle of tilt was significantly negative during the first post-flight sessions (Seated Head-Feet, R+1: $t_4 = -3.56$, $p = 0.024$; Supine Front-Back, R+5: $t_4 = -3.61$, $p = 0.023$), but was back to zero at R+12.

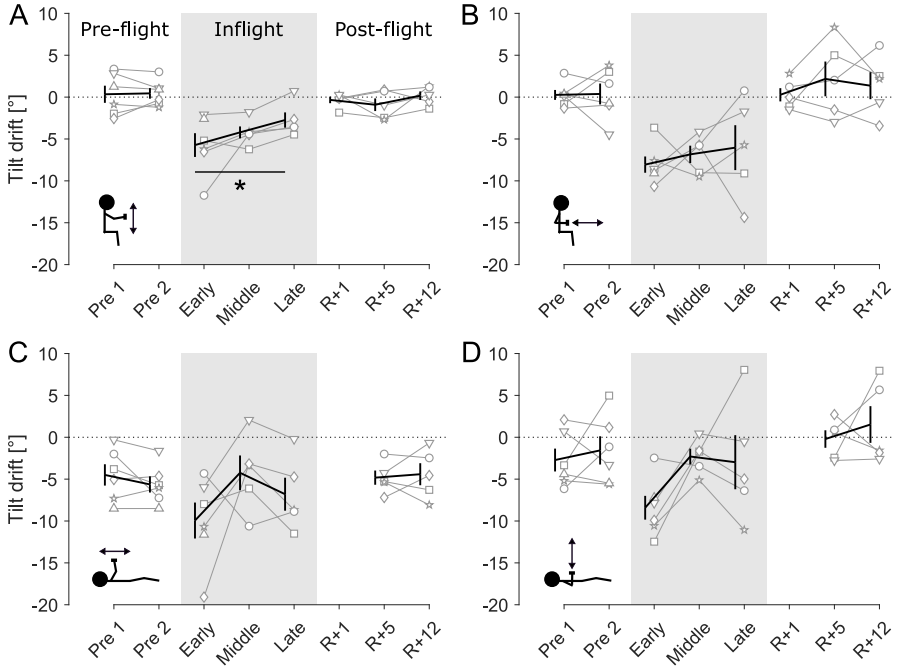

Figure 5.4 – Total drift of the hand-path tilt across sessions in the Seated Head-Feet (A), Seated Front-Back (B), Supine Head-Feet (C) and Supine Front-Back (D) configurations. Grey symbols show individual means, while black lines and error bars show mean ± standard error. The asterisk shows the main effect of *Session* for Seated Head-Feet movements in flight ($^*p < 0.05$).

5.3.2 Movement amplitude

Prior to flight, movement amplitude (Fig. 5.5A) was of course influenced by movement configuration ($F_{3,15} = 153.7$, $p < 0.001$) but not by the vision condition (main effect: $F_{1,5} = 1.14$, $p = 0.33$; *Configuration*×*Vision*: $F_{3,15} = 2.32$, $p = 0.12$). There was a significant effect of *Configuration* on amplitude drift ($F_{3,15} = 4.96$, $p = 0.014$) but no main effect of vision ($F_{1,5} = 0.08$, $p = 0.78$) and no significant interaction effect ($F_{3,15} = 2.57$, $p = 0.093$). Post-hoc tests failed to find any significant amplitude drift in any condition ($p > 0.1$).

In contrast, in microgravity movement amplitude decreased significantly

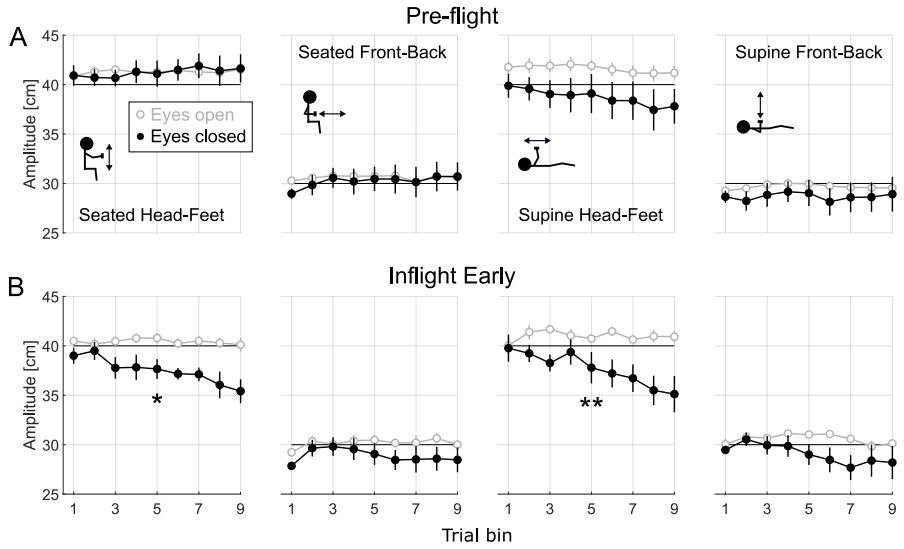

Figure 5.5 – Movement amplitude in all conditions during the pre-flight sessions (A) and during the Early inflight session (B). Each panel shows the evolution of the amplitude during the course of a block when performed with eyes open (grey lines) and with eyes closed (black lines). Each bin shows the mean of two consecutive trials (one in each direction) × two blocks × the number of sessions (two pre-flight sessions, one Early inflight session). Circles and error bars show mean ± standard error. Asterisks show slopes that are significantly different from zero ($^{*}p < 0.05$; $^{**}p < 0.01$).

across trials with eyes closed, but only in some configurations, as illustrated in Fig. 5.5B. There was a significant main effect of *Configuration* on amplitude drift ($F_{3,15} = 4.67$, $p = 0.017$), a non-significant main effect of *Vision* ($F_{1,5} = 5.16$, $p = 0.072$) and a significant interaction effect ($F_{3,15} = 3.90$, $p = 0.030$). Amplitude drift was significantly negative only for Head-Feet movements (Seated: $t_5 = -3.83$, $p = 0.012$; Supine: $t_5 = -4.12$, $p = 0.009$). Amplitude remained stable across trials when eyes were open. We found no significant change in the slopes of the amplitude decrease across inflight sessions.

5.3.3 End-point variability

From the average traces in Fig. 5.2, it can be observed that the divergence of hand path between the two vision conditions was largest when the shoulder and the elbow were extended, i.e. at the end of headward movements and at

the end of forward movements. To quantify this, we computed, within each block, the variability of the end points in the sagittal plane along the axis that maximizes variability (see Section 5.2.5). Not surprisingly, end-point variability was larger when eyes were closed in all configurations, both prior to and during flight (main effect of *Vision*, $p < 0.05$). Furthermore, whether movements were performed on Earth or in Space there was a significant main effect of *Direction* and/or a significant *Vision*×*Direction* interaction in all movement configurations. Post-hoc analyses revealed that prior to flight, when eyes were closed end-point variability was larger for headward than feetward movements in the two postures (paired t-tests: $t_5 > 2.7$, $p < 0.05$) and larger for forward than backward movements in the two postures ($t_5 > 2.7$, $p < 0.05$). No effect of movement direction was found when eyes were open. During the Early inflight session, we observed the same effect of movement direction on end-point variability when eyes were closed, although the difference between headward and feetward movements was only marginal in the Seated Head-Feet condition ($t_5 = 2.44$, $p = 0.059$).

5.4 Discussion

In this chapter, we investigated the interaction between visual, gravitational and proprioceptive cues during reaching arm movements in the sagittal plane. We found that in the absence of vision, gravitational cues played an important role in maintaining accurate and stable movements. On Earth, movements were more aligned with the target axis when the latter was parallel to gravity than when it was perpendicular to gravity, in both body postures. Furthermore, when the longitudinal body axis and the target axis were both perpendicular to gravity (the Supine Head-Feet condition), hand path rotated almost systematically in the same direction at an average rate of $-0.3\,°$/trial. In microgravity, a similar rotation of hand path was observed in the two body postures and along the two target axes when eyes were closed, in the same direction as in the Supine posture on Earth, at an average rate between -0.3 and $-0.6\,°$/trial depending on the movement configuration.

On Earth, the accuracy of pointing movements toward remembered target locations has been observed to be lower when participants are lying in a supine or prone posture (Smetanin, 1997) or upside-down (Hondzinski et al., 2016) compared to when they are upright. The poorer performance in supine posture was attributed to an erroneous motor program that did not take into account

the change in body orientation relative to gravity (Smetanin, 1997). This explanation seems rather unlikely in our case, given that the movements were also practiced with eyes open (allowing calibration of the motor plan) and that we observed no improvement in performance across pre-flight and post-flight sessions.

In microgravity, pointing movements in the absence of visual feedback have been reported to be less accurate and more variable than in 1-g, both during parabolic flight maneuvers (Fisk et al., 1993; Bock et al., 1992; Whiteside, 1961) and orbital space flights (Watt, 1997; Young et al., 1993). These poorer performances in 0-g have been attributed to inappropriate motor commands (Bock et al., 1992), inaccurate external spatial maps (Watt, 1997; Young et al., 1993) and/or inaccurate proprioceptive feedback (Fisk et al., 1993; Bock et al., 1992; Young et al., 1993).

Studies performed in parabolic flight (Fisk et al., 1993) and onboard space shuttles (Young et al., 1993, 1984) as well as anecdotal reports from astronauts (Lackner and DiZio, 2000; Young et al., 1993) have indicated that proprioception could indeed be less reliable in microgravity. Impairments in proprioception have been attributed to a decrease in the sensitivity of the muscle spindles caused by a reduction of the vestibulo-spinal influence (Fisk et al., 1993; Lackner and DiZio, 1992) or to slack developing in the spindles as a result of lower tonic activity (Proske, 2019). The reduction in movement amplitude that we observed in some movement configurations in 0-g in the absence of vision indicate indeed that the position of the arm was probably not estimated correctly. However, besides one anecdotal observation (Young et al., 1993), we found no paper reporting a systematic drift in limb position in microgravity or in a supine posture in 1-g.

It is known that limb position sense tends to drift in the absence of visual feedback on Earth (Paillard and Brouchon, 1968; Wann and Ibrahim, 1992). Proprioceptive drift might occur because of receptor adaptation at the level of muscle spindles (Tsay et al., 2014). Additionally, the trajectory of repeated movements of the unseen arm tends to drift, potentially because of the accumulation of movement errors (Brown et al., 2003). To our knowledge, it is however unknown why the proprioceptive drift or the movement errors would be biased in a particular direction in 0-g or in a supine posture in 1-g.

If one considers that the hand-path drift observed in 0-g was caused by a proprioceptive drift, then the results indicate that the participants were overestimating elbow flexion and underestimating shoulder flexion during Head-Feet

movements. In contrast, they were underestimating elbow flexion and overestimating shoulder flexion during Front-Back movements (see Appendix B for more details). Joint angle estimations were therefore biased in opposite directions for Head-Feet and Front-Back movements, which is not impossible given that the range of joint motion was different in the two types of movement (see Appendix B).

An alternative hypothesis is that hand-path tilt was caused by an erroneous perception of body orientation. Indeed, hand-position drift was consistently characterized by a progressive clockwise *rotation* of hand path across repeated trials which was not necessarily correlated with a decrease in movement amplitude. This clockwise rotation was observed whether movements were performed in a seated or in a supine posture and whether movements were parallel or perpendicular to the longitudinal body axis. The same phenomenon was moreover observed on Earth in the Supine posture. In all cases, the results would correspond to a perceived gradual backward inclination of the body with respect to the true body orientation.

This hypothesis would be consistent with the fact that spatial orientation is more accurate when the body is upright in 1-g (Aubert, 1861; Mittelstaedt, 1983; Schöne and De Haes, 1968; Kaptein and Van Gisbergen, 2004) and more accurate in 0-g than in 1-g (Clément et al., 2007; Lackner and DiZio, 2000; Carriot et al., 2004). On Earth, backward body tilts have been reported to be overestimated at large tilt angles close to the supine posture (Ebenholtz, 1970; Bortolami et al., 2006a). In microgravity, illusions of pitch motions, and in particular illusions of being inclined backward, have been reported by astronauts on orbit (Kornilova, 1997). When asked to adopt a vertical posture relative to the ground, astronauts have been observed to lean forward, while reporting feeling perfectly vertical, meaning that the perceived posture was tilted backward relative to the true posture (Clément et al., 1984). However, astronauts' postures were back to normal after three days in Space. During parabolic flight maneuvers, novice subjects asked to point to their subjective horizon tend to aim too low, as if they perceive themselves as leaning backward (Carriot et al., 2004). However, subjects that have prior experience with parabolic flights do not show such a biased subjective horizon (Carriot et al., 2004).

If the astronauts were indeed overestimating backward body tilt when supine on the ground, one could then wonder why no tilt of hand path was observed during Front-Back movements. A first possible explanation is that the perceived vertical and horizontal axes are not necessarily orthogonal (Betts and Curthoys, 1998). A second possible explanation stems from the fact that arm

movements influence the perception of the vertical (Tani et al., 2021; Bringoux et al., 2004; Fouque et al., 1999). A good reason for this is that the gravitational torques at the shoulder and elbow joints can provide cues about the orientation of the arm relative to gravity (Worringham and Stelmach, 1985; Bringoux et al., 2012). The patterns of the gravitational torques being completely different between Head-Feet (horizontal) and Front-Back (vertical) movements, the perceived orientation of the arm as well as the sensitivity to hand-path tilt probably differed between the two types of movements. These two hypotheses could also explain why Seated Front-Back movements showed a slight upward tilt, while Seated Head-Feet movements were well aligned with the target axis.

But why would the perceived perception of body orientation be tilted backward relative to the true orientation on the ISS ? Tactile information provided by the straps and by the contact with the chair or with the mattress could have influenced spatial orientation[2] (Bringoux et al., 2003; Trousselard et al., 2003) but it is difficult to predict whether this influence would bias the perceived body tilt in a particular direction. Another possibility is that the hypothetical perception of backward tilt originates from a bias in the vestibular system. For instance, it has been suggested that the inversion illusion[3] often experienced in 0-g could be due to a difference, in the otolith organs, between the resting activities of hair cells polarized in the rostral direction and those polarized in the caudal direction (Mittelstaedt and Glasauer, 1993). Similarly, a sensation of leaning backward would be elicited if a difference existed between the resting activities of hair cells polarized in the ventral direction and those polarized in the dorsal direction. The small reduction in the drift of the angle of tilt observed across inflight sessions could then be due to a reinterpretation of this bias by the CNS. However, we found no evidence for such bias in the literature.

In conclusion, we have shown that gravity is essential for maintaining directional accuracy when performing repeated reaching movements without visual feedback. This was evidenced on Earth by the stability and directional accuracy of vertical movements performed in an upright posture with eyes closed, contrasting with the larger and accumulating directional errors observed during horizontal movements performed while lying down. Strikingly, when all gravitational and visual cues were removed (i.e. in microgravity with eyes closed), reaching directions started to drift in all movement configurations. The direction of the drift being always the same, we suspect that it reflects a systematic

[2]One astronaut reported that he used the tension of the shoulder straps to better estimate arm position (with little success, according to the data).

[3]The sensation of feeling upside-down relative to one's surroundings.

misperception of body orientation relative to the target axes, although a biased proprioceptive drift or erroneous motor commands could contribute as well. These results open the door to new experiments that could be performed both in normal and altered gravity to disentangle the contributions of proprioceptive and vestibular signals to spatial orientation during reaching movements. They also stress the crucial importance of having reliable visual feedback during spaceflight operations.

Chapter 6

General discussion and perspectives

6.1 Main contributions

The present thesis forms a new volume in a series of theses devoted to the study of dexterous object manipulation in parabolic flights. In the previous volumes, a large set of tasks were studied including rhythmic movements (Augurelle et al., 2003a; White et al., 2005, 2008), point-to-point movements (Crevecoeur et al., 2009a,b, 2010a, 2014), self-generated collisions (White et al., 2012) and manipulation of unbalanced objects (Giard et al., 2015). These studies have all highlighted the robustness of the grip-load force coupling with respect to altered gravity and have provided pieces of evidence indicating that this coupling could be achieved thanks to flexible internal forward models and acute sensory feedback. By studying object manipulation in partial-gravity, in unusual body postures and in Space, we hope we could improve our global understanding of the GF-LF coupling and of the sensorimotor adaptation to altered gravito-inertial environments and provide new tools for better preparing future space explorations.

First, we have provided additional pieces of evidence to the accumulating observations that the sensorimotor mechanisms underlying object manipulation can adapt very quickly to various altered-gravity environments, by studying the GF-LF coupling in partial gravity (Chapter 2). Furthermore, we showed that the learning of a reduced-gravity environment could be transferred to lower

gravity levels in the context of object manipulation. Whether this learning reflects the calibration of forward models, a global habituation to an uncommon environment or a reduction in stress or excitement is not clear. What is clear, though, is that novices that had prior experience in partial gravity adapted faster to microgravity than novices that did not (Augurelle et al., 2003a).

We have further shown that the GF-LF coordination is robust to a reversal of body orientation relative to gravity (the upside-down posture studied in Chapter 3). So, despite the overwhelming preponderance of movements performed in an upright posture in everyday life, the CNS can easily change the group of muscles to be coordinated during object manipulation, allowing for an allocentric (gravity-centered) control of GF. By contrast, hand velocity reflected an egocentric programming of kinematics and a progressive adaptation to the unusual posture, reinforcing the idea that predicting the consequences of movements and adapting movement trajectories rely on distinct mechanisms. Interestingly, we observed some similarities between the patterns of adaptation in the upside-down posture and the patterns of adaptation in changed gravity levels in parabolic flights. These similarities indicate that common mechanisms may be involved in the adaptation to altered gravity and adaptation to uncommon body postures on Earth.

The experiments performed in parabolic flights paved the way for the development of an integrative set of experiments conducted on the International Space Station, thanks to which the long-term adaptation of the GF-LF coupling to microgravity could be studied for the first time. Thanks to these experiments, we could possibly settle the question of whether complete adaptation can be achieved in weightlessness in terms of grip dynamics (Chapter 4). From the middle of the first inflight session onward, the parameters characterizing the GF-LF coupling did not change any further and GF was finely tuned to the specificities of each task and of each gravity condition. Grip dynamics appeared to account for very fine aspects of the finger-object interface, such as load direction and range, unequal distributions of load between the fingers and possibly even frictional anisotropies of the fingerpad.

Finally, investigations of reaching arm movements on Earth and in Space suggested a bias in the aiming direction that accumulated across trials when neither visual nor gravitational cues were available (Chapter 5). Such directional bias was also observed during horizontal movements performed in a supine posture on Earth. These results were signs of a possible progressive rotation of the internal representation of the orientation of the body. Although a decrease in aiming and spatial orientation accuracy have already been observed in separate

studies in microgravity, such a biased drift in hand position has to our knowledge never been reported. This drift could put astronauts at risks in situations where visual feedback is not available or not reliable.

These works all emphasize the importance of taking into account gravity's effect and the importance of making use of gravitational cues during motor planning and control. They further emphasize the crucial role played by tactile feedback in object manipulation and the tight relationship that exists between feedback and feed-forward control. The underlying mechanisms likely involve flexible internal forward models continuously calibrated during movements thanks to the rapid integration of cutaneous and proprioceptive feedback (Witney et al., 2004; White et al., 2020). This would allow to coordinate movements along various motion axes and in various body postures on Earth and, incidentally, in altered-gravity environments.

6.2 Gravity, adaptation and after-effects during object manipulation

An important observation that was made in all experiments conducted for this work was the absence of sensible after-effects in the dynamics of precision grip following repeated practice in parabolic flight, in Space or in an upside-down posture. This observation raises the question of the type of adaptation that was occurring in those circumstances. Indeed, it seems contradictory with the idea that adaptation through the re-calibration of a forward model generally requires a time of de-adaptation when the perturbation is removed (Martin et al., 1996; Lackner and DiZio, 1994; Shadmehr and Mussa-Ivaldi, 1994; Fleury et al., 2019). It also contrasts with the re-adaptation patterns of arm kinematics observed after repeated practice in an upside-down posture (Chapter 3). At the same time, the tight coupling between GF and LF observed in very different contexts constitutes strong evidence that malleable predictive mechanisms were at play and it is difficult to explain predictive mechanisms without invoking forward models. How can we reconcile these contradictions?

Once again, an efficient integration of sensory feedback could be one explanation. In all experiments presented here, sensory feedback informing about the "perturbation" was available before movement initiation through the vestibular and somatosensory systems. Furthermore, the weight of the object (but not its mass) could be estimated during static holding. Therefore, the calibration of the sensory predictions could already start before the task started. In contrast,

for perturbations such like force-fields, visuomotor rotations or Coriolis forces, the perturbation can only be sensed during active movements.

Furthermore, the specificity of the goal must be considered when studying motor adaptation. For instance, adjusting grip force adequately to avoid slippage should be intuitively much easier than adjusting arm kinematics to optimize movements. In the former case, tactile feedback at the fingertips directly informs us about the increment of grip force that should be applied to avoid slippage. In the latter case, sensory feedback does not provide information about how far from optimal the movement is, because in a novel environment the optimal cost is unknown. Thus, different trajectories must be explored before selecting the best one.

Actually, it is possible that no update of the forward models underlying grip control is required in constant gravitational backgrounds if the internal models already consider the gravitational force as an input that can vary (White et al., 2020). This might sound unlikely given the timeless nature of gravity on Earth. It gets however more plausible when remembering that gravity's effects on movements depend on the direction of the movement relative to gravity and are therefore varying constantly.

Another point worth discussing in more depth is the distinct adaptation patterns observed between grip force timing and grip force scaling following exposure to microgravity or to an unusual body orientation. Changes in GF lag relative to LF remained generally very limited in all experiments conducted here, while the mean level of grip force could vary substantially from one condition to another and from one participant to another. A reasonable explanation is that the timing of LF peaks is very easy to predict because these peaks correspond to the peaks of hand acceleration, which in the case of harmonic movements correspond to motion extrema. In contrast, the required amount of grip force depends on multiple factors: hand acceleration, object mass, contact surface material, finger moisture, location of the center of pressures and desired safety margin. In particular, the applied safety margin is expected to be quite idiosyncratic as it depends on subject's confidence, stress and grip strength in addition to task context. These considerations can also explain why grip force scaling, but not timing, is affected by finger anesthesia (Augurelle et al., 2003b; Nowak et al., 2002a), finger cooling (Nowak and Hermsdörfer, 2003) or cerebellar pathologies (Rost et al., 2005).

6.3 Limitations, open questions and suggestions for future works

Almost all parabolic-flight or spaceflight studies are characterized by a small sample size and a stressful environment. These elements should be kept in mind when interpreting the results. In particular, they could explain some inconsistencies between studies. Additionally, the small number of participants reduces the size of the panel of idiosyncratic behaviors. However, the growing number of studies performed in parabolic flight allows now to pinpoint consistent results and to be more confident about the generalization to the population. A meta-analysis studying idiosyncratic behaviors following exposure to microgravity could provide interesting clues about the mechanisms underlying motor adaptation to new gravitational fields.

Spaceflight studies related to sensorimotor coordination remain unfortunately scarce. Hopefully, the sample size of the studies presented in Chapters 4 and 5 might grow soon. Furthermore, other types of movements (self-generated collisions and targeted movements) are currently studied in Space and should widen our understanding of the adaptation of arm control to microgravity. For instance, controlled collisions performed on the ISS will allow to test the strength of the prior according to which upward collisions are more prone to generate accidental slips than downward collisions (White et al., 2012). Furthermore, point-to-point movements to various targets in the horizontal and vertical planes will hopefully provide new information on the cost function that is putatively minimized when generating movements and on the impact of microgravity on mass perception.

In Space, we observed a directional asymmetry in the GF modulation, with a grip-load force ratio being on average greater for negative (feetward) load forces than for positive (headward) load forces. The data strongly suggest that this asymmetry was generated to account for unequal distributions of the negative load force on the two fingers and direction-dependencies of the static coefficient of friction. Other factors possibly contributing to this asymmetry could be an erroneous prediction of LF, a misperception of negative tangential forces or an increased safety margin applied for negative loads to cope with larger prediction uncertainties. These alternative factors deserve further exploration. Interestingly, such directional dependency of the GF modulation has also been observed on Earth for horizontal movements (unpublished data). Experiments could therefore be conducted on the ground to estimate the contribution of

each factor to the asymmetry observed in Space.

The study of reaching movements in Space was particularly fruitful considering the number of new questions that was raised. The systematic drift of hand-path tilt observed in microgravity is intriguing and, although we favor the contribution of a biased internal estimate of body orientation, the data do not allow us to disregard the contributions of proprioceptive or movement errors to this phenomenon. Luckily, a very similar drift was observed on the ground in the Supine posture. This phenomenon could therefore be studied on Earth and the results potentially generalized to Space. For instance, one could measure hand drift over longer periods of time, as the drift did not seem to saturate after the 25 seconds of a single block of trials. Another question that could be easily tested is whether hand-path tilt increased as a function of time or as a function of movement repetition. If repeated reaching arm movements are necessary for hand-path drift to be observed, it would suggest a major contribution of movement error (Brown et al., 2003). An investigation of the impact of body orientations between 0 and 90° and beyond should also be carried out to better characterize the drifting phenomenon. To probe the contribution of the subjective perception of body orientation, one could start by studying the effect of head orientation, in the supine posture, on hand-path tilt. And to probe the contribution of proprioception, a perceptual task measuring the perception of hand position in a body-centered reference frame could be imagined. Finally, a virtual-reality setup could be used to test the effect of visual feedback more thoroughly.

Ground studies will probably not be sufficient to cover all the questions left regarding sensorimotor adaptation to altered gravity. Parabolic-flight and spaceflight studies still have great days ahead of them. In particular, adaptation patterns across partial-gravity environments should be examined more thoroughly in other paradigms than the GF-LF couplings. For instance, the kinematics of arm pointing movements, which have been shown to adapt progressively to microgravity, could be studied in Mars, Moon and micro- gravity in order to test the possible transfer of adaptation across gravity levels but also to better characterize the effect of gravity on movement optimization (Gaveau et al., 2016). Hypergravity has been linked to an erroneous attribution of a change in weight to a change in mass; this phenomenon could also be observed in partial gravity and can be easily tested using the same protocols as Crevecoeur et al. (2014). Partial-gravity could furthermore be particularly useful to see if the drifting phenomenon observed in Chapter 5 is specific to microgravity or can also occur at reduced levels of gravity. Such an experiment could

allow to relate the drifting phenomenon to the subjective vertical, as the latter has been shown to be impaired when gravity was below a participant-specific threshold (de Winkel et al., 2012).

6.4 Concluding words

In this thesis, we took another step towards the understanding of the adaptation of sensorimotor coordination to altered-gravity environments and of the mechanisms underlying object manipulation on Earth. A rigorous scrutiny of the new patterns of finger forces and arm kinematics in altered gravity and in different body postures in normal gravity revealed interesting new insights on the predictive mechanisms of the brain. We saw that changes in gravity level can quite easily be taken into account during object manipulation but that gravity is also essential to perform accurate movements. In the end, one can only be convinced of the incredible capacity of the brain to use every available resource at its disposal to ensure that we move safely and efficiently. As far as object manipulation is concerned, space exploration should be a piece of cake for the brain ! Do not try to bake that extraterrestrial cake with eyes closed though, you might fail by a few degrees.

Appendix A

Influence of hypergravity on the GF-LF coupling in partial gravity

A.1 Introduction

In Chapter 2, we analyzed the evolution of grip dynamics during rhythmic arm movements across parabolas reproducing Mars, Moon and micro- gravity. For these analyses, we excluded the last two parabolas of each gravity condition (parabolas 12, 13, 24, 25, 30 and 31; see Fig. 2.1B). The reason for this was that during these parabolas, the subjects performed the task continuously throughout the entire parabolic maneuver, including the hypergravity and transition phases. In contrast, during the other parabolas the subjects only performed the task during the stable partial-gravity phases and during the level-flight 1-g periods in-between two parabolic maneuvers. Performing the task during the hypergravity and transition phases could have had an influence on task performance in the subsequent partial-gravity phase and we did not want this potential influence to interfere with the effect of adaptation. In this appendix we analyze these specific parabolas in more details.

A.2 Statistical analyses

First, we used the same linear mixed-effects (LME) model as in Chapter 2 (Equation 2.2) to characterize the evolution of grip dynamics across parabolas in the Mars, Moon and microgravity conditions, including the last two parabolas of each condition. Please note that even for these parabolas, only the oscillation cycles performed during the partial-gravity phase are considered here.

Second, within each gravity condition we compared the parabolas during which the task was performed continuously with the two parabolas directly preceding them, using paired t-tests. For instance, in the *Mars* condition we compared the average between parabolas 10 and 11 (task performed only during the stable partial-gravity phase) with the average between parabolas 12 and 13 (task performed continuously throughout all phases of the parabola).

A.3 Results

Including the last two parabolas of each condition to the LME model did not modify the main conclusions of Chapter 2 (Fig. A.1). The GF/LF ratio at the time of peak LF still decreased significantly across parabolas in the Mars condition, with a similar slope as when excluding these parabolas ($b_1 = -0.034$, $t = -3.46$, $p < 0.001$). The GF/LF ratio was not significantly smaller during these parabolas than during the two preceding ones ($t_7 = 0.18$, $p = 0.86$). In addition, the R^2-coefficient characterizing the grip-load force correlation still increased significantly across Mars parabolas ($b_1 = 0.013$, $t = 3.22$, $p = 0.002$). It was slightly reduced in the last two parabolas, but not significantly ($t_7 = 1.68$, $p = 0.14$). The effect of the parabola on the GF/LF ratio and R^2 coefficient was not significant in the Moon and Micro conditions.

There was however a (non-significant) tendency for the R^2 coefficient to be slightly reduced when the task was performed in reduced gravity after performing the task in hypergravity (filled dots in Fig. A.1). The same tendency can be observed for the GF gain (first row of Fig. A.1). The decrease of GF gain was actually significant in microgravity (LME: $b_1 = -0.057$, $t = -2.52$, $p = 0.016$; t-test: $t_7 = 2.69$, $p = 0.03$).

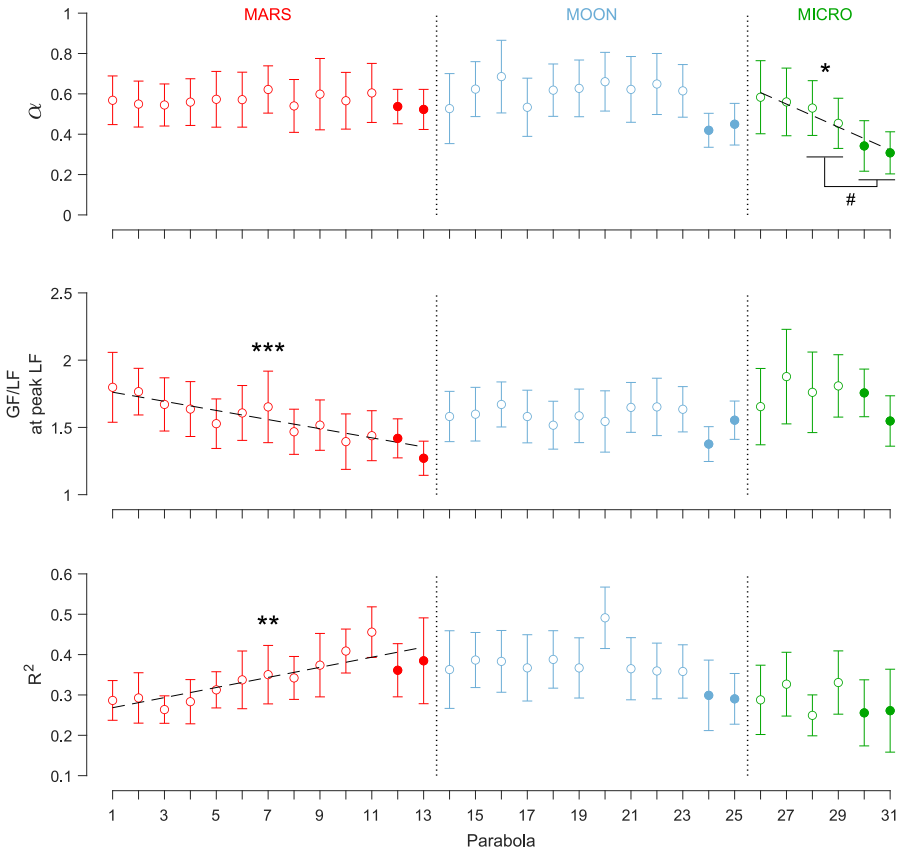

Figure A.1 – Grip dynamics across Mars, Moon and micro- gravity parabolas during the experiment presented in Chapter 2. From top to bottom: GF gain (α), GF/LF ratio at the time of peak LF, and R^2 coefficient. The regression lines estimated by the mixed-effects models are plotted (dashed lines) when their slope is significantly different from zero ($^{*}p < 0.05$; $^{**}p < 0.01$; $^{***}p < 0.001$). During the last two parabolas of each condition (filled dots), participants performed the task throughout all phases of the parabola (see Section 2.2). The hash symbol shows the significant difference between pairs of parabolas (paired t-test, $^{\#}p < 0.05$).

A.4 Conclusion

The complementary analyses performed in this appendix suggest that the GF gain, representing the increase of GF for a unit increase of LF, was reduced in partial and micro- gravity when the task was performed during the preceding hypergravity phase compared to when the task was only performed during the stable reduced-gravity phase. The difference was significant during the

microgravity session. However, because these parabolas were always performed at the end of each session, it cannot be concluded whether this reduction was a consequence of performing the task in hypergravity or a continuation of the adaptation to the microgravity environment.

It is possible that the GF gain was reduced because of the greater variability in LF peaks caused by the varying gravitational level, as compared to the distribution of LF peaks when gravity level is stable. However, the mean level of GF was not increased during these parabolas, which is not consistent with an increase in uncertainty for LF predictions (Hadjiosif and Smith, 2015; Crevecoeur et al., 2010a). Alternatively, manipulating the object during the hypergravity and transition phases could have influenced the perception of object mass and hence the GF gain (Crevecoeur et al., 2014).

Appendix B

Joint angles during reaching arm movements (two-link model)

B.1 Introduction

In Chapter 5, it was observed that hand path progressively deviated from the target axis when reaching movements were performed repeatedly with eyes closed. Here, we describe this deviation in terms of shoulder and joint angles instead of hand-path tilt.

B.2 Methods

For a detailed description of the experimental procedure, see Section 5.2. We focus here on the Head-Feet and Front-Back movements performed in a seated posture on the ISS, as the conclusions are similar for the supine posture in flight and on the ground.

Joint angles were not measured during the experiment and thus had to be estimated from the coordinates of the hand and from arm measurements. To that end, we considered a two-link system (first link = upper arm, second link = forearm + hand + manipulandum) in a two-dimensional space (the sagittal plane), as illustrated in Fig. B.1. The upper arm length L_1 and the forearm

length L_2 were measured for each participant during the first pre-flight session and are reported in Table B.1. L_1 was defined as the distance between the acromion and the elbow joint; $L2$ was defined as the distance between the elbow joint and the center of thumb fingertip when the hand is in the precision grip configuration, which corresponds approximately to the distance between the elbow joint and the center of the manipulandum.

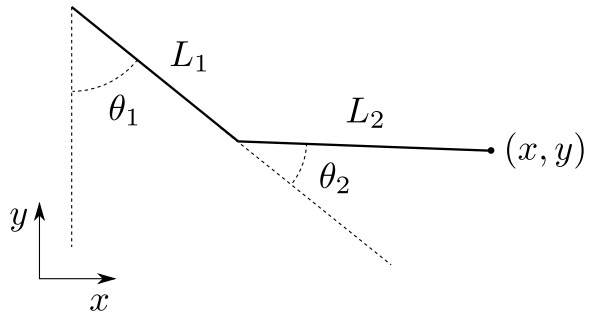

Figure B.1 – Two-dimensional representation of a two-link system representing the upper arm (of length L_1) and forearm (of length L_2) in the sagittal plane. The shoulder angle θ_1 is defined as the angle between the $y-$axis and the upper arm. The elbow angle θ_2 is defined as the angle between the upper arm and the forearm.

Subject	L_1 [cm]	L_2 [cm]
S1	30	43
S2	32	39
S3	35	35
S4	34	37
S5	33	38.5
S6	34	42
Mean	33	39

Table B.1 – Subjects' upper arm (L_1) and forearm (L_2) lengths.

During the reaching movements, the position of the hand was measured in an external reference frame whose origin was located on the utility box. To compute the joint angles, this position has to be expressed relative to the shoulder acromion, whose position was not measured. Hence, we had to estimate the initial configuration of the arm before movement onset on the basis of photographs taken during the experimental sessions. This estimation is inevitably a quite rough approximation (as is the assumption of a two-dimensional system), however the goal here is to extract some tendencies for the behavior of joint

angles to provide additional possible explanations for the observed hand-path tilt.

Given an initial pair of joint coordinates $(\theta_{0,1}, \theta_{0,2})$ at movement onset (estimated from the photographs), the coordinates (x, y) of the hand in a reference frame centered on the acromion can be computed easily. From there, the shoulder angle θ_1 and the elbow angle θ_2 during subsequent movements are uniquely related to the coordinates (x, y) of the hand if one imposes that θ_2 must be in the interval $[0, \pi]$. These joint angles can be computed using the following formulas:

$$\theta_2 = \cos^{-1}\left(\frac{x^2 + y^2 - L_1^2 - L_2^2}{2L_1L_2}\right) \tag{B.1}$$

$$\theta_1 = \frac{\pi}{2} + \tan^{-1}\left(\frac{y}{x}\right) - \sin^{-1}\left(\frac{L_2 \sin\theta_2}{\sqrt{x^2 + y^2}}\right). \tag{B.2}$$

With this method, we could transform any trajectory from a pair of (x, y) coordinates describing the position of the hand into a pair of joint angles (θ_1, θ_2) describing the configuration of the shoulder and elbow joints.

The trajectories were first averaged across trials and participants within each condition. To that end, each trial was temporally normalized. Then, the trajectories were converted into joint angles using equations B.1 and B.2 and the mean L_1 and L_2 measurements reported in Table B.1. For the blocks of reaching movements performed with eyes closed, only the last four trials of each block (hence eight trials in total) were considered (two forward and two backward movements) since the path tilt was most pronounced during these last trials. For the blocks performed with eyes open, all 36 trials were included.

B.3 Results

The average temporal evolution of the shoulder and elbow angles during headward and feetward movements performed in weightlessness in a seated posture are presented in Fig. B.2. Light and dark traces show the average angle profiles for movements performed with eyes open and closed, respectively. As described in Chapter 5, at the end of the blocks performed with eyes closed hand paths deviated significantly from the hand paths of movements performed with eyes open. This deviation was mainly explained by a decrease in the value of elbow angle, i.e. the elbow was more extended with eyes closed than with eyes open

(by more than 10° at the end of headward movements). In contrast, the profile of the shoulder angle was very similar in both vision conditions.

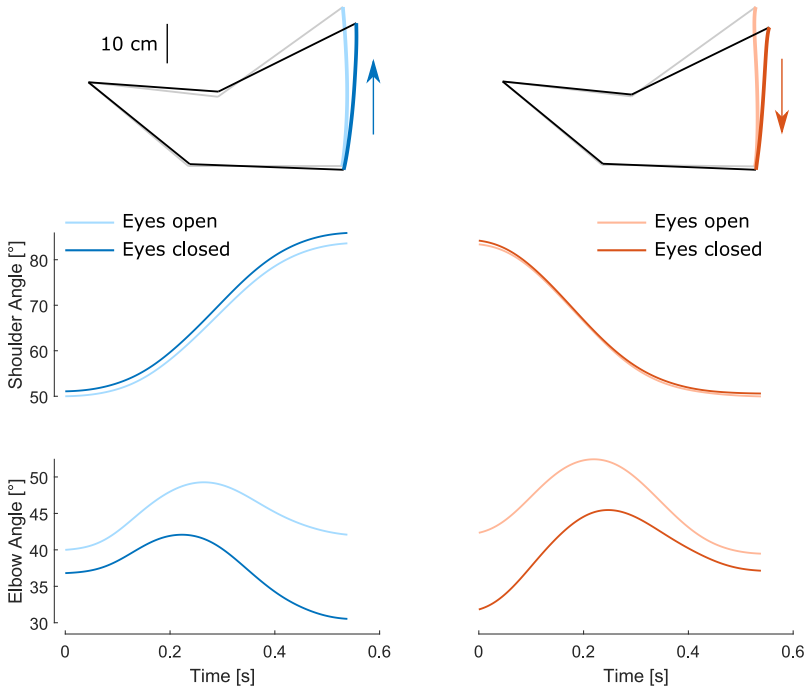

Figure B.2 – Shoulder and elbow joint angles during Head-Feet reaching movements performed in flight in a seated posture. The top rows show the average hand paths across subjects of all trials performed with eyes open (light traces) and of the last two trials of each block performed with eyes closed (dark traces). Gray and black lines show the computed configuration of the arm at the start and at the end of the trajectory when eyes are open and closed, respectively.

For Front-Back movements, differences in joint angles between the two vision conditions are also present although more subtle (Fig. B.3). Overall, the elbow was less extended during the eyes-closed trials than during the eyes-open trials. Furthermore, the shoulder angle was slightly smaller when eyes were closed, i.e. shoulder flexion was reduced. Note that in the supine posture, the same tendencies were observed for both motion axes.

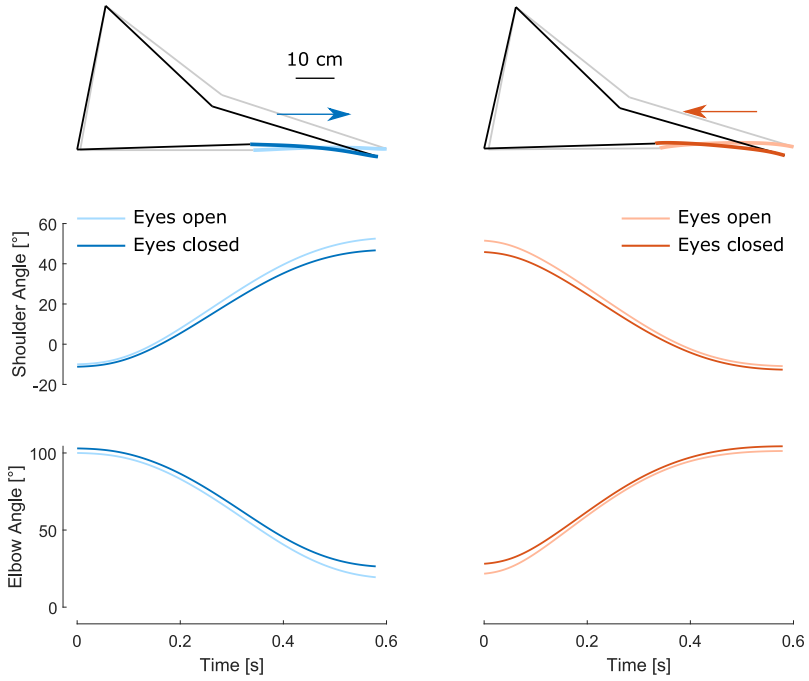

Figure B.3 – Shoulder and elbow joint angles during Front-Back reaching movements performed in flight in a seated posture. The top rows show the average hand paths across subjects of all trials performed with eyes open (light traces) and of the last two trials of each block performed with eyes closed (dark traces). Gray and black lines show the computed configuration of the arm at the start and at the end of the trajectory when eyes are open and closed, respectively.

B.4 Discussion

According to the two-dimensional two-link model presented here, the hand-path tilts observed in flight when no vision was allowed correspond to distinct joint angle errors between Head-Feet and Front-Back movements. If the participants were trying to reproduce the same joint configurations with eyes closed as with eyes open, the results show that they overestimated elbow angle during Head-Feet movements while underestimating elbow angle during Front-Back movements. In addition, they slightly underestimated shoulder angle during Head-Feet movements while overestimating it during Front-Back movements.

It is therefore possible that joint angle estimations were biased in opposite directions for Head-Feet and Front-Back movements. This could be explained by the fact that the configuration of the arm is different in the two types of

movements (see angles range in Fig. B.2 and B.3).

Alternatively, it is also possible that joint angles were not misperceived (intact proprioception) but that the participants were trying to reach for different points in space than with eyes open (inaccurate external spatial map; Watt 1997) because of an erroneous perception of body orientation. As explained in Chapter 5, this would be consistent with the fact that hand-path deviation is biased in a consistent direction in the sagittal plane, whatever the posture of the body or the movement direction. Additional experiments should be carried out in the future to distinguish the contributions of limb position sense and target position sense to hand-path tilt in microgravity.

Bibliography

Adams, M. J., B. J. Briscoe, and S. A. Johnson
2007. Friction and lubrication of human skin. *Tribology Letters*, 26(3):239–253.

Adams, M. J., S. A. Johnson, P. Lefèvre, V. Lévesque, V. Hayward, T. André, and J.-L. Thonnard
2013. Finger pad friction and its role in grip and touch. *Journal of the Royal Society, Interface*, 10(80):20120467.

Alberts, B. B., L. P. Selen, G. Bertolini, D. Straumann, W. P. Medendorp, and A. A. Tarnutzer
2016. Dissociating vestibular and somatosensory contributions to spatial orientation. *Journal of Neurophysiology*, 116(1):30–40.

André, T., P. Lefèvre, and J.-L. Thonnard
2009. A continuous measure of fingertip friction during precision grip. *Journal of Neuroscience Methods*, 179(2):224–229.

André, T., V. Levesque, V. Hayward, P. Lefèvre, and J.-L. Thonnard
2011. Effect of skin hydration on the dynamics of fingertip gripping contact. *Journal of The Royal Society, Interface*, 8(64):1574–1583.

Angelaki, D. E. and K. E. Cullen
2008. Vestibular System: The Many Facets of a Multimodal Sense. *Annual Review of Neuroscience*, 31(1):125–150.

Angelaki, D. E., M. Q. McHenry, J. D. Dickman, S. D. Newlands, and B. J. Hess
1999. Computation of inertial motion: neural strategies to resolve ambiguous otolith information. *Journal of Neuroscience*, 19(1):316–327.

Appelle, S.
1972. Perception and discrimination as a function of stimulus orientation: The "oblique effect" in man and animals. *Psychological Bulletin*, 78(4):266–278.

Asch, S. E. and H. A. Witkin
1948. Studies in space orientation. II. Perception of the upright with displaced visual fields and with body tilted. *Journal of Experimental Psychology*, 38(4):455–477.

Atkeson, C. G. and J. M. Hollerbach
1985. Kinematic features of unrestrained vertical arm movements. *Journal of Neuroscience*, 5(9):2318–30.

Aubert, H.
1861. Eine scheinbare bedeutende Drehung von Objecten bei Neigung des Kopfes nach rechts oder links. *Archiv für Pathologische Anatomie und Physiologie und für Klinische Medicin*, 20(3-4):381–393.

Augurelle, A.-S., M. Penta, O. White, and J.-L. Thonnard
2003a. The effects of a change in gravity on the dynamics of prehension. *Experimental Brain Research*, 148(4):533–540.

Augurelle, A.-S., A. M. Smith, T. Lejeune, and J.-L. Thonnard
2003b. Importance of Cutaneous Feedback in Maintaining a Secure Grip During Manipulation of Hand-Held Objects. *Journal of Neurophysiology*, 89(2):665–671.

Barbieri, G., A. S. Gissot, F. Fouque, J. M. Casillas, T. Pozzo, and D. Pérennou
2008. Does proprioception contribute to the sense of verticality? *Experimental Brain Research*, 185(4):545–552.

Barbiero, M., C. Rousseau, C. Papaxanthis, and O. White
2017. Coherent Multimodal Sensory Information Allows Switching between Gravitoinertial Contexts. *Frontiers in Physiology*, 8(MAY):290.

Barmack, N. H.
2003. Central vestibular system: Vestibular nuclei and posterior cerebellum. *Brain Research Bulletin*, 60(5-6):511–541.

Barra, J., A. Marquer, R. Joassin, C. Reymond, L. Metge, V. Chauvineau, and D. Pérennou
2010. Humans use internal models to construct and update a sense of verticality. *Brain*, 133(12):3552–63.

Barrea, A., D. C. Bulens, P. Lefèvre, and J.-L. Thonnard
2016. Simple and Reliable Method to Estimate the Fingertip Static Coefficient of Friction in Precision Grip. *IEEE Transactions on Haptics*, 9(4):492–498.

Bastian, A. J.
2006. Learning to predict the future: the cerebellum adapts feedforward movement control. *Current opinion in neurobiology*, 16(6):645–649.

Bastian, A. J.
2008. Understanding sensorimotor adaptation and learning for rehabilitation. *Current Opinion in Neurology*, 21(6):628–633.

Bell, C.
1981. An efference copy which is modified by reafferent input. *Science*, 214(4519):450–453.

Bennett, S. J., J.-J. O. de Xivry, P. Lefèvre, and G. R. Barnes
2010. Oculomotor prediction of accelerative target motion during occlusion: long-term and short-term effects. *Experimental Brain Research*, 204(4):493–504.

Berret, B., E. Chiovetto, F. Nori, and T. Pozzo
2011. Evidence for composite cost functions in arm movement planning: An inverse optimal control approach. *PLoS Computational Biology*, 7(10):e1002183.

Berret, B., C. Darlot, F. Jean, T. Pozzo, C. Papaxanthis, and J. P. Gauthier
2008. The inactivation principle: Mathematical solutions minimizing the absolute work and biological implications for the planning of arm movements. *PLoS Computational Biology*, 4(10).

Betts, G. A. and I. S. Curthoys
1998. Visually perceived vertical and visually perceived horizontal are not orthogonal. *Vision Research*, 38(13):1989–1999.

Birznieks, I., M. K. Burstedt, B. B. Edin, and R. S. Johansson
1998. Mechanisms for force adjustments to unpredictable frictional changes

at individual digits during two-fingered manipulation. *Journal of Neurophysiology*, 80(4):1989–2002.

Birznieks, I., V. G. Macefield, G. Westling, and R. S. Johansson
2009. Slowly adapting mechanoreceptors in the borders of the human fingernail encode fingertip forces. *Journal of Neuroscience*, 29(29):9370–9379.

Bisdorff, A. R., C. J. Wolsley, D. Anastasopoulos, A. M. Bronstein, and M. A. Gresty
1996. The perception of body verticality (subjective postural vertical) in peripheral and central vestibular disorders. *Brain*, 119(5):1523–34.

Blakemore, S. J., C. Frith, and D. M. Wolpert
2001. The cerebellum is involved in predicting the sensory consequences of action. *Neuroreport*, 12(9):1879–1884.

Blakemore, S. J., S. J. Goodbody, and D. M. Wolpert
1998. Predicting the consequences of our own actions: the role of sensorimotor context estimation. *Journal of Neuroscience*, 18(18):7511–7518.

Blank, R., A. Breitenbach, M. Nitschke, W. Heizer, S. Letzgus, and J. Hermsdörfer
2001. Human development of grip force modulation relating to cyclic movement-induced inertial loads. *Experimental Brain Research*, 138(2):193–199.

Bock, O.
1998. Problems of sensorimotor coordination in weightlessness. *Brain Research Reviews*, 28(1-2):155–60.

Bock, O. and B. S. Cheung
1998. Control of isometric force in hypergravity. *Aviation Space and Environmental Medicine*, 69(1):27–31.

Bock, O., I. P. Howard, K. E. Money, and K. E. Arnold
1992. Accuracy of aimed arm movements in changed gravity. *Aviation Space and Environmental Medicine*, 63(11):994–8.

Bortolami, S. B., A. Pierobon, P. DiZio, and J. R. Lackner
2006a. Localization of the subjective vertical during roll, pitch, and recumbent yaw body tilt. *Experimental Brain Research*, 173(3):364–373.

Bortolami, S. B., S. Rocca, S. Daros, P. DiZio, and J. R. Lackner
2006b. Mechanisms of human static spatial orientation. *Experimental Brain Research*, 173(3):374–388.

Brandt, T. and M. Dieterich
1999. The Vestibular Cortex: Its Locations, Functions, and Disorders. *Annals of the New York Academy of Sciences*, 871:293–312.

Bresciani, J.-P., J. Blouin, K. E. Popov, C. Bourdin, F. R. Sarlegna, J. L. Vercher, and G. M. Gauthier
2002. Galvanic vestibular stimulation in humans produces online arm movement deviations when reaching towards memorized visual targets. *Neuroscience Letters*, 318(1):34–38.

Bringoux, L., J. Blouin, T. Coyle, H. Ruget, and L. Mouchnino
2012. Effect of gravity-like torque on goal-directed arm movements in microgravity. *Journal of Neurophysiology*, 107(9):2541–8.

Bringoux, L., V. Nougier, L. Marin, P.-A. Barraud, and C. Raphel
2003. Contribution of Somesthetic Information to the Perception of Body Orientation in the Pitch Dimension. *The Quarterly Journal of Experimental Psychology Section A*, 56(5):909–923.

Bringoux, L., K. Tamura, M. Faldon, M. A. Gresty, and A. M. Bronstein
2004. Influence of whole-body pitch tilt and kinesthetic cues on the perceived gravity-referenced eye level. *Experimental Brain Research*, 155(3):385–392.

Brooks, J. X., J. Carriot, and K. E. Cullen
2015. Learning to expect the unexpected: rapid updating in primate cerebellum during voluntary self-motion. *Nature Neuroscience*, 18(9):1310–1317.

Brown, H. and R. Prescott
2006. Normal Mixed Models. In *Applied Mixed Models in Medicine, Second Edition*, chapter 2, Pp. 33–107. Chichester, UK: John Wiley and Sons, Ltd.

Brown, L. E., D. A. Rosenbaum, and R. L. Sainburg
2003. Movement speed effects on limb position drift. *Experimental Brain Research*, 153(2):266–274.

Buckingham, G. and M. A. Goodale
2010. The influence of competing perceptual and motor priors in the context of the size-weight illusion. *Experimental Brain Research*, 205(2):283–288.

Burstedt, M. K., B. B. Edin, and R. S. Johansson
1997. Coordination of fingertip forces during human manipulation can emerge from independent neural networks controlling each engaged digit. *Experimental Brain Research*, 117(1):67–79.

Burstedt, M. K., J. R. Flanagan, and R. S. Johansson
1999. Control of grasp stability in humans under different frictional conditions during multidigit manipulation. *Journal of Neurophysiology*, 82(5):2393–2405.

Carriot, J., L. Bringoux, C. Charles, F. Mars, V. Nougier, and C. Cian
2004. Perceived body orientation in microgravity: Effects of prior experience and pressure under the feet. *Aviation Space and Environmental Medicine*, 75(9):795–799.

Casellato, C., M. Tagliabue, A. Pedrocchi, C. Papaxanthis, G. Ferrigno, and T. Pozzo
2012. Reaching while standing in microgravity: A new postural solution to oversimplify movement control. *Experimental Brain Research*, 216(2):203–215.

Clément, G. R.
2007. Using your head: Cognition and sensorimotor functions in microgravity. *Gravitational and Space Biology*, 20(2):65–78.

Clément, G. R., T. N. Arnesen, M. H. Olsen, and B. Sylvestre
2007. Perception of longitudinal body axis in microgravity during parabolic flight. *Neuroscience Letters*, 413(2):150–153.

Clément, G. R., A. Berthoz, and F. G. Lestienne
1987. Adaptive changes in perception of body orientation and mental image rotation in microgravity. *Aviation Space and Environmental medicine*, 58(9):159–63.

Clément, G. R., V. S. Gurfinkel, F. G. Lestienne, M. Lipshits, and K. E. Popov
1984. Adaptation of postural control to weightlessness. *Experimental Brain Research*, 57(1):61–72.

Clément, G. R., S. T. Moore, T. Raphan, and B. Cohen
2001. Perception of tilt (somatogravic illusion) in response to sustained linear acceleration during space flight. *Experimental Brain Research*, 138(4):410–418.

Cohen, Y. E. and R. A. Andersen
2002. A common reference frame for movement plans in the posterior parietal cortex. *Nature Reviews Neuroscience*, 3(7):553–562.

Comaish, S. and E. Bottoms
1971. The skin and friction: deviations from Amonton's laws, and the effects of hydration and lubrication. *British Journal of Dermatology*, 84(1):37–43.

Coppola, D. M., H. R. Purves, A. N. Mccoy, and D. Purves
1998. The distribution of oriented contours in the real world. *Neurobiology*, 95:4002–4006.

Crevecoeur, F., A. Barrea, X. Libouton, J.-L. Thonnard, and P. Lefèvre
2017. Multisensory components of rapid motor responses to fingertip loading. *Journal of Neurophysiology*, 118(1):331–343.

Crevecoeur, F., T. Giard, J.-L. Thonnard, and P. Lefèvre
2011. Adaptive control of grip force to compensate for static and dynamic torques during object manipulation. *Journal of Neurophysiology*, 106(6):2973–2981.

Crevecoeur, F., J. McIntyre, J.-L. Thonnard, and P. Lefèvre
2010a. Movement stability under uncertain internal models of dynamics. *Journal of Neurophysiology*, 104(3):1301–13.

Crevecoeur, F., J. McIntyre, J.-L. Thonnard, and P. Lefèvre
2014. Gravity-dependent estimates of object mass underlie the generation of motor commands for horizontal limb movements. *Journal of Neurophysiology*, 112(April):384–392.

Crevecoeur, F., J.-L. Thonnard, and P. Lefèvre
2009a. Forward models of inertial loads in weightlessness. *Neuroscience*, 161(2):589–598.

Crevecoeur, F., J.-L. Thonnard, and P. Lefèvre
2009b. Optimal Integration of Gravity in Trajectory Planning of Vertical Pointing Movements. *Journal of Neurophysiology*, 102(2):786–796.

Crevecoeur, F., J.-L. Thonnard, and P. Lefèvre
2010b. Sensorimotor Mapping for Anticipatory Grip Force Modulation. *Journal of Neurophysiology*, 104(3):1401–1408.

Cullen, K. E.
2004. Sensory signals during active versus passive movement. *Current Opinion in Neurobiology*, 14(6):698–706.

Dakin, C. J., A. Peters, P. Giunti, and B. L. Day
2018. Cerebellar Degeneration Increases Visual Influence on Dynamic Estimates of Verticality. *Current Biology*, 28(22):3589–3598.e3.

Dakin, C. J. and A. Rosenberg
2018. Gravity estimation and verticality perception. In *Handbook of Clinical Neurology*, B. L. Day and S. Lord, eds., volume 159.

Danion, F. R.
2004. How dependent are grip force and arm actions during holding an object? *Experimental Brain Research*, 158(1):109–119.

Danion, F. R., J. S. Diamond, and J. Randall Flanagan
2013. Separate contributions of kinematic and kinetic errors to trajectory and grip force adaptation when transporting novel hand-held loads. *Journal of Neuroscience*, 33(5):2229–2236.

Danion, F. R. and F. R. Sarlegna
2007. Can the Human Brain Predict the Consequences of Arm Movement Corrections When Transporting an Object? Hints from Grip Force Adjustments. *Journal of Neuroscience*, 27(47):12839–12843.

Davare, M.
2006. Dissociating the Role of Ventral and Dorsal Premotor Cortex in Precision Grasping. *Journal of Neuroscience*, 26(8):2260–2268.

de Winkel, K. N., G. R. Clément, E. L. Groen, and P. J. Werkhoven
2012. The perception of verticality in lunar and Martian gravity conditions. *Neuroscience Letters*, 529(1):7–11.

Delhaye, B. P., K. H. Long, and S. J. Bensmaia
2018. Neural Basis of Touch and Proprioception in Primate Cortex. *Comprehensive Physiology*, In Press(October):1575–1602.

Demontis, G. C., M. M. Germani, E. G. Caiani, I. Barravecchia, C. Passino, and D. Angeloni
2017. Human Pathophysiological Adaptations to the Space Environment. *Frontiers in Physiology*, 8(AUG):547.

Descoins, M., F. R. Danion, and R. J. Bootsma
2006. Predictive control of grip force when moving object with an elastic load applied on the arm. *Experimental Brain Research*, 172(3):331–342.

Desmurget, M., C. M. Epstein, R. S. Turner, C. Prablanc, G. E. Alexander, and S. T. Grafton
1999. Role of the posterior parietal cortex in updating reaching movements to a visual target. *Nature Neuroscience*, 2(6):563–567.

Diamond, J. S., J. Y. Nashed, R. S. Johansson, D. M. Wolpert, and J. Randall Flanagan
2015. Rapid visuomotor corrective responses during transport of hand-held objects incorporate novel object dynamics. *Journal of Neuroscience*, 35(29):10572–10580.

Dichgans, J., R. Held, L. R. Young, and T. Brandt
1972. Moving visual scenes influence the apparent direction of gravity. *Science*, 178(4066):1217–1219.

Dyde, R. T., M. R. Jenkin, and L. R. Harris
2006. The subjective visual vertical and the perceptual upright. *Experimental Brain Research*, 173(4):612–622.

Ebenholtz, S. M.
1970. Perception of the vertical with body tilt in the median plane. *Journal of Experimental Psychology*, 83(1):1–6.

Edin, B. B., G. Westling, and R. S. Johansson
1992. Independent control of human finger-tip forces at individual digits during precision lifting. *Journal of Physiology*, 450(1992):547–64.

Ehrsson, H. H.
2003. Evidence for the Involvement of the Posterior Parietal Cortex in Coordination of Fingertip Forces for Grasp Stability in Manipulation. *Journal of Neurophysiology*, 90(5):2978–2986.

Fisk, J., J. R. Lackner, and P. DiZio
1993. Gravitoinertial force level influences arm movement control. *Journal of Neurophysiology*, 69(2):504–11.

Flanagan, J. R. and S. Lolley
2001. The inertial anisotropy of the arm is accurately predicted during movement planning. *Journal of Neuroscience*, 21(4):1361–1369.

Flanagan, J. R. and J. Tresilian
1994. Grip-load force coupling: a general control strategy for transporting objects. *Journal of experimental psychology. Human perception and performance*, 20(5):944–957.

Flanagan, J. R., J. Tresilian, and A. M. Wing
1993. Coupling of grip force and load force during arm movements with grasped objects. *Neuroscience Letters*, 152(1-2):53–56.

Flanagan, J. R., P. Vetter, R. S. Johansson, and D. M. Wolpert
2003. Prediction precedes control in motor learning. *Current Biology*, 13(2):146–150.

Flanagan, J. R. and A. M. Wing
1993. Modulation of grip force with load force during point to point arm movements. *Experimental Brain Research*, 95:131–143.

Flanagan, J. R. and A. M. Wing
1995. The stability of precision grip forces during cyclic arm movements with a hand-held load. *Experimental Brain Research*, 105(3):455–464.

Flanagan, J. R. and A. M. Wing
1997. The role of internal models in motion planning and control: evidence from grip force adjustments during movements of hand-held loads. *Journal of Neuroscience*, 17(4):1519–1528.

Flash, T. and N. Hogan
1985. The coordination of arm movements: an experimentally confirmed mathematical model. *Journal of Neuroscience*, 5(7):1688–1703.

Fleury, L., C. Prablanc, and A.-E. Priot
2019. Do prism and other adaptation paradigms really measure the same processes? *Cortex*, 119:480–496.

Fleury, M., C. Bard, N. Teasdale, J. Paillard, J. Cole, Y. Lajoie, and Y. Lamarre
1995. Weight judgment: The discrimination capacity of a deafferented subject. *Brain*, 118(5):1149–1156.

Forssberg, H., H. Kinoshita, A. C. Eliasson, R. S. Johansson, G. Westling, and A. M. Gordon
1992a. Development of human precision grip I: Basic coordination of force. *Experimental Brain Research*, 90(2):393–398.

Forssberg, H., H. Kinoshita, A. C. Eliasson, R. S. Johansson, G. Westling, and A. M. Gordon
1992b. Development of human precision grip II: Anticipatory control of isometric forces targeted for object's weight. *Experimental Brain Research*, 90(2):393–398.

Fouque, F., B. G. Bardy, T. A. Stoffregen, and R. J. Bootsma
1999. Action and Intermodal Information Influence the Perception of Orientation. *Ecological Psychology*, 11(1):1–43.

Gandevia, S. C., J. L. Smith, M. Crawford, U. Proske, and J. L. Taylor
2006. Motor commands contribute to human position sense. *Journal of Physiology*, 571(3):703–710.

Gao, F., M. L. Latash, and V. M. Zatsiorsky
2008. Similar motion of a handheld object may trigger non-similar grip force adjustments. *J Hand Ther*, 20(4):300–309.

Gaveau, J., B. Berret, D. E. Angelaki, and C. Papaxanthis
2016. Direction-dependent arm kinematics reveal optimal integration of gravity cues. *eLife*, 5(NOVEMBER2016):1–17.

Gaveau, J., B. Berret, L. Demougeot, L. Fadiga, T. Pozzo, and C. Papaxanthis
2014. Energy-related optimal control accounts for gravitational load: comparing shoulder, elbow, and wrist rotations. *Journal of Neurophysiology*, 111(1):4–16.

Gaveau, J., S. Grospretre, D. E. Angelaki, and C. Papaxanthis
2021. A cross-species neural integration of gravity for motor optimisation. *Science Advances*, 7(15):eabf7800.

Gaveau, J. and C. Papaxanthis
2011. The temporal structure of vertical arm movements. *PLoS ONE*, 6(7):e22045.

Gentili, R., V. Cahouet, and C. Papaxanthis
2007. Motor planning of arm movements is direction-dependent in the gravity field. *Neuroscience*, 145(1):20–32.

Giard, T., F. Crevecoeur, J. McIntyre, J.-L. Thonnard, and P. Lefèvre
2015. Inertial torque during reaching directly impacts grip-force adaptation to weightless objects. *Experimental Brain Research*, 233(11):3323–3332.

Girgenrath, M., S. Göbel, O. Bock, and H. Pongratz
2005. Isometric force production in high Gz: Mechanical effects, proprioception, and central motor commands. *Aviation Space and Environmental Medicine*, 76(4):339–343.

Goodwin, G. M., D. I. Mccloskey, and P. B. Matthews
1972. Proprioceptive illusions induced by muscle vibration: Contribution by muscle spindles to perception? *Science*, 175(4028):1382–1384.

Gordon, A. M., H. Forssberg, R. S. Johansson, and G. Westling
1991. Visual size cues in the programming of manipulative forces during precision grip. *Experimental Brain Research*, 83:477–482.

Gordon, A. M., G. Westling, K. J. Cole, and R. S. Johansson
1993. Memory representations underlying motor commands used during manipulation of common and novel objects. *Journal of Neurophysiology*, 69(6):1789–1797.

Graybiel, A.
1952. Oculogravic illusion. *A.M.A. Archives of Ophthalmology*, 48(5):605–615.

Graybiel, A. and R. S. Kellogg
1967. Inversion illusion in parabolic flight: its probable dependence on otolith function. *Aerospace medicine*, 38(11):1099–103.

Graybiel, A. and J. L. Patterson
1955. Thresholds of stimulation of the otolith organs as indicated by the oculogravic illusion. *Journal of applied physiology*, 7(6):666–70.

Green, A. M. and D. E. Angelaki
2010. Internal models and neural computation in the vestibular system. *Experimental Brain Research*, 200(3-4):197–222.

Gysin, P., T. R. Kaminski, and A. M. Gordon
2003. Coordination of fingertip forces in object transport during locomotion. *Experimental Brain Research*, 149:371–379.

Haarmeier, T., F. Bunjes, A. Lindner, E. Berret, and P. Thier
2001. Optimizing visual motion perception during eye movements. *Neuron*, 32(3):527–535.

Hadjiosif, A. M. and M. A. Smith
2015. Flexible Control of Safety Margins for Action Based on Environmental Variability. *Journal of Neuroscience*, 35(24):9106–9121.

Häger-Ross, C., K. J. Cole, and R. S. Johansson
1996. Grip-force responses to unanticipated object loading: load direction reveals body- and gravity-referenced intrinsic task variables. *Experimental Brain Research*, 110(1):142–50.

Hallgren, E., L. Kornilova, E. Fransen, D. Glukhikh, S. T. Moore, G. R. Clément, A. Van Ombergen, H. MacDougall, I. Naumov, and F. L. Wuyts
2016. Decreased otolith-mediated vestibular response in 25 astronauts induced by long-duration spaceflight. *Journal of Neurophysiology*, 115:2045–3051.

Harris, L. R., M. R. Jenkin, H. Jenkin, J. E. Zacher, and R. T. Dyde
2017. The effect of long-term exposure to microgravity on the perception of upright. *npj Microgravity*, 3(1).

Hermsdörfer, J., C. Marquardt, J. Philipp, A. Zierdt, D. A. Nowak, S. Glasauer, and N. Mai
1999. Grip forces exerted against stationary held objects during gravity changes. *Experimental Brain Research*, 126(2):205–214.

Hermsdörfer, J., C. Marquardt, J. Philipp, A. Zierdt, D. A. Nowak, S. Glasauer, and N. Mai
2000. Moving weightless objects. Grip force control during microgravity. *Experimental Brain Research*, 132(2000):52–64.

Hollerbach, J. M. and T. Flash
1982. Dynamic interactions between limb segments during planar arm movement. *Biological Cybernetics*, 44(1):67–77.

Hondzinski, J. M., C. M. Soebbing, A. E. French, and S. A. Winges
2016. Different damping responses explain vertical endpoint error differences between visual conditions. *Experimental Brain Research*, 234(1575-1587).

Hupfeld, K. E., H. R. McGregor, P. Reuter-Lorenz, and R. Seidler
2021. Microgravity Effects on the Human Brain and Behavior: Dysfunction and Adaptive Plasticity. *Neuroscience and Biobehavioral Reviews*, 122(12):176–189.

Indovina, I., V. Maffei, G. Bosco, M. Zago, E. Macaluso, and F. Lacquaniti
2005. Representation of visual gravitational motion in the human vestibular cortex. *Science*, 308(5720):416–419.

Indovina, I., V. Maffei, K. Pauwels, E. Macaluso, G. A. Orban, and F. Lacquaniti
2013. Simulated self-motion in a visual gravity field: Sensitivity to vertical and horizontal heading in the human brain. *NeuroImage*, 71(2013):114–124.

Iwase, S., N. Nishimura, K. Tanaka, and T. Mano
2020. Effects of Microgravity on Human Physiology. In *Beyond LEO - Human Health Issues for Deep Space Exploration*. IntechOpen.

Izawa, J., T. Rane, O. Donchin, and R. Shadmehr
2008. Motor Adaptation as a Process of Reoptimization. *Journal of Neuroscience*, 28(11):2883–2891.

Jenkin, H., R. T. Dyde, M. R. Jenkin, I. P. Howard, and L. R. Harris
2003. Relative role of visual and non-visual cues in determining the direction of "up": experiments in the York tilted room facility. *Journal of Vestibular Research*, 13(4-6):287–293.

Jenkin, H., R. T. Dyde, J. E. Zacher, D. C. Zikovitz, M. R. Jenkin, R. S. Allison, I. P. Howard, and L. R. Harris
2005. The relative role of visual and non-visual cues in determining the perceived direction of "up": Experiments in parabolic flight. In *Acta Astronautica*, volume 56, Pp. 1025–1032.

Jian, B., T. Shintani, B. Emanuel, and B. J. Yates
2002. Convergence of limb, visceral, and vertical semicircular canal or otolith inputs onto vestibular nucleus neurons. *Experimental Brain Research*, 144(2):247–257.

Johansson, R. S. and Å. B. Vallbo
1983. Tactile sensory coding in the glabrous skin of the human hand. *Trends in Neurosciences*, 6(C):27–32.

Johansson, R. S. and G. Westling
1984. Roles of glabrous skin receptors and sensorimotor memory in automatic control of precision grip when lifting rougher or more slippery objects. *Experimental Brain Research*, 56(3):550–564.

Johansson, R. S. and G. Westling
1987a. Signals in tactile afferents from the fingers eliciting adaptive motor responses during precision grip. *Experimental Brain Research*, 66(1):141–154.

Johansson, R. S. and G. Westling
1987b. Tactile afferent input influencing motor coordination during precision grip. *Clinical aspects of sensory motor integration*, 4:3–13.

Johansson, R. S. and G. Westling
1988a. Coordinated isometric muscle commands adequately and erroneously programmed for the weight during lifting task with precision grip. *Experimental Brain Research*, 71(1):59–71.

Johansson, R. S. and G. Westling
1988b. Programmed and triggered actions to rapid load changes during precision grip. *Experimental Brain Research*, 71(1):72–86.

Jörges, B. and J. López-Moliner
2017. Gravity as a Strong Prior: Implications for Perception and Action. *Frontiers in Human Neuroscience*, 11(April):1–16.

Kaptein, R. G. and J. A. Van Gisbergen
2004. Interpretation of a Discontinuity in the Sense of Verticality at Large Body Tilt. *Journal of Neurophysiology*, 91:2205–2214.

Karmali, F. and M. J. Shelhamer
2008. The dynamics of parabolic flight: Flight characteristics and passenger percepts. *Acta Astronautica*, 63(5-6):594–602.

Kawato, M.
1999. Internal models for motor control and trajectory planning. *Current Opinion in Neurobiology*, 9(6):718–727.

Kawato, M., T. Kuroda, H. Imamizu, E. Nakano, S. Miyauchi, and T. Yoshioka
2003. Internal forward models in the cerebellum: fMRI study on grip force and load force coupling. In *Progress in Brain Research*, volume 142, Pp. 171–188. Elsevier.

Keyser, J., W. P. Medendorp, and L. P. Selen
2017. Task-dependent vestibular feedback responses in reaching. *Journal of Neurophysiology*, 118(1).

Kim, I. K. and E. S. Spelke
1992. Infants' Sensitivity to Effects of Gravity on Visible Object Motion. *Journal of Experimental Psychology: Human Perception and Performance*, 18(2):385–393.

Kinoshita, H., A. Bäckström, J. R. Flanagan, and R. S. Johansson
1997. Tangential torque effects on the control of grip forces when holding objects with a precision grip. *Journal of Neurophysiology*, 78(3):1619–1630.

Kornilova, L.
1997. Orientation illusions in spaceflight. *Journal of Vestibular Research: Equilibrium and Orientation*, 7(6):429–439.

Kuhtz-buschbeck, J. P., H. H. Ehrsson, and H. Forssberg
2001. Human brain activity in the control of fine static precision grip forces : an fMRI study. *European Journal of Neuroscience*, 14:382–390.

Kurtzer, I. L., J. A. Pruszynski, and S. H. Scott
2008. Long-Latency Reflexes of the Human Arm Reflect an Internal Model of Limb Dynamics. *Current Biology*, 18(6):449–453.

Lackner, J. R. and P. DiZio
1992. Gravitoinertial force level affects the appreciation of limb position during muscle vibration. *Brain Research*, 592(1-2):175–180.

Lackner, J. R. and P. DiZio
1993. Multisensory, cognitive, and motor influences on human spatial orientation in weightlessness. *Journal of Vestibular Research*, 3(3):361–372.

Lackner, J. R. and P. DiZio
1994. Rapid adaptation to Coriolis force perturbations of arm trajectory. *Journal of Neurophysiology*, 72(1):299–313.

Lackner, J. R. and P. DiZio
2000. Human orientation and movement control in weightless and artificial gravity environments. *Experimental Brain Research*, 130(1):2–26.

Lackner, J. R. and P. DiZio
2018. Dynamic Sensory-Motor Adaptation to Earth Gravity. In *Stevens' Handbook of Experimental Psychology and Cognitive Neuroscience*, Pp. 1–27.

Lackner, J. R., P. DiZio, and J. Fisk
1992. Tonic vibration reflexes and background force level. *Acta Astronautica*.

Lackner, J. R. and A. Graybiel
1979. Parabolic flight: Loss of sense of orientation. *Science*, 206:1105–1108.

Lackner, J. R. and A. Graybiel
1981. Illusions of postural, visual, and aircraft motion elicited by deep knee bends in the increased gravitoinertial force phase of parabolic flight - Evidence for dynamic sensory-motor calibration to earth gravity force levels. *Experimental Brain Research*, 44:312–316.

Lacquaniti, F., G. Bosco, S. Gravano, I. Indovina, B. La Scaleia, V. Maffei, and M. Zago
2014. Multisensory integration and internal models for sensing gravity effects in primates. *BioMed Research International*, 2014:615854.

Lacquaniti, F. and C. Maioli
1989a. Adaptation to suppression of visual information during catching. *Journal of Neuroscience*, 9(1):149–159.

Lacquaniti, F. and C. Maioli
1989b. The role of preparation in tuning anticipatory and reflex responses during catching. *Journal of Neuroscience*, 9(1):134–48.

Laurens, J., H. Meng, and D. E. Angelaki
2013. Neural representation of orientation relative to gravity in the macaque cerebellum. *Neuron*, 80:1508–1518.

Le Séac'h, A. B. and J. McIntyre
2007. Multimodal reference frame for the planning of vertical arms movements. *Neuroscience Letters*, 423(3):211–215.

Le Séac'h, A. B., P. Senot, and J. McIntyre
2010. Egocentric and allocentric reference frames for catching a falling object. *Experimental Brain Research*, 201(4):653–662.

Lechner-Steinleitner, S., H. Schöne, and N. J. Wade
1979. Perception of the visual vertical: Utricular and somatosensory contributions. *Psychological Research*, 40(4):407–414.

Lipshits, M., A. Bengoetxea, G. Cheron, and J. McIntyre
2005. Two reference frames for visual perception in two gravity conditions. *Perception*, 34:545–555.

Lipshits, M. and J. McIntyre
1999. Gravity affects the preferred vertical and horizontal in visual perception of orientation. *NeuroReport*, 10:1085–1089.

Lukos, J., C. Ansuini, and M. Santello
2007. Choice of contact points during multidigit grasping: Effect of predictability of object center of mass location. *Journal of Neuroscience*, 27(14):3894–3903.

Lyons, J. L., S. Hansen, S. Hurding, and D. Elliott
2006. Optimizing rapid aiming behaviour: Movement kinematics depend on the cost of corrective modifications. *Experimental Brain Research*, 174(1):95–100.

Martin, T. A., J. G. Keating, H. P. Goodkin, A. J. Bastian, and W. T. Thach
1996. Throwing while looking through prisms II. Specificity and storage of multiple gaze-throw calibrations. *Brain*, 119(4):1199–1211.

Maschke, M., C. M. Gomez, T. J. Ebner, and J. Konczak
2004. Hereditary Cerebellar Ataxia Progressively Impairs Force Adaptation During Goal-Directed Arm Movements. *Journal of Neurophysiology*, 91(1):230–238.

McCall, A. A., D. M. Miller, and B. J. Yates
2017. Descending influences on vestibulospinal and vestibulosympathetic reflexes. *Frontiers in Neurology*, 8(MAR):1–15.

McCloskey, D. I., P. Ebeling, and G. M. Goodwin
1974. Estimation of weights and tensions and apparent involvement of a "sense of effort". *Experimental Neurology*, 42(1):220–232.

McIntyre, J., A. Berthoz, and F. Lacquaniti
1998. Reference frames and internal models for visuo-manual coordination: What can we learn from microgravity experiments? *Brain Research Reviews*, 28(1-2):143–154.

McIntyre, J. and M. Lipshits
2008. Central Processes Amplify and Transform Anisotropies of the Visual System in a Test of Visual-Haptic Coordination. *Journal of Neuroscience*, 28(5):1246–1261.

McIntyre, J., M. Zago, A. Berthoz, and F. Lacquaniti
2001. Does the brain model Newton's laws? *Nature neuroscience*, 4(7):693–694.

McNamee, D. and D. M. Wolpert
2019. Internal Models in Biological Control. *Annual Review of Control, Robotics, and Autonomous Systems*, 2(1):339–364.

Mechtcheriakov, S., M. Berger, E. Molokanova, G. Holzmueller, W. Wirtenberger, S. Lechner-Steinleitner, C. De Col, I. B. Kozlovskaya, and F. Gerstenbrand
2002. Slowing of human arm movements during weightlessness: The role of vision. *European Journal of Applied Physiology*, 87(6):576–583.

Merfeld, D. M., L. R. Young, C. M. Oman, and M. J. Shelhamer
1993. A multidimensional model of the effect of gravity on the spatial orientation of the monkey. *Journal of Vestibular Research*, 3:141–161.

Merfeld, D. M., L. Zupan, and R. J. Peterka
1999. Humans use internal models to estimate gravity and linear acceleration. *Nature*, 398(6728):615–618.

Miall, R. C. and D. M. Wolpert
1996. Forward Moldels for Physiological Motor Control. *Neural Networks*, 9(8):1265–1279.

Mierau, A., M. Girgenrath, and O. Bock
2008. Isometric force production during changed-Gz episodes of parabolic flight. *European Journal of Applied Physiology*, 102(3):313–318.

Mittelstaedt, H.
1983. A new solution to the problem of the subjective vertical. *Naturwissenschaften*, 70:272–281.

Mittelstaedt, H.
1996. Somatic graviception. *Biological Psychology*, 42(1-2):53–74.

Mittelstaedt, H.
1997. Interaction of eye-, head-, and trunk-bound information in spatial perception and control. *Journal of Vestibular Research*, 7(4):283–302.

Mittelstaedt, H.
1999. The role of the otoliths in perception of the vertical and in path

integration. In *Annals of the New York Academy of Sciences*, volume 871, Pp. 334–344. New York Academy of Sciences.

Mittelstaedt, H. and E. Fricke
1988. The relative effect of saccular and somatosensory information on spatial perception and control. *Advances in oto-rhino-laryngology*, 42:24–30.

Mittelstaedt, H. and S. Glasauer
1993. Crucial effects of weightlessness on human orientation. *Journal of Vestibular Research*, 3(3):307–314.

Monzée, J., Y. Lamarre, and A. M. Smith
2003. The effects of digital anesthesia on force control using a precision grip. *Journal of Neurophysiology*, 89(2):672–683.

Morasso, P.
1981. Spatial control of arm movements. *Experimental Brain Research*, 42(2):223–227.

Mulliken, G. H., S. Musallam, and R. A. Andersen
2008. Forward estimation of movement state in posterior parietal cortex. *Proceedings of the National Academy of Sciences*, 105(24):8170–8177.

Nowak, D. A., S. Glasauer, and J. Hermsdörfer
2004a. How predictive is grip force control in the complete absence of somatosensory feedback? *Brain*, 127(1):182–192.

Nowak, D. A. and J. Hermsdörfer
2003. Digit cooling influences grasp efficiency during manipulative tasks. *European journal of applied physiology*, 89(2):127–33.

Nowak, D. A., J. Hermsdörfer, S. Glasauer, J. Philipp, L. Meyer, and N. Mai
2002a. The effects of digital anaesthesia on predictive grip force adjustments during vertical movements of a grasped object. *European Journal of Neuroscience*, 14(4):756–762.

Nowak, D. A., J. Hermsdörfer, C. Marquardt, and H. H. Fuchs
2002b. Grip and load force coupling during discrete vertical arm movements with a grasped object in cerebellar atrophy. *Experimental Brain Research*, 145(1):28–39.

Nowak, D. A., J. Hermsdörfer, J. Philipp, C. Marquardt, S. Glasauer, and N. Mai
2001. Effects of changing gravity on anticipatory grip force control during point-to-point movements of a hand-held object. *Motor Control*, 5(3):231–253.

Nowak, D. A., J. Hermsdörfer, E. Schneider, and S. Glasauer
2004b. Moving objects in a rotating environment: rapid prediction of Coriolis and centrifugal force perturbations. *Experimental Brain research*, 157(2):241–54.

Olivier, E., M. Davare, M. Andres, and L. Fadiga
2007. Precision grasping in humans: from motor control to cognition. *Current Opinion in Neurobiology*, 17(6):644–648.

Opsomer, L., V. Théate, P. Lefèvre, and J.-L. Thonnard
2018. Dexterous Manipulation During Rhythmic Arm Movements in Mars, Moon, and Micro-Gravity. *Frontiers in Physiology*, 9(July):1–10.

Oya, T., T. Takei, and K. Seki
2020. Distinct sensorimotor feedback loops for dynamic and static control of primate precision grip. *Communication Biology*, 3(156).

Paillard, J. and M. Brouchon
1968. Active and passive movements in the calibration of position sense. In *The neuropsychology of spatially oriented behavior*, S. Freedman, ed., Pp. 37–55. Dorsey Press.

Papaxanthis, C., T. Pozzo, and J. McIntyre
2005. Kinematic and dynamic processes for the control of pointing movements in humans revealed by short-term exposure to microgravity. *Neuroscience*, 135(2):371–383.

Papaxanthis, C., T. Pozzo, K. E. Popov, and J. McIntyre
1998a. Hand trajectories of vertical arm movements in one-G and zero-G environments. Evidence for a central representation of gravitational force. *Experimental Brain Research*, 120(4):496–502.

Papaxanthis, C., T. Pozzo, and M. Schieppati
2003. Trajectories of arm pointing movements on the sagittal plane vary with both direction and speed. *Experimental Brain Research*, 148(4):498–503.

Papaxanthis, C., T. Pozzo, and P. Stapley
1998b. Effects of movement direction upon kinematic characteristics of vertical arm pointing movements in man. *Neuroscience Letters*, 253(2):103–106.

Papaxanthis, C., T. Pozzo, A. Vinter, and A. Grishin
1998c. The representation of gravitational force during drawing movements of the arm. *Experimental Brain Research*, 120(2):233–242.

Pérennou, D., G. Mazibrada, V. Chauvineau, R. Greenwood, J. Rothwell, M. A. Gresty, and A. M. Bronstein
2008. Lateropulsion, pushing and verticality perception in hemisphere stroke: A causal relationship? *Brain*, 131:2401–2413.

Pilon, J.-F., S. J. D. Serres, and A. G. Feldman
2007. Threshold position control of arm movement with anticipatory increase in grip force. *Experimental Brain Research*, 181(1):49–67.

Popa, L. S. and T. J. Ebner
2019. Cerebellum, Predictions and Errors. *Frontiers in Cellular Neuroscience*, 12:524.

Pozzo, T., C. Papaxanthis, P. Stapley, and A. Berthoz
1998. The sensorimotor and cognitive integration of gravity. *Brain Research Reviews*, 28(1-2):92–101.

Proske, U.
2019. Exercise, fatigue and proprioception: a retrospective. *Experimental Brain Research*, 237(10):2447–2459.

Proske, U. and S. C. Gandevia
2009. The kinaesthetic senses. *Journal of Physiology*, 587(Pt 17):4139–4146.

Purves, D., G. J. Augustine, D. Fitzpatrick, W. C. Hall, A.-S. LaMantia, and L. E. White
2012. The Vestibular System. In *Neuroscience 5th edition*, Pp. 303–311. Sinauer Associates, Inc.

Rabbitt, R. D., E. R. Damiano, and J. W. Grant
2004. Biomechanics of the Semicircular Canals and Otolith Organs. In *The Vestibular System*, Pp. 153–201. Springer, New York, NY.

Reschke, M. F., D. J. Anderson, and J. L. Homick
1984. Vestibulospinal reflexes as a function of microgravity. *Science*, 225:212–214.

Roll, R., J. C. Gilhodes, J. P. Roll, K. E. Popov, O. Charade, and V. S. Gurfinkel
1998. Proprioceptive information processing in weightlessness. *Experimental Brain Research*, 122:393–402.

Ross, H. E., E. Brodie, and A. J. Benson
1986. Mass-discrimination in weightlessness and readaptation to earth gravity. *Experimental Brain Research*, 64(1986):358–366.

Rost, K., D. A. Nowak, D. Timmann, and J. Hermsdörfer
2005. Preserved and impaired aspects of predictive grip force control in cerebellar patients. *Clinical Neurophysiology*, 116:1405–1414.

Roy, J. E. and K. E. Cullen
2004. Dissociating Self-Generated from Passively Applied Head Motion: Neural Mechanisms in the Vestibular Nuclei. *Journal of Neuroscience*, 24(9):2102–2111.

Santello, M., G. Baud-Bovy, and H. Jörntell
2013. Neural bases of hand synergies. *Frontiers in Computational Neuroscience*, 7:23.

Sarlegna, F. R., G. Baud-Bovy, and F. R. Danion
2010. Delayed Visual Feedback Affects Both Manual Tracking and Grip Force Control When Transporting a Handheld Object. *Journal of Neurophysiology*, 104:641–653.

Sawtell, N. B.
2016. Neural Mechanisms for Predicting the Sensory Consequences of Behavior: Insights from Electrosensory Systems. *Annual Review of Physiology*, 79:381–399.

Schaal, S., D. Sternad, R. Osu, and M. Kawato
2004. Rhythmic arm movement is not discrete. *Nature Neuroscience*, 7(10):1136–1143.

Schneider, S., V. Brümmer, S. Göbel, H. Carnahan, A. Dubrowski, and H. K. Strüder
2007. Parabolic flight experience is related to increased release of stress hormones. *European Journal of Applied Physiology*, 100(3):301–308.

Schöne, H.
1964. On the role of gravity in human spatial orientation. *Aerospace medicine*, 35:764–772.

Schöne, H. and H. U. De Haes
1968. Perception of gravity-vertical as a function of head and trunk position. *Zeitschrift für Vergleichende Physiologie*, 60(4):440–444.

Scotto Di Cesare, C., L. Bringoux, C. Bourdin, F. R. Sarlegna, and D. R. Mestre
2011. Spatial localization investigated by continuous pointing during visual and gravitoinertial changes. *Experimental Brain Research*, 215:173–182.

Seilheimer, R. L., A. Rosenberg, and D. E. Angelaki
2014. Models and processes of multisensory cue combination. *Current Opinion in Neurobiology*, 25:38–46.

Senot, P., M. Zago, F. Lacquaniti, and J. McIntyre
2005. Anticipating the Effects of Gravity When Intercepting Moving Objects: Differentiating Up and Down Based on Nonvisual Cues. *Journal of Neurophysiology*, 94:4471–4480.

Shadmehr, R. and J. W. Krakauer
2008. A computational neuroanatomy for motor control. *Experimental Brain Research*, 185(3):359–381.

Shadmehr, R. and F. A. Mussa-Ivaldi
1994. Adaptive representation of dynamics during learning of a motor task. *Journal of Neuroscience*, 14(5):3208–3224.

Shortt, T. L. and C. A. Ray
1997. Sympathetic and vascular responses to head-down neck flexion in humans. *American Journal of Physiology*, 272(4):1780–1784.

Smetanin, B. N.
1997. Effect of body orientation with respect to gravity on directional accuracy of human pointing movements. *European Journal of Neuroscience*, 9(1):7–11.

Smith, A. M. and S. H. Scott
1996. Subjective scaling of smooth surface friction. *Journal of Neurophysiology*, 75(5):1957–1962.

Smith, C. P., J. E. Allsop, M. Mistry, and R. F. Reynolds
2017. Co-ordination of the upper and lower limbs for vestibular control of balance. *Journal of Physiology*, 595(21):6771–6782.

Soechting, J. F. and F. Lacquaniti
1981. Invariant characteristics of a pointing movement in man. *Journal of Neuroscience*, 1(7):710–720.

Tagliabue, M. and J. McIntyre
2012. Eye-hand coordination when the body moves: Dynamic egocentric and exocentric sensory encoding. *Neuroscience Letters*, 513(1):78–83.

Tani, K., S. Yamamoto, Y. Kodaka, and K. Kushiro
2021. Dynamic arm movements attenuate the perceptual distortion of visual vertical induced during prolonged whole-body tilt. *PLOS ONE*, 16(4):e0250851.

Tarnutzer, A. A., G. Bertolini, C. J. Bockisch, D. Straumann, and S. Marti
2013. Modulation of Internal Estimates of Gravity during and after Prolonged Roll-Tilts. *PLoS ONE*, 8(10):e78079.

Tarnutzer, A. A., C. J. Bockisch, D. Straumann, and I. Olasagasti
2009. Gravity dependence of subjective visual vertical variability. *Journal of Neurophysiology*, 102:1657–1671.

Thonnard, J.-L., L. Opsomer, P. Lefèvre, V. Pletser, and J. McIntyre
2020. GRIP: Dexterous Manipulation of Objects in Weightlessness. In *Preparation of Space Experiments*, V. Pletser, ed., chapter GRIP: Dext, Pp. 1–19. IntechOpen.

Todorov, E.
2004. Optimality principles in sensorimotor control. *Nature Neuroscience*, 7(9):907–915.

Todorov, E. and M. I. Jordan
2002. Optimal feedback control as a theory of motor coordination. *Nature Neuroscience*, 5(11):1226–35.

Toma, S., V. Caputo, and M. Santello
2020. Visual Feedback of Object Motion Direction Influences the Timing of Grip Force Modulation During Object Manipulation. *Frontiers in Human Neuroscience*, 14(May):1–17.

Trousselard, M., P. A. Barraud, V. Nougier, C. Raphel, and C. Cian
2004. Contribution of tactile and interoceptive cues to the perception of the direction of gravity. *Cognitive Brain Research*, 20(3):355–362.

Trousselard, M., C. Cian, V. Nougier, S. Pla, and C. Raphel
2003. Contribution of somesthetic cues to the perception of body orientation and subjective visual vertical. *Perception and Psychophysics*, 65(8):1179–87.

Tsay, A., G. Savage, T. J. Allen, and U. Proske
2014. Limb position sense, proprioceptive drift and muscle thixotropy at the human elbow joint. *The Journal of Physiology*, 592(Pt 12):2679.

Tseng, Y. W., J. Diedrichsen, J. W. Krakauer, R. Shadmehr, and A. J. Bastian
2007. Sensory prediction errors drive cerebellum-dependent adaptation of reaching. *Journal of Neurophysiology*, 98(1):54–62.

Turrell, Y., F. X. Li, and A. M. Wing
1999. Grip force dynamics in the approach to a collision. *Experimental Brain Research*, 128(1-2):86–91.

Udo De Haes, H. A.
1970. Stability of apparent vertical and ocular countertorsion as a function of lateral tilt. *Perception and Psychophysics*, 8(3):137–142.

van Kuilenburg, J., M. A. Masen, and E. van der Heide
2013. A review of fingerpad contact mechanics and friction and how this affects tactile perception. *Proceedings of the Institution of Mechanical Engineers, Part J: Journal of Engineering Tribology*, 229(3):243–258.

Viviani, P. and F. Lacquaniti
2015. Grip forces during fast point-to-point and continuous hand movements. *Experimental Brain Research*, 233:3201–3220.

von Holst, E. and H. Mittelstaedt
1950. The principle of reafference. *Naturwissenschaften*, 3(37):464–476.

Wade, N. J.
1970. Effect of Prolonged Tilt on Visual Orientation. *Quarterly Journal of Experimental Psychology*, 22(3):423–439.

Wann, J. and S. Ibrahim
1992. Does limb proprioception drift? *Experimental Brain Research*, 91(1):162–166.

Watt, D. G.
1997. Pointing at memorized targets during prolonged microgravity. *Aviation Space and Environmental Medicine*, 68(2):99–103.

Werremeyer, M. M. and K. J. Cole
1997. Wrist action affects precision grip force. *Journal of Neurophysiology*, 78(1):271–280.

Westling, G. and R. S. Johansson
1984. Factors influencing the force control during precision grip. *Experimental Brain Research*, 53(2):277–284.

Westling, G. and R. S. Johansson
1987. Responses in glabrous skin mechanoreceptors during precision grip in humans. *Experimental Brain Research*, 66(1):128–140.

White, O.
2015. The brain adjusts grip forces differently according to gravity and inertia: a parabolic flight experiment. *Frontiers in Integrative Neuroscience*, 9(February):1–10.

White, O., Y. Bleyenheuft, R. Ronsse, A. M. Smith, J.-L. Thonnard, and P. Lefèvre
2008. Altered gravity highlights central pattern generator mechanisms. *Journal of Neurophysiology*, 100(5):2819–2824.

White, O., J. Gaveau, L. Bringoux, and F. Crevecoeur
2020. The gravitational imprint on sensorimotor planning and control. *Journal of Neurophysiology*, 124(1):4–19.

White, O., P. Lefèvre, A. M. Wing, R. M. Bracewell, and J.-L. Thonnard
2012. Active Collisions in Altered Gravity Reveal Eye-Hand Coordination Strategies. *PLoS ONE*, 7(9).

White, O., J. McIntyre, A.-S. Augurelle, and J.-L. Thonnard
2005. Do novel gravitational environments alter the grip-force/load-force coupling at the fingertips? *Experimental Brain Research*, 163(3):324–334.

White, O., J.-L. Thonnard, P. Lefèvre, and J. Hermsdörfer
2018. Grip force adjustments reflect prediction of dynamic consequences in varying gravitoinertial fields. *Frontiers in Physiology*, 9(FEB):1–11.

White, O., J.-L. Thonnard, A. M. Wing, R. M. Bracewell, J. Diedrichsen, and P. Lefèvre
2011. Grip force regulates hand impedance to optimize object stability in high impact loads. *Neuroscience*, 189:269–276.

Whiteside, T. C.
1961. Hand-eye coordination in weightlessness. *Aeromedica acta*, 32:719–725.

Wing, A. M., J. R. Flanagan, and J. Richardson
1997. Anticipatory postural adjustments in stance and grip. *Experimental Brain Research*, 116(1):122–130.

Witney, A. G., A. M. Wing, J.-L. Thonnard, and A. M. Smith
2004. The cutaneous contribution to adaptive precision grip. *Trends in Neurosciences*, 27(10):637–643.

Wolpert, D. M., R. C. Miall, and M. Kawato
1998. Internal models in the cerebellum. *Trends in Cognitive Sciences*, 2(9):338–347.

Worringham, C. J. and G. E. Stelmach
1985. The contribution of gravitational torques to limb position sense. *Experimental Brain Research*, 61(1):38–42.

Young, L. R., C. M. Oman, D. M. Merfeld, D. G. Watt, S. Roy, C. DeLuca, D. Balkwill, J. Christie, N. Groleau, D. K. Jackson, G. Law, S. Modestino, and W. Mayer
1993. Spatial orientation and posture during and following weightlessness: Human experiments on spacelab life sciences. *Journal of Vestibular Research*, 3:231–239.

Young, L. R., C. M. Oman, D. G. Watt, K. E. Money, and B. K. Lichtenberg
1984. Spatial orientation in weightlessness and readaptation to Earth's gravity. *Science*, 225(July):205–208.

Zaehle, T., K. Jordan, T. Wüstenberg, J. Baudewig, P. Dechent, and F. W. Mast
2007. The neural basis of the egocentric and allocentric spatial frame of reference. *Brain Research*, 1137(1):92–103.

Zago, M. and F. Lacquaniti
2005. Visual perception and interception of falling objects: A review of

evidence for an internal model of gravity. *Journal of Neural Engineering*, 2(3):S198–S208.

Zatsiorsky, V. M., F. Gao, and M. L. Latash

2005. Motor control goes beyond physics: Differential effects of gravity and inertia on finger forces during manipulation of hand-held objects. *Experimental Brain Research*, 162(3):300–308.